Influence of Isoflurane on the Integrity of the Blood Brain Barrier

by

John N. Litchfield

Dissertation submitted to the Faculty of the Daniel K. Inouye
Graduate School of Nursing, Uniformed Services University of the Health Sciences
In partial fulfillment of the requirements for the degree of
Doctor of Philosophy 2018

Distribution Statement

Distribution A: Public Release.

The views presented here are those of the author and are not to be construed as official or reflecting the views of the Uniformed Services University of the Health Sciences, the Department of Defense or the U.S. Government.

USU Uniformed Services University | GRADUATE NURSING Daniel K. Inouye Graduate School of Nursing

GSN PhD Dissertation Defense
Doctor of Philosophy in Nursing Science Degree

NAME: LCDR John Litchfield

TITLE: Influence of Isoflurane on the Integrity of the Blood Brian Barrier in Rats

Date of Defense: 12 July 2018

The decision of the Dissertation Committee is:

PASS

(A.) Both the dissertation and the oral defense are satisfactory:
B. Minor changes are recommended by the Dissertation Committee that is to be made to the satisfaction of the Dissertation Chairperson:

DEFER

A. Major changes in the dissertation are required. Changes must be made to the satisfaction of the Dissertation Chairperson:
B. Major changes in the dissertation are required. Changes must be made to the satisfaction of the Dissertation Committee and at that time the oral defense will be rescheduled:

FAIL: Neither the oral performance nor the dissertation is adequate:

SIGNATURES OF THE COMMITTEE:

Chairperson: Christine E. Kasper, PhD, RN, FAAN, FACSM Signatu[redacted]

Member: Lisa A. Osborne Smith, PhD, CRNA Signatu[redacted]

Member: Chantal M. Moratz, PhD Signatu[redacted]

Member: Clifton L. Dalgard, PhD, CLS Signatu[redacted]

Approved/Disapproved
PhD Program Director: [redacted] Date: 9/28/2018

Approved/Disapproved
Dean, Graduate School of Nursing: [redacted] Date: 10/4/2018

ACKNOWLEDGMENTS

This dissertation was not accomplished in singularity. I had immense help from multiple different professors, faculty, staff members and friends. Unfortunately, this is cannot be an exhaustive list. So, if you don't find your name listed here, please do not feel forgotten or slighted.

First, I would like to thank Dr. Lisa Osborne-Smith who encourage me to return to school and then finagled a way to make it happen. You provided unending support, guidance, and reoccurring doses of reality. Her countless hour of making sure this dissertation was scientifically sound and clinically relevant made this project enjoyable and hopefully meaningful for those entrusted into our care that require multiple surgical procedures.

To Dr. Christine Kasper – I am particularly grateful and thankful that your focused wisdom and experience kept this dissertation moving in the right direction and prevented me from adding more aims. If you hadn't, I would still be working! You somehow always knew when to let me run, real me in, and appear out of nowhere to answer pressing questions.

To my troubleshooter, Dr. Chantal Moratz – thank you for allowing me to use your lab equipment and providing me a space to work. Your guidance and encouragement during the incalculable number of hours spent troubleshooting previously validated western blots and immunohistochemistry slides was invaluable. I will never look at a pressure cooker or microwave the same again.

To Dr. Clifton Dalgard – I feel tremendously fortunate to have worked with you this past 5 years. You provided irreplaceable mentorship, advise, guidance, and material

support for the RT-qPCR and RNA-sequencing portions of this dissertation. Additionally, you were ever present and quick to respond to my growing list of questions no matter how busy you were.

I am eternally grateful to my wife, Heather Litchfield, who in my continued absence over the past five years has meant that you had to act as a single parent more than I wished. You did it with unwavering grace and class (and a little wine). Thank you for allowing me to pursue my dream while putting yours on hold. Truly selfless…

To my children, Jacob and Emma. I marvel at how easily you take things in stride and make the best of any situation. In your few short years here, you have done and seen a lot – unfortunately without me. Thank you for keeping me company on long weekends in the lab, providing me and my classmates with a continuous supply of baked goods, and sometimes, not so subtle reminders of what's important - dad time.

To the other members of the "Wolf Pack" my classmates, Dr. Lalon Kasuske and Dr. Dawn Kimberly Hawkins your continued friendship to this date is a cherished gift. I look back at all the experiences that we have shared, "at least 99" I think, and would not wanted to experience them with anyone else. I am looking forward to making more!

I am particularly grateful to Dr. Luke Michelson and Dr. Andre Bhloken for easing the stress of learning new basic science techniques and answering the millions of questions about tissue destruction, antibody binding, cryostat cutting, immunohistochemistry, microscopy, and basic lab management.

I need to personally thank Dr. Maureen Hood for allowing me to use her shiny new western blot transfer system and digital fluorescent western blot imager. Moving from overnight wet transfers and 30 minute imaging times to 6 minute transfers and 3

minute imaging times has saved me countless hours of waiting. Also, thank you for keeping the lab supplied with cheesecake.

This dissertation was generously supported by a Jonas Nursing and Veterans Healthcare Scholarship, a Tri-Service Nursing Research Program grant, and two Uniformed Services University Intramural grants. A thank you to all those who had a hand in moving money around, purchasing supplies, and tracking me down for required reports. I'll do better next time; I promise (fingers crossed).

DEDICATION

For those Warriors with complex wounds requiring multiple surgeries.

You are in my continued thought and prayers.

COPYRIGHT STATEMENT

The author hereby certifies that the use of any copyrighted material in the dissertation manuscript entitled: “Influence of Isoflurane on the Integrity of the Blood Brain Barrier” is appropriately acknowledged and, beyond brief excerpts, is with the permission of the copyright owner.

_____

John Newman Litchfield

June 24, 2018

DISCLAIMER

The views presented here are those of the author and are not to be construed as official or reflecting the views of the Uniformed Services University of the Health Sciences, the Department of Defense or the U.S. Government.

ABSTRACT

Title of Dissertation: Influence of Isoflurane on the Integrity of the Blood Brain Barrier

by

John N. Litchfield, PhD, CRNA, 2018

Thesis directed by: Christine E. Kasper, PhD, RN, FAAN, FASCM

Professor, Doctor of Philosophy in Nursing Science Program

Daniel K. Inouye Graduate School of Nursing

Uniformed Services University of the Health Science

ABSTRACT

Background: The blood brain barrier (BBB) is a highly regulated structure that provides a stable microenvironment for proper neuronal functioning. An emerging body of evidence suggests that a single exposure to volatile anesthetics, like isoflurane, can reversibly alter BBB structure and function. Complex trauma patients often require multiple operations. The effects of repeated isoflurane exposures on BBB structure and function remain unidentified. Therefore, the purpose of this dissertation is to evaluate the effects of repeated exposures to isoflurane on the structure, function, and permeability of the BBB.

Methods: Adult (8-10 Week) male Sprague Dawley Rats were divided into 4 groups: control, single prolonged exposure (1PE), single brief exposure (1BE), and multiple brief exposures (5BE). Animals were anesthetized with 1.5% isoflurane for 4 hours, 2 hours,

or 2 hours on 5 consecutive days. Physiological parameters, arterial blood gases (ABG's), and metabolic parameters were measured. Expression of tight junction proteins (CL-5, occludin & ZO-1) were measured by RT-qPCR, western blot, and immunohistochemistry, while BBB permeability was measured by FITC -dextran extravasation at 4 and 24 hours following anesthesia exposure.

Results: All physiological, ABG, and metabolic parameters were within normal reference values. A single prolonged exposure to isoflurane showed a significant decrease in CL-5 levels at 4 hours with full recovery by 24 hours, while occludin levels were significantly reduced at both 4 and 24 hours by western blot and immunohistochemistry analysis. Dextran extravasation was significant at both 4 and 24 hours following exposure. No changes in BBB structure or function were noted following a single brief exposure. Following 5 BE's to isoflurane, protein levels of occludin were significantly reduced at 4 hours but showed partial recovery at 24 hours. The amount of ZO-1 located at tight junctions was significantly decreased at both 4 and 24 hours. Loss of tight junction proteins resulted in significant dextran extravasation at 4 hours.

Conclusion: These findings suggest that a single prolonged exposure or multiple brief exposures to isoflurane can induce substantial BBB disruption at 4 hours with partial recovery by 24 hours. Additionally, a single brief exposure failed to disrupt BBB structure and function.

TABLE OF CONTENTS

Abstract ix

LIST OF TABLES xv

LIST OF FIGURES xvi

CHAPTER 1: Introduction 1

Introduction 1
Postoperative Cognitive Dysfunction 1
Definition 1
Incidence 2
Manifestations and Risk Factors 3
Neuropathology of POCD 4
Volatile Anesthetics 5
Mechanism of Action 5
Side Effects 6
Blood Brain Barrier 7
History 10
Structure of the BBB 11
Astrocytes 12
Microglia 13
Pericytes 14
Basal Lamina 14
Endothelial Cells 15
Molecules of the BBB 16
Occludin 16
Claudin-5 18
Zonula Occludens 19
Volatile Anesthetics at the BBB 21
Specific Aims 23
Specific Aim: 23
Hypotheses: 24

CHAPTER 2: Background and Significance 25

Introduction 25
Wounding Pattern 25
Surgical Repair 26
Postoperative Cognitive Dysfunction 27
Blood Brain Barrier 28
Volatile Anesthetics 31
Volatile Anesthetic: Characteristics 32
Volatile Anesthetics: Gene Alterations 32

Volatile Anesthetics: Hippocampus 33
Volatile Anesthetics: Drug Combinations 33
Volatile Anesthetics: Repeated Exposures 34
Volatile Anesthetics: Blood Brain Barrier 35
Volatile Anesthetics: Cellular Pathways and Blood Brain Barrier 38
Conclusion 40

CHAPTER 3: Methods 41

Research Design 41
Power Analysis 41
Animal Model 41
Anesthesia Exposure 42
Overview 42
Control Group 43
Single Exposure Groups 43
Repeated Brief Exposures 44
Monitoring Physiological Parameters 44
Weight 44
Agent Monitoring 44
Vital Signs 45
Arterial Blood Gas and Lactate 46
Blood Glucose 47
Hemoglobin 47
Dextran Injection 47
Tissue Preparation 48
Euthanasia and Hippocampal Dissection 48
Whole Animal Perfusion 48
Western Blot 50
Protein Extraction 50
Protein Quantification 50
Sodium Dodecyl Sulfate-Polyacrylamide Gel Electrophoresis (SDS-PAGE) 51
Quantitative Real Time Polymerase Chain Reaction 53
RNA Isolation 53
Determining RNA purity, quantification, & integrity 54
Spectrophotometer 54
Quant-iT Fluorescence Quantification 55
RNA Integrity 56
Complementary DNA Synthesis (cDNA) 58
Primer Design 58
Quantitative Real Time Polymerase Chain Reaction (PCR) 59
RNA Sequencing 60
Immunofluorescence 60
Tissue Sectioning 60
Immunofluorescence 61
Proteins of Interest (Occludin, CL-5, and ZO-1) 61
Dextran Extravasation 63

Image Acquisition 65
Image Analysis 66
Immunohistochemistry 66
Dextran Extravasation 67

CHAPTER 4: Results 69

Physiological Parameters 69
Physiological Parameters: Between Groups 69
Physiological Parameters: Between Repeated Exposures 70
Arterial Blood Gas 72
Arterial Blood Gas: Between Groups 72
Arterial Blood Gas: Between Exposures 73
Glucose and Hemoglobin Results 74
Glucose and Hemoglobin Results: Between Groups 74
Glucose and Hemoglobin: Between Exposures 75
Quantitative Real Time Polymerase Chain Reaction Results 76
RNA Sequencing Results 79
Overview 79
Gene Ontology Biological Process Analysis 80
RNA-Seq: Study Proteins 80
RNA-Seq: BBB Accessory Proteins 81
RNA-Seq: Specific Brain Cell Markers 83
Oligodendrocyte RT-PCR 87
RNA-Seq: Volatile Anesthetic Targets 87
RNA-Seq: Volatile Anesthesia Targets: Inhibitory 88
RNA-Seq: Volatile Anesthetics - Excitatory 89
RNA-Seq: Excitatory - Glutamate receptors 89
RNA-Seq: Excitatory - Acetylcholine Receptors 91
RNA-Seq: Excitatory - Histamine Receptors 91
RNA-Seq: Opioid Receptors 92
RNA-Seq: Ion Channels 93
Western Blot 96
Single Prolonged Exposure 96
Single Brief Exposure 97
5 Brief Exposures 97
Immunohistochemistry 100
Single Prolonged Exposure 100
Single Brief Exposure 103
5 Brief Exposures 103
Dextran Extravasation 106

CHAPTER 5: Discussion 108

Physiological Parameters 108
Cardiorespiratory Parameters 108
Arterial Blood Gas Parameters 110
Metabolic Parameters 112

RNA-Sequencing 114
Tight Junction Proteins 120
Transmembrane Proteins 121
Cytoplasmic Proteins 122
Dextran Extravasation 123
Limitations and Future Work 124
Conclusion ..... **Error! Bookmark not defined.**

LIST OF TABLES

Table 1: Animal groups, sections, and cohorts. 41
Table 2. Animal Exposure Timeline 43
Table 3. Western blot primary and secondary Antibodies 53
Table 4: RNA Purity and Quantification 54
Table 5: Quant-iT Quantification Results 56
Table 6. RNA Quality Number: Sample number (RQN value) 57
Table 7. Primer Design Characteristics 58
Table 8. Forward and reverse primer sequences. 59
Table 9. Immunofluorescence primary and secondary antibodies. 65
Table 10. Physiological parameters by group listed as mean ± SEM. 70
Table 11. Physiological parameters by anesthesia exposure listed as mean ± SEM. 71
Table 12. Arterial blood gas parameters by group, listed at mean ± SEM. 73
Table 13. Arterial blood gas parameters by exposure, listed by mean ± SEM. 74
Table 14. Glucose and hemoglobin results by group, listed as mean ± SEM. 75
Table 15. Glucose and hemoglobin values by exposure, listed as mean ± SEM. 76
Table 16. RT-qPCR mean ΔΔCt values, fold change, and p-values for study proteins 77
Table 17. Top 15 up and down regulated genes following 1 PE to 1.5% isoflurane. 79
Table 18. Top 10 Gene Ontology Processes. 80
Table 19. RNA Seq values for study proteins (Cl-5, occludin, & ZO-1) 81
Table 20. Differently expressed BBB transcripts including fold changes and p-value. 82
Table 21. RNA-Seq results for brain specific markers listed by cell type. 85
Table 22. Oligodendrocyte PCR values and fold change. 87
Table 23. Inhibitory Anesthesia Targets (GABA & Glycine) 89
Table 24. Volatile anesthetics: Excitatory glutamate receptor subunits. 90
Table 25. Excitatory volatile anesthesia targets: Acetylcholine 91
Table 26. Excitatory volatile anesthetics: Histamine 92
Table 27: Volatile anesthesia targets: Opioid receptors. 92
Table 28. Volatile anesthesia targets: Ion channels 94

LIST OF FIGURES

Figure 1: ZO-1 protein domains. The PDZ-1 domain primarily binds claudin molecules, PDZ-2 domains bind junctional adhesion molecules and other ZO proteins, a combination of the U5/GK domains bind occludin, and the proline rich (P) c-terminal binds actin and other cytoskeleton proteins. Multiple other proteins interact with these domains, but were not included in this figure for clarity. Adapted from: Bauer, H., Zweimueller-Mayer, J., Steinbacher, P., Lametschwandtner, A., & Bauer, H.C. The Dual Role of Zonula Occludens (ZO) Proteins. Journal of Biomedical and Biotechnology, Volume 2010, Article ID: 402593..... 21
Figure 2. Slide pattern for immunofluorescence..... 61
Figure 3. Real-time RT-PCR analysis of CL-5, occludin, and ZO-1 mRNA levels following a 1 Prolonged Exposure (4 hour) to 1.5% isoflurane. 77
Figure 4. RT-PCR analysis of CL-5, occludin, and ZO-1 mRNA levels following 5 Brief (2 Hour) exposures to 1.5% isoflurane on consecutive days. 78
Figure 5. RT-PCR analysis of CL-5, occludin, and ZO-1 mRNA levels following 1 Brief Exposure (2 Hours) to 1.5% isoflurane..... 78
Figure 6. Heat map of study genes (CL-5, occludin, & ZO-1) and accessory transmembrane and cytoplasmic proteins. 82
Figure 7. Heat map of specific brain cell markers. 86
Figure 8. Heap map of inhibitory and excitatory anesthesia targets, and ion channels... 95
Figure 9. Western blot analysis of CL-5 (9A), occludin (9B), and ZO-1 (9C) protein levels following 1 PE to 1.5% isoflurane. * $p < 0.05$ compared to control group; † $p < 0.05$ compared to 1_PE4 group 98
Figure 10. Western blot analysis of CL-5 (10A), occludin (10B), and ZO-1 (10C) protein levels following 5 BE's to 1.5% isoflurane. * $p < 0.05$ compared to control group; † $p < 0.05$ compared to 1_PE4 group 99
Figure 11. Immunofluorescence microscopy results for CL-5 (Figure 11A), occludin (Figure 11B), and ZO-1 (Figure 11C) in the 1 Prolonged Exposure group. * $p < 0.05$ compared to control group; † $p < 0.05$ compared to 1_PE4 group..... 102
Figure 12. Immunofluorescence microscopy results for CL-5 (Figure 12A), occludin (Figure 12B), and ZO-1 (Figure 12C) in the 1 Brief Exposure Group. *$p < 0.05$ compared to control; † $p < 0.05$ compared to 1_BE4 cohort. 104
Figure 13. Immunofluorescence microscopy results for CL-5 (Figure 13A), occludin (Figure 13B), and ZO-1 (Figure 13C) in the 5 Brief Exposure Group. 105
Figure 14. Dextran results following 1_PE (14A), 1_BE (14B) or 5_BE's (14C) to isoflurane. *$p< 0.05$ compared to control; † $p < 0.05$ compared to 4 hour cohort. 107

CHAPTER 1: Introduction

INTRODUCTION

Postoperative cognitive dysfunction (POCD) remains a common, but poorly understood disorder of cognitive function following exposure to anesthesia and surgery (94; 235). Manifestations of POCD include alterations in memory, attention, concentration, executive function, and socialization leading to increased length of hospital stays and decreased quality of life (4). The etiology of POCD is a complex, multifactorial process with the specific role of anesthesia exposure not being well described. Recent evidence indicates that a single exposure to a volatile anesthetic, such as isoflurane, can alter synaptic function, trigger an innate immune response, and alter the structure and function of the blood brain barrier (BBB), all of which can alter cognitive processes (133; 228; 239). However, complex trauma patients often require multiple exposures to volatile anesthetics before definitive repairs can be completed (149). The effects of these repeated exposures to volatile anesthetics on the structure and function of the BBB remains largely unknown. Therefore, the purpose of this dissertation is to identify the structural and functional changes to the BBB following repeated exposures to volatile anesthetics. Knowledge gained from this research can be utilized to inform best clinical practice models for individuals who require multiple operations.

POSTOPERATIVE COGNITIVE DYSFUNCTION

Definition

Postoperative cognitive dysfunction is defined as new impairment of cognitive functioning following anesthesia and surgery (94; 235). Manifestations of POCD include alterations in memory, attention, concentration, speed of processing, executive function,

and socialization (107; 221). Initially, the initial signs of POCD maybe subtle and confused for the acute effects of residual anesthetics, pain medications, or surgical recovery.

Postoperative cognitive dysfunction also needs to be distinguished from other cognitive changes that can occur postoperatively such as emergence delirium (ED) or postoperative delirium (POD). Emergence delirium is characterized as restlessness, confusion, somnolence, agitation, excitement, or aggression during the immediate emergence from anesthesia and is fully resolved before discharge from the post-anesthesia care unit (PACU) (31; 128). Patients who experience POD typically have a more complex PACU stay and postoperative course resulting in increased lengths of stay and increased cost (196; 204). Postoperative delirium is described as acute changes in consciousness, disturbances in attention or awareness, impairment of cognition and language, and emotional dysregulation that fluctuates throughout the day(58). Postoperative delirium is divided into hypoactive, hyperactive, or mixed subtypes, with hyperactive being the most common. Typically, POD occurs between postoperative days 1 to 3 and is related to increased length of hospital stay, admissions to skilled nursing facility, reductions in cognitive function, decline in functional capabilities, and increased mortality at 1 year (148; 204). The major difference between ED and POD compared to POCD is alterations in consciousness. In both ED and POD, patients have a reduced level of consciousness while patients with POCD do not (58).

Incidence

Due to differing clinical definitions and study methodologies, the actual incidence of POCD is difficult to determine. The most common way to diagnosis POCD is to

compare post-operative neurocognitive test scores to individual pre-operative scores or those of aged matched controls. However, the type and number of neuropsychological tests employed, analysis of the results, and when statistical significance reaches clinical relevance has yet to be resolved.

The International Study of Postoperative Cognitive Dysfunction (ISPOCD) was an international study involving 13 different hospitals in 8 different countries. This study involved 1,218 elderly participants (> 60) and 145 aged matched control that underwent formal neuropsychological testing prior to, and again at 1 week, and 3 months following surgery. For a diagnosis of POCD, the calculated Z-score in two or more individual test or the overall combined score needed to be greater than 1.96 from controls scores to be considered positive. Compared to controls, POCD was present in 25.8% of patients at 1 week and 9.9% at 3 months (164). Further evaluation of POCD in patients greater than 18, using the same methodology as the ISPOCD study, reported the incidence of POCD at hospital discharge to be 36.6% in the young (18-39), 30.4% in the middle age (40-59), and 41.4% in the elderly (>60) (114). Additionally, 3 months following surgery, the rates were 5.7% for the young, 5.6% for the middle aged, and 12.7% for the elderly (114).

Manifestations and Risk Factors

The presence of POCD increases the risk for postoperative complications, length of stay, admission to rehabilitation facilities, and cost (164; 165). Initially, these cognitive changes can be limited to subtle irritation, or lead to changes in overall level of daily functioning, decreased social integration, relationship difficulties, and a decreased quality of life (165; 221) . If POCD does not resolve, however, it can be come permeant leading to loss of independence, premature departure from the job market, and increased

dependence on social programs (4; 114; 165; 221). Additionally, POCD present at hospital discharge shortens the time to a diagnosis of dementia and increased mortality at the 1 year mark following surgery (221). Therefore, POCD not only poses a substantial burden on individuals and their family, it poses a significant burden on communities and society as well.

Numerous risk factors that might dispose individuals to POCD have been developed and are divided in patent and surgical related factors. Patient related factors include current burden of illness, education level, preoperative cognitive status, advanced age (>60), and certain genetic dispositions (21; 164). The surgical related factors can be subdivided into intraoperative risk and postoperative risks. Intraoperative risks include large operations under general anesthesia especially cardiac or orthopedic procedures, duration of anesthesia and surgery, hypothermia, or intraoperative complications such as cerebral hypoxia (107; 164). Postoperative infection, respiratory complications, uncontrolled pain, sleep deprivation, prolonged immobilization, and subsequent operations are postoperative risk factors (21; 207) .

Neuropathology of POCD

The exact neuropathological basis of POCD remains unclear. What remains uncertain is whether anesthesia alone can cause POCD or if a combination of anesthesia and surgical trauma is required. Studying the effect of anesthesia exposure independently of surgery offers great control, but is unrealistic clinically because individuals do not receive anesthesia without undergoing some sort of invasive procedure. Additionally, studying the effect of surgery on POCD without anesthesia would be considered unethical. Because of this, multiple different animal models have been developed. These

models suggest that exposure to volatile anesthetics may lead to changes in cognitive function by altering synaptic functioning, triggering neuroinflammation, or by altering the structure and function of the BBB.

VOLATILE ANESTHETICS

Volatile anesthetics, such as isoflurane, create a complex state of reversible loss of consciousness, sedation, amnesia, analgesia, and immobility (102). Volatile anesthetics are administered via the lungs as gaseous vapors and are delivered to the CNS dissolved in the bloodstream (68). This unique characteristic of inhaled anesthetics gives them distinct pharmacodynamics and pharmacokinetic properties. Additionally, despite the fact that they have been used in clinical practice for over 150 years, the exact mechanism of action at the cellular level remains elusive.

Mechanism of Action

There is a wide range of structurally diverse compounds that can induce general anesthesia and produce immobility. Since there was no structural relationship between these compounds, it was believed that the compounds worked via a common manner on global structures in the brain and not on specific receptors (28). This unity theory of action proposed that membrane structures of the neurons were perturbed leading to loss of function and general anesthesia (117). Later on, it was discovered that there was a strong correlation between solubility of the volatile anesthetic in olive oil and potency. This relationship between lipid solubility and potency spanned several orders of magnification and was comparable across species (205). This lipid solubility theory suggests that the diverse compounds dissolve in the lipid bilayers of neurons altering their signaling properties.

Newer evidence, however, indicates that volatile anesthetics bind directly to specific protein ion channels and either block their excitatory effects or enhance their inhibitory effects. Volatile anesthetics enhance the inhibitory effects of chloride (Cl-) by activating gama-aminobutryic acid (GABA) and glycine receptors, and by altering the resting membrane potential of neurons by opening inward rectifying two-pore domain potassium (K+) channels (83; 102; 205). Additionally, volatile anesthetics diminish excitatory activity at both acetylcholine (nicotinic and muscarinic) and glutamate (N-methyl-D-asparate [NMDA]) receptors (83; 102; 205).

Side Effects

Volatile anesthetics are commonly chosen for their ease of use, ready availability, lack of known major side effects, and their ability to quickly be eliminated from the body. In addition to their desired effects, volatile anesthetics can alter cerebral, respiratory, thermoregulatory, and metabolic parameters (67). Understanding these effects is important for study outcomes and animal welfare (8; 57).

Even in extremely low concentrations, volatile anesthetics are potent respiratory depressants (66), decreasing minute ventilation (MV) by decreasing tidal volume (TV), typically without a co-contaminant increase in respiratory rate, leading to increased PaCO2 levels (68). This indicates that individuals may develop hypoxemia, hypercarbia, and respiratory acidosis.

Volatile anesthetics have minimal effects on cardiovascular parameters. In a dose dependent manner, volatile anesthetics cause vasodilation leading to a decrease in arterial blood pressure through a decrease in systemic vascular resistance (66). However, cardiac

output (CO) is maintained by a slight rise in heart rate due to preservation of the carotid baroreceptors (66).

The decrease in systemic vascular resistance leads to a 33% increase in cerebral blood flow at normal concentrations (<1.5%) and 63% at high concentrations. However, this increase in cerebral blood flow leads to a 25% increase in intracranial pressure which can be prevented with hyperventilation (66; 68). Additionally, volatile anesthetics leads to a slowing of the electroencephalogram (EEG) and a decrease in the cerebral metabolic rate for oxygen and glucose (245). Conversely, the increased blood flow, combined with decreased cerebral metabolic rate for oxygen, am offer some degrees of neuroprotection during anesthesia (66).

BLOOD BRAIN BARRIER

The blood brain barrier (BBB) is a highly regulated structure that provides a stable microenvironment for proper neuronal functioning. To accomplish this, specialized vascular endothelial cells block neurotoxic substances in the blood from reaching the brain parenchyma, contain specific transporters that allow for the influx of required nutrients and metabolic substrates, conduct extrusion of brain generated toxins, and allow for bi-directional communication between the brain and periphery (262). However, these specialized endothelial cells do not function in isolation. For proper functioning, the specialized endothelial cells of the BBB require intimate cell to cell interactions with astrocytes, pericytes, microglia, and neurons. This complex interaction between central nervous system (CNS) cell types forms a dynamic functional unit, termed the neurovascular unit (111).

The CNS is the most complex organ system of the body and is comprised of the nerves and supporting glial cells of the brain and spinal cord. The brain constitutes about 2% of the body mass, consumes about 20% of the bodies oxygen and glucose supply (173). However, because the brain has no local reserve of either oxygen or glucose, a constant supply of blood is required (126). Blood is supplied to the anterior portion of the brain by the internal carotid arteries and the posterior section is supplied by the vertebral arteries. In addition to connecting the anterior with the posterior circulation, the Circle of Willis provides for collateral circulation in case one of the sections become damaged. The venous drainage is comprised of a superficial system drainage system that drains into a deep venous system. The deep venous system then drains into either the internal or external jugular vein and then into the superior vena cava. A vast network of capillaries connect the arterial supply with the venous drainage (86).

Capillaries connect arteries to veins and are the smallest blood vessels in the body. Typically, capillaries are a single endothelial cell thick, and are responsible for supplying nutrients to the tissue while removing waste products. Capillaries can be divided into sinusoid, fenestrated, and continuous. Sinusoid capillaries are found in the liver, spleen, or bone marrow and display large pores and a discontinuous basal membrane while fenestrated capillaries are found in the intestines, pancreas, endocrine glands, and kidney glomeruli and display small pores with a continuous basal membrane. Continuous capillaries have an uninterrupted lining of endothelial cells that typically only allow small molecules to pass through intercellular gaps and are found in the skin or skeletal muscles (33; 48).

The brain also contains continuous capillaries. However, the continuous capillaries of the brain display a unique phenotype with several distinct structural and functional features not found in other tissue. Cerebral capillary endothelial cells differ from regular endothelial cells by their ability to limit passage of ions, proteins, cells, and other solutes from the blood into the CNS and vice a versa. It is these specialized characteristics that make the vascular endothelial cells of the brain capillaries the anatomical basis of the BBB (254).

The BBB localizes to all areas of the brain except for the highly specialized areas that participate in the sensing and secreting function of the neuroendocrine system. These specialized areas are termed circumventricular organs and are located at the surface of the third and fourth ventricle, laminal terminalis, subfornical organ, subcommissural organ, and the pineal gland (118). These particular areas contain specialized brain microvessels that allows neuronal tissue to sample to the vascular compartment and respond as necessary (225).

The other 99% of the brain microvascular makes up about 3% of the total brain volume and is estimated to be about 400 miles in length (254). The capillary density varies with metabolic demand, and gray matter is 3 times more metabolically active than white matter. The gray matter is made up of neuronal cell bodies, dendrites, synapses, axons, both myelinated and un-myelinated, glial cells (astrocytes, pericytes, oligodendrocytes, and microglia), and cerebral vascular cells while the white matter is mostly myelinated axons, glial cells (oligodendrocytes and microglia), and endothelial cells (254). Most of the energy consumed in the brain is used by neurons to in order to maintain resting membrane potential and for generation of action potentials (264). Thus,

the gray matter consumes about 75% of the brain's energy demand resulting in a capillary density that is 2-4 times that of white matter (264).

During pathological insults, such as hypertension, hypoxia, infection, pain, or from the direct influence of drugs such as mannitol or volatile anesthetics the complex interaction between the different cell types may become compromised leading to BBB and CNS dysfunction (30; 142; 182; 255).

History

The concept of a barrier restricting the passage of materials from the vascular system to the CNS was first described in the 19th century by the German scientist, Paul Ehrlich. He noted that when water soluble dyes were injected peripherally, the animal was stained except the brain and spinal cord. Initially, Ehrlich attributed this lack of staining to either the brain being extremely porous or lacking an affinity for the type of dye used (70). Complementary studies by Ehrlich's student, Edwin Goldman furthered the concept of a barrier separating the vascular system from the brain. In these studies, Goldman injected water-soluble dyes directly into the cerebral spinal fluid (CSF) where they stained the brain and spinal cord but not the rest of the animal (89). However, when he injected the same dyes intravascularly, the body of the animal was stained but the brain was not. The difference in staining was attributed to proprieties of the CSF and not the vascular system (89).

The existence of a physical barrier at the level of the cerebral vasculature was first hypothesized by Max Lewandowsky. Using sodium ferrocyanide or cholic acid, Lewandowsky noted minimal CNS effects when they were injected peripherally, but strong pharmacological actions when injected into the CNS. Based on these results,

Lewandowsky introduced the term “bluthirnschranke” or blood brain barrier to describe the limited effects of these toxic substances when injected into the vascular system (129).

Despite these observations, a demonstrated physical barrier separating the brain from the peripheral circulation was lacking. Additionally, if there was a physical barrier, controversy surrounded whether the capillary endothelium, astrocytic end-feet or the basal lamina or a combination of structures constituted the barrier (134). It was not until the advent of the electron microscope that these questions could begin to be resolved.

Initial electron microscope studies, however, added more controversy. One of the first electron microscope studies of the rat brain indicated that there was almost no interstitial space between neurons and glial cells. Since there was almost no interstitial space, there was also almost no interstitial fluid to stain and therefore the physical barrier properties simply resided in the lipid membranes (202).

However, subsequent electron microscope studies indicated that intravenously administered horseradish peroxidase was able to enter the space between cerebral endovascular cells but not beyond. Ultrastructure analysis indicated the presence of tight junction proteins on adjacent cells interacting to form protective intercellular barrier (201). Additionally, it was noted, that the tight junction protein barrier was bi-directional and when horseradish peroxidase was injected directly into the brain it could make its way through astrocytic end-feet and basal lamina, but was stopped from entering the vascular endothelial space by tight junctions (25).

Structure of the BBB

Brain vascular endothelial cells form the anatomical basis of the BBB. However, development of their unique characteristics requires cross talk from other glial cells. To

better understand this, non-vascularized brain tissue from quails was transplanted into the coelomic cavity of chick embryos. Additionally, mesoderm grafts from quails were transplanted into the cerebral cavity of chick embryos. Since none of these grafts were vascularized prior to implantation, determining the origin of the invading vascular structure was possible. Results indicated that neuronal tissue transplanted into the coelomic cavity developed into cerebral vascular- like structures with tight junction while the mesoderm grafts transplanted into the cerebral cavity developed into leaky gut capillaries. Thus, it was concluded that interactions of cells in the surrounding microenvironment are critical for the development of nascent vascular tissue (223).

Astrocytes

Astrocytes are star shaped cells that help support and protect neurons. Currently, there are as many as 10 different types of astrocytes and they help maintain the microenvironment of the CNS by linking neurons to cerebral vascular endothelial cells (71; 91). Their end processes provide scaffolds to guide neuronal growth, encapsulate synapses to prevent neurotransmitter escape, and cover up to 85-99% of the abluminal surface of cerebral vascular capillaries to help maintain BBB tightness (2). Additionally, astrocytic end feet contain abundant amounts of aquaporin-4, a water channel protein, important for maintaining extracellular fluid balance and brain water content (191). Finally, they provide a cellular link between neurons and cerebral vascular blood vessels. To accomplish this, astrocytes, supply energy to neurons, synthesize, release, take up, and recycle of neurotransmitters such as glutamate and gamma aminobutyric acid, maintain the BBB phenotype of endothelial cells, regulate tight junction protein expression and

assist in localizing endothelial transporters to both the luminal and abluminal sides of vascular endothelial cells(32; 91).

Microglia

Microclia account for 10-20% of the glial population and are the resident immune cells of the brain responsible for innate immunity (243). In addition to immune functions, microglia play a vital role in brain homeostasis by constantly scanning the biochemical makeup of the extracellular fluid for changes in biochemical composition and cellular debris. If changes in biochemical composition or cellular debris are encountered, microglia change from their resting shape of small cell body and long ramification to activated microglia with large cell bodies and small ramifications. Once activated, either by pathogens or aseptic injury such as ischemia or surgical trauma, microglia display two distinct phenotypes: M1 or M2 (178). Typically, the M1 phenotypes secrete pro-inflammatory mediators such as tumor necrosis alpha (TNF-a), interleukin -1B (IL-1B), IL-6 and IL-12 and therefore are considered neurotoxic. Conversely, the M2 phenotypes are considered neuroprotective because they release anti-inflammatory substances such as IL-4 and IL-10 (178).

With a smooth transition from M1 to M2 phenotypes, neuronal damage can be limited and properly repaired. However, if the M2 response is impaired or there is chronic microglia activation, a M1 phenotype response predominates. This leads to an imbalance of pro-inflammatory mediators compared to anti-inflammatory mediators and ultimately neuroinflammation. In addition to decreasing long term potentiation (LTP), the cellular mechanism of learning and memory, neuroinflammation is associated with BBB dysfunction, both of which can cause cognitive impairment (40; 178).

Pericytes

Pericytes have multiple processes that attach to the abluminal side of vascular endothelial cells and are fully embedded within the basal lamina. They cover about 20-30% of the brain capillaries and are responsible for BBB induction, maintenance of junctional integrity, producing basal lamina proteins, guiding astrocyte end feet, initiating phagocytic activity, and regulating capillary diameter (82; 172). During development, pericytes appear about 7 days before astrocytes, and are crucial for establishing the BBB properties of vascular endothelial cells (56). In pericytes deficient mice, tight junctions fail to form properly leading to increased vascular permeability, micro-hemorrhages, and embryonic lethality (137) .

In addition to releasing multiple different angiogenic growth factors during development, pericytes continue to release signals that help regulate tight junction protein expression and astrocytic end feet migration into adulthood (14). Pericytes contain multiple receptors that can sense and respond to decreased tissue oxygen levels or increased lactate levels by vasodilating and increasing local blood flow through the tissue (98; 154). Conversely, when sensing increased extracellular potassium levels, pericytes contract leading to vasoconstriction (257). Additionally, granular pericytes, which contain a high concentration of lysosomes, participate in phagocytosis of substances that make it through the BBB (208; 230).

Basal Lamina

The basal lamina is a specialized extracellular matrix that surrounds astrocytic end feet, pericytes, and endothelial cells to provide cellular attachment points and mechanical support (97; 172). Focal adhesion junctions, selectins, and integrins anchor

the basal lamina to the endothelial cells (231). The basal lamina is comprised of three distinct layers of proteins synthesized by astrocytes and endothelial cells. The inner most layer is comprised of predominately laminin 4 and 5 proteins produced by endothelial cells, while the outer most layer is predominately laminin 1 and 2 produced by astrocytes. The middle layer, is primarily collagen IV and other glycoproteins that are produced by both endothelial cells and astrocytes (5; 172). This inner layer contains multiple different signaling molecules to help maintain endothelial cell phenotype, cytoskeleton stability, and negatively charged particles to help repel the passage of negatively charged molecules (1; 34; 110).

Endothelial Cells

Specialized endothelial cells form the anatomic basis of the BBB (1). Large arteries, arterioles, and veins are formed by multiple interconnected endothelial cells while the cerebral microvessels are formed by a single monolayer of endothelial cells folded over on themselves. The cerebral microvasculature makes up about 3% of the brain tissue volume and covers a surface area of 15-25 m^2 or roughly 600 km in an adult brain (174). The intracapillary distance is 40 µm while the distance between capillaries and neurons is only about 10-20 µm (64; 214). This short distance between neurons and capillaries indicate that each neuron may have its own vascular supply (254).

Gases substances such as oxygen, carbon dioxide, and volatile anesthetics rapidly diffuse across the lipid membranes from the blood into the brain parenchyma. Additionally, small lipophilic molecules and drugs with less than 8 hydrogen bods and molecular weight of 400 Da can also cross the BBB (185). However, the presence of junctional complexes, such as tight and adheren junctions, eliminate the fenestrae

between endothelial cells and restrict the paracellular passage of larger molecules into the brain parenchyma (1; 172).

In addition to junctional complexes, specialized transporters selectively regulate the passage of substances from the blood into the brain and from the brain back to the blood (32). Efflux transporters, located on the luminal or blood side, actively remove toxins and therapeutic agents that make it into the endothelial cell cytoplasm (1; 172). Conversely, influx transporters, facilitate the transportation of glucose, amino acids, fatty acids, and vitamins from the blood into the brain (172). Some of these transporters move substances against the concentration gradient and require large amounts of energy (195). To compensate for this, cerebral vascular endothelial cells contain an increased volume of mitochondria (179).

Molecules of the BBB

Occludin

Occludin is a 65 kDa transmembrane protein that localizes to both endothelial and epithelial cells and was the first transmembrane protein identified (84). Structurally, occludin consists of four transmembrane domains, two extracellular loops, and three intracellular domains with the N-terminal and larger C-terminal present in the cytoplasm. The two extracellular loops are the same size (44-45 amino acids) but are very distinct, especially the first loop which contains more than 50% tyrosine and glycine residues (53; 78). Additionally, the two extracellular loops protrude into the intracellular space and interact with occludin molecules on adjacent endothelial cells fusing them together. For proper localization and barrier function, both extracellular loops need to be present (17). In Madin-Darby Canine Kidney (MDCK) cells, occludin transfection lacking the first

loop was able to co-localize with ZO-1 and form tight junctions, whereas, occludin lacking the second loop, or both loops, were unable to localize with ZO-1and form paracellular barriers (161). The cytoplasmic C-terminal, which is conserved among species, is essential for occludin interaction with Zonula Occludens-1 (ZO-1), F-actin, and other regulatory proteins (155). Additionally, the C-terminal is often phosphorylated by multiple different protein kinases to help regulate the function of the BBB (38; 150). The precise role of the N-terminal, however, remains unknown. Recent evidence, thought, indicates that the N-terminal interacts with Itch, a E3 ubiquitin-protein ligase that can decrease barrier function (232).

To better understand the function of occludin, multiple different in vivo and vitro studies have been conducted. Transfecting occludin into cells that lack tight junctions, such as Sf9 or L-fibrobloasts, the presence of occludin induces the formation of tight junction barriers and in increases transepithelial resistance (TEER) (242). Furthermore, over expression of occludin in MDCK cells, leads to enhanced TEER suggesting that occludin plays an important role in barrier function (17). However, in knockout mice (occludin -/-), a complex BBB phenotype emerges. In these mice, the morphology of the tight junction is intact, but thinning of the compact bone, testicular atrophy, gastric inflammation, salivary gland dysfunction, and brain calcification are noted (209).

Besides acting as a barrier protein, occludin is important in signal transduction and apoptosis (20). Recent evidence suggests that occludin is required for the extracellular transduction of interferon-gamma and tumor necrosis factor-alpha (TNF-α) signals from the periphery to the brain parenchyma (37; 151).

Claudin-5

Claudins are transmembrane tight junction proteins that are genetically distinct from occludin. They are a family of 24 different isoforms (20-27 kDa's) that form the major structural components of paracellular barriers (238). Claudins contain four transmembrane domains, two extracellular loops, and three intracellular domains with both the N and C-terminal located in the cytoplasm (120). The C-terminal is highly conserved among the different isoforms and contains a PDZ/ZO-1 (PDZ) binding domain that allows for direct interaction with ZO proteins (206). The extracellular loops can form homotrophic dimers with adjacent claudins on the same endothelial cell (loop 1) or heterotrophic dimers with claudin isoforms on adjacent endothelial cells (loop 2) where they specialize in restricting the paracellular passage of substances (121; 190; 250). Additionally, claudins, especially CL-5 play an essential role in angiogenesis.

Claudin isoforms display distinct expression and tissue specific patterns, which are currently not well understood, with most cells expressing at least two different isoforms (32; 96). This is evident by the different levels of TEER and paracellular size selectivity of barriers formed in the stomach, intestine, liver, testis, retina, ear, lungs and brain. Claudin-1, 2, 5, 11, and 12 are found in the brain with claudin-5 predominating at the BBB (138; 167).

In barrier free cells, such as CaCo-2 and fibroblasts, transfection of CL-5 contribute to the development of endothelial cell like tight junctions and increased TEER (9; 168). In a an animal model of CL-5 (-/-) mice, the blood vessels appeared normal, but allowed rapid expansion of small molecule (less than 800 kDa) into the brain parenchyma (176). Additionally, all CL-5 negative animals died within 10 hours of birth (176).

Lastly, in a model of CNS inflammation, a downregulation of CL-5 was accompanied by an increase of dye extravasation (13).

Zonula Occludens

The three zonula occludens proteins, ZO-1, ZO-2, & ZO-3 are members of the membrane-associated guanylate kinase (MAGUK) family and are responsible for the assembly, location and regulation of tight junctions (32; 77). Additionally, they coordinate the actions of multiple signaling pathways and actively interact multiple cytoskeleton proteins (18). The ZO proteins are multi-domain peptides that contain 3 PSD-95/discs-large/Zonula occludins-1 (PDZ) domains, a Src homology 3 (SH3) domain, a guanylate kinase domain (GUK), and a proline rich C terminal. Additionally, interspersed between these set domains are 6 variable unique binding (U 1-6) domains (Figure 1).

Zonula occludens-1 (ZO-1) is a 220 kD protein and was the first identified and is the most characterized of the ZO proteins (222). Through the PDZ-1 domain, ZO-1 interacts with the c-terminal of claudin molecules and is crucial for the formation of tight junctions (112). The PDZ-2 domain is important for binding of JAMs, and the other two ZO molucules (ZO-2 and ZO-3) while the U5/GK domain is crucial for occludin binding. The proline rich c-terminal, of all ZO proteins, is important for direct interaction with actin filaments (77). Multiple different signaling proteins interact with either ZO-1 or the ZO-1/ZO-2/ZO-3 complex for regulating gene expression, cell cycle progression, subcellular location of signaling proteins, and cytoplasmic protein-protein interactions(18; 92).

In multiple cellular models, loss of ZO-1 does not prevent the formation of tight junctions (158; 241). However, the assembly of tight junctions was noticeably delayed and a decrease in claudins and occludens proteins at the tight junctions was noted. This indicates the potential for ZO-2 to be substituted for ZO-1 under pathological circumstances. In mice, ZO-1 knock out proves lethal during gestation (116). In fact, no embryo is viable past E11.5 with delayed angiogenesis and embryonic growth noted (116). Additionally, massive apoptosis was noted in the neural tube and notochord. The expression and location of ZO-2/ZO-3, however, was unaltered.

Cellular levels of ZO-1 expression is linked to cellular tightness, measured by transepithelial electrical resistance (TEER) levels, or a quantitative measure for tight junction integrity. When ZO-1 expression is increased, TEER increases, and conversely, when ZO-1 expression is decreased, TEER decreases (26; 109). Pathological conditions such as ischemia, inflammatory pain, infection, stroke, or cancer can alter the expression of ZO proteins at the tight junction (18; 26). Additionally, under pathological conditions, ZO-1 can translocate from the cytoskeleton to nucleus and act as signaling molecules to relay the conditions of the tight junction conditions to the cell (93).

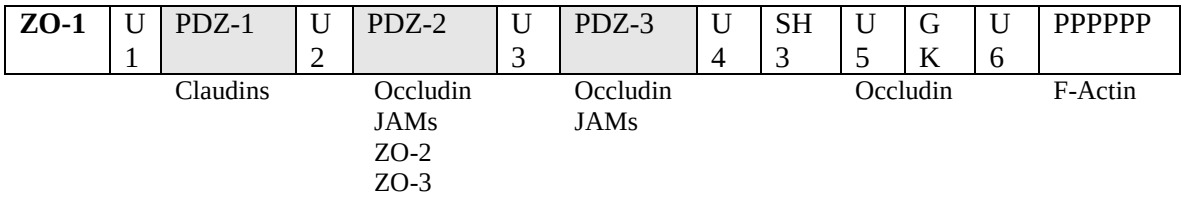

Figure 1: ZO-1 protein domains. The PDZ-1 domain primarily binds claudin molecules, PDZ-2 domains bind junctional adhesion molecules and other ZO proteins, a combination of the U5/GK domains bind occludin, and the proline rich (P) c-terminal binds actin and other cytoskeleton proteins. Multiple other proteins interact with these domains, but were not included in this figure for clarity. Adapted from: Bauer, H., Zweimueller-Mayer, J., Steinbacher, P., Lametschwandtner, A., & Bauer, H.C. The Dual Role of Zonula Occludens (ZO) Proteins. Journal of Biomedical and Biotechnology, Volume 2010, Article ID: 402593.

VOLATILE ANESTHETICS AT THE BBB

Adequate BBB function is essential for proper neuronal and glial functioning. Multiple different disease states and pharmacological agents have been show to alter normal BBB functioning. Recent evidence in multiple cellular animal models suggests that the volatile anesthetics can modify tight junction proteins and disrupt the BBB (6; 29; 263). Both indirect, through multiple different cellular pathways, and direct damaged to vascular endothelial cells are proposed mechanism responsible for tight junction modification.

Fluctuation in tight junction protein expression and permeability following exposure to isoflurane may involve alteration in several regulatory pathways. Activation of the extracellular kinase 1 and 2 (ERK 1/2) pathway, which plays an active role in regulating the expression of occludin and ZO-1, in Calu-3 epithelial cells is associated with a 15% reduction in the co-localization of occludin and ZO-1 leading to increased paracellular permeability to both small and large molecular weight substances (141). Additionally, exposure to 1.4% isoflurane for 4 hours to adult mice significantly

increased the expression of the ERK 1/2 pathway and cognitive changes through day 10 following exposure (140) .

Prolonged exposure, greater than 3 or 4 hours, can disrupt the ultrastructure of the BBB, decrease the expression of occludin, and increase the permeability to large molecule dyes for up to 24 hours (101). Additionally, as the concentration of volatile anesthetics increase, so does the extent of dye extravasation into the brain parenchyma.

To better understand toe permeability of the BBB to both small and large molecular weight substances over time, aged Sprague Dawley rats were evaluated at 30 minutes, 1, 2, and 4 hours during a single 1.5% isoflurane exposure and again at 24, 48, and 72 hours following termination of anesthesia (30). The content of NaFL in the hippocampus did not differ from controls following either a 30 minutes, or 1 or 2 hour exposure. However, after a 4 hour exposure, significant amounts of NaFL was noted in the hippocampus where it remained elevated for at least 24 hours before returning to normal. Additionally, following the 4 hour exposure, a significant number of IgG antibodies were noted in the hippocampus where they remained for 24 hours (29).

In addition to dye permeability studies, transmission electron microscopy can be utilized to evaluate the ultrastructure of the BBB. Following a 2 hour exposure, minimal collapse of the basal lamina was noted (29; 30; 218). However, following either a 3 or 4 hour exposure to 1.5% isoflurane, the basal lamina collapses, astrocytic end feet are swollen, tight junctions expression decreases leading to identifiable gaps between adjacent endothelial cells and edema (29; 101; 218). Over the next 48 to 72 hours, however, the basal lamina recovers and tight junction proteins reappear and close the gaps between endothelial cells.

Overall, anesthesia exposure times up to 2 hours display minimal alterations in the structure and function of the BBB that are quickly repaired. However, exposure times greater than 3 hours is associated with alterations in the ultrastructure of the BBB evidenced by decreased expression of occludin and increased permeability to both small and large molecular weight dyes for at least 24 hours(30; 218; 263). Currently, there is no evidence on the effects of multiple brief exposures to isoflurane on the structure and function of the BBB. Therefore, the purpose of this study is to evaluate the expression of tight junction proteins along with the permeability of the BBB following multiple brief exposures to the volatile anesthetic isoflurane.

SPECIFIC AIMS

The long term goal of this research is to delineate the structural and functional changes in the BBB following repeated exposures to isoflurane in order to provide better insight into the development of best clinical practices for patients that require multiple operations. The objective of this dissertation is to evaluate the expression and location of tight junction proteins as well as the permeability of the BBB following multiple exposures to isoflurane. The central hypothesis is that multiple exposures will decrease the expression of occludin, CL-5, and ZO-1 thereby increasing the paracellular permeability of the BBB to injected dextrans. We plan to test this hypothesis by pursing the following specific aims:

Specific Aim:

To identify changes in the expression and location of tight junction proteins and to evaluate the permeability of the BBB following a single prolonged (4 hour) or multiple brief (2 hour) exposures to isoflurane.

Hypotheses:

H1: Animals exposed to a single prolonged or multiple brief exposures to isoflurane will demonstrate a reduction in the expression of occludin, CL-5, and ZO-1 at 4 and 24 hours following exposure.

H2: Animals exposed to a single prolonged or multiple brief exposure to isoflurane will display alterations in the location of occludin, CL-5, and ZO-1 at 4 and 24 hours following exposure.

H3: Animals exposed to a single prolonged or multiple brief exposure to isoflurane will exhibit increased BBB permeability to high molecular weight dextrans at 4 and 24 hours following exposure.

This research will be utilized to inform best clinical practice models for anesthetic drug choice to enhance recovery and prevent complications for wounded warriors injured during combat operations and civilians in need of multiple operations following trauma.

CHAPTER 2: Background and Significance

INTRODUCTION

Wounding Pattern

Since 2011, over 50,000 US service members have been wounded in action with 60-70% sustaining musculoskeletal trauma (63). Damage from exploding ordnances such as bombs, grenades, land mines, and artillery shells predominate accounting for 70-80% of the injuries (63; 181). However, more personnel are surviving the initial blast because of improved body armor and acute trauma care (87). While the increased use of body armor and other protective equipment reduces the effects of blast to the chest and abdomen, injuries to the extremities remains a serious problem. Wounding patterns indicate that a high percentage of combatants' suffer a high percentage of either upper extremity (47.3%) or lower extremity (43.2%) injuries while 27% of casualties' sustain both an upper and lower extremity injury (63).

Those with extremity injuries did not differ from other types of injures based on age, gender, military rank, or branch of service. The mean age of the combat wounded is 24 ± 5 years with junior enlisted (E1-E4) predominating (41.6%) (76). Additionally, males make up 99% of the casualties' (76). Those with extremity injuries were more likely to be seriously wounded, require a medivac, receive an operative procedure at a forward deployed field hospital, and suffer from higher incidences of postoperative complications (63).

The explosive blast contains two distinct phases, a high pressure shock wave followed by a blast wind (160). Injury patterns are characterized as primary (direct effects of over and under pressurization), secondary (penetrating injuries from flying objects),

tertiary (being displaced into objects), or quaternary (damage from burns or smoke) (59; 197). However, these different injury mechanisms don't occur in isolation and can create complex injury pattern involving many different body systems. The complexity of IED blast injuries is highlighted by the number of repeated operations required to prepare the wound for definitive reconstruction.

Surgical Repair

Treating massive musculoskeletal injuries has evolved over the past 15 years of military conflict. Damage control surgery, or brief repeated surgical procedures, to control hemorrhage, remove major contaminants, and stabilize fractures before definitive repair and reconstruction is now standard practice (88; 122). Prolonged surgical operations in acute trauma patients can result in hypothermia, acidosis, and coagulopathy leading to adverse outcomes (103). The Bethesda Limb Salvage protocol was designed to standardize the care of these complex injuries. This protocol features multiple repeated marginal debridement's to remove as much debris and necrotic tissue as possible while minimizing damage to healthy tissue (88). Prior to arrival at Walter Reed National Military Medical Center, the median number of operations per patient was 2.6 (range 1-6) (136). After arrival, the average number of operations from admission to definitive closure was 6 (range 3-22) for upper extremity injuries and 5 (range 2-13) for lower extremity injuries while the average time to definitive reconstruction was 24 days (range 15-62) (122; 123).

Each of these brief operations require exposure to some form of anesthesia, with most received a volatile anesthetic such as isoflurane (248). Volatile anesthetics create a complex state of unconsciousness, amnesia, analgesia, and immobility by altering

multiple different cellular pathways within the brain and spinal cord (27). Volatile anesthetics are commonly chosen because of their ease of use, ready availability, lack of major side effects, and their ability to be quickly eliminated from the body following discontinuation (143; 216). However, recent evidence from multiple different cellular and animal models suggest that even a single exposure to volatile anesthetics can institute molecular changes that ultimately lead to alterations in the structure and function of the blood brain barrier (BBB) and eventually alterations in cognitive functioning (30; 101).

Postoperative Cognitive Dysfunction

Cognitive changes following anesthesia exposure is termed postoperative cognitive dysfunction (POCD) and can affect up to 35% of middle aged adults acutely (114; 164; 165). Risk factors for POCD include increased duration of anesthesia exposure, severity of the surgical wound, advanced age (>60), low education attainment, and multiple exposures to anesthesia (164; 203). Manifestations of POCD include alterations in processing speed, decreased attention span, and loss of memory functions leading to impairments of daily functioning, loss of independence, premature departure from the job market, increased dependence on social programs, and increased mortality (4; 221). Thus, POCD not only poses a substantial burden on individuals and their families, it poses a significant burden on communities and society as well. The exact neuropathological basis of POCD, however, remains a mystery. Several different models have been developed to clarify the effects of anesthesia, surgery, and the combined effects of anesthesia and surgery on the structure and function of the BBB and cellular pathways that can potentially lead to alterations in cognitive function. This study will

utilize a rodent model to elucidate the effects of anesthesia, specifically repeated anesthesia exposures, on the structure and function of the BBB.

Blood Brain Barrier

The concept of a physical barrier separating the peripheral circulation from the central nervous system (CNS) was conceived from dye studies in the late 19th century. Water soluble blue dyes injected into the peripheral circulation failed to stain the brain and spinal cord. Conversely, when the same blue dye was injected into the spinal fluid, the brain and spinal cord were stained blue while the rest of the internal organs were not. The results of these two studies introduced the concept of a physical barrier possibly separating the brain and spinal cord from the rest of the body (72; 172; 202).

Initially, defining the exact anatomical basis of the BBB provided much controversy. Preliminary evaluation of the vascular bed in the cerebral cortex of rats failed to identify an interstitial space between adjacent endothelial cells, leading to the conclusion that a true physical barrier between cells did not actually exist. It was hypothesized that the transfusion barrier resisted with the cellular membrane of each individual endothelial cell (156). Further evaluation noted that horseradish peroxidase, a small enzymatically active protein, remains confined to the vessel lumen within the brain, but freely moved into the interstitial space between adjacent muscle cells (50). Ultrastructural analysis noted that the capillaries in the periphery exhibited gaps between adjacent endothelial cells allowing for movement from the vascular space to the interstitial space while capillaries in the brain displayed overlapping endothelial cells creating tight junction between adjacent endothelial cells thereby limiting the paracellular

passage of substance into the brain (201). This evidence establishes the special properties displayed by the cerebral vascular endothelial cells as the anatomical basis of the BBB.

Cerebral vascular endothelial cells differ from the peripheral endothelial cells by the presence of tight junctions proteins at the apical membrane, minimal pinocytic activity, lack of fenestrations, few cytoplasmic vesicles, increased concentrations of mitochondria, and dedicated transport systems to extrude toxic substances generated in the brain while simultaneously admitting essential nutrients and oxygen (80; 179; 201; 215; 266). These specialized structures allow the BBB to precisely regulate the passage of ions, proteins, immune cells and other solutes from the blood into the CNS while rapidly eliminating metabolic waste products, thereby creating a stable microenvironment for optimal neuronal functioning (100). The dedicated transport systems of influx and efflux transporters create a biochemical barrier while the tight junctions create a physical barrier (1).

Tight junction proteins are complexes of multiple transmembrane proteins that link adjacent endothelial cells together and several cytoplasmic scaffolding proteins that link the transmembrane proteins to the actin components of the cell. Junctional adhesion molecules (JAM), the claudin family, and occludin make up the transmembrane proteins while the zonula occludens (ZO) family of proteins make up the cytoplasmic scaffolding proteins (1; 100). In addition to a physical barrier, tight junction proteins are involved in fencing and signaling functions. As a fence, the endothelial cells limit lateral diffusion and movement of the membrane while barrier function involves selectively limiting paracellular passage between cells (187).

Structurally, the JAMs have a single transmembrane domain that forms a disulfide bond with JAMs on adjacent endothelial cells (19). Functionally, JAMs promote the localization of occludin to the cellular membrane and aid in the paracellular transfer of leukocytes from the blood into the brain parenchyma (19; 187). The claudin family of tight junction proteins is responsible for forming the primary seal of the BBB (85). Mice born with a claudin-5 deficiency display an increased permeability to substances under 800 kDa and die within 10 hours of birth (176). Currently, there are over 24 different isoforms identified with, claudin-1 and claudi-5 being primarily expressed within the CNS (244). The claudin family displays four transmembrane domains, which interact homotrophically with claudin molecules expressed on adjacent endothelial cells, and two end terminals that reside within the cytoplasm and complex with ZO molecules (85; 237). Additionally, in experimental model of autoimmune encephalomyelitis, downregulation of claudin molecules is associated with increased trafficking of immune cells into the brain and neuroinflammation (74).

Like the claudin family, occludin is a four transmembrane protein with cytoplasmic tails that is highly expressed in cerebral endothelial cells (105). The expression of occludin displays a distinct staining pattern along the margins of endothelial cells (100). The cytoplasmic portion of occludin express multiple sites of phosphorylation that function to regulate permeability to different substances based on response to multiple external and internal signaling pathways. Experiments in occludin deficient or reduced mice reveal that the presence of occludin is not responsible for the formation of the BBB but can lead to growth retardation and increased mineral deposits in the brain (209; 226). However, after the BBB is formed, alterations in expression or

location of occludin can be used as an early indicator of BBB dysfunction (62). Additionally, chronic alteration in expression and location of occludin is associated with chronic neurological diseases live Alzheimer's and vascular cognitive impairment (265).

Zonula occludens, especially ZO-1 and ZO-2, are widely distributed throughout the brain and anchor both transmembrane proteins (occludin and claudin-5) to the endothelial cell cytoskeleton (241). Besides their anchoring roles, zonula occludens are essential for tight junction formation. In cultured epithelial cells that did not express ZO-1 or ZO-2, tight junctions failed to form despite the presence of claudins (240; 241). Deletions of ZO-1 and ZO-2 proteins in mice lead to early embryonic death (258). Additionally, zonula occludens are key signaling proteins for growth, development, and danger processing. Dissociation of zonula occludens from the tight junction complex increases the permeability of the BBB (3; 81). Normally, ZO-1 is found along the entire perimeter of the endothelial cell; however, following injury, ZO-1 dissociates from the tight junctions and moves toward the nucleus increasing BBB permeability (81).

Volatile Anesthetics

Recent evidence indicates that prolonged exposures to volatile anesthetics may alter the structure and function of the BBB an ultimately lead to cognitive dysfunction (30; 140). Volatile anesthetics, like isoflurane, are commonly used in basic research and clinical practice to induce a reversible loss of consciousness, amnesia, analgesia, and produce immobility(27). Volatile anesthetics can be considered "dirty drugs" because they interact with multiple pathways in the brain, spinal cord, and various other organ systems. Several lines of evidence indicate that volatile anesthetics enhance the inhibitory ligand gated ion channels for gamma-aminobutyric acid (GABA) and glycine, while

inhibiting the excitatory ligand gated ion channels for glutamate, serotonin, histamine, and acetylcholine (153; 180; 205). Additionally, volatile anesthetics can alter the conduction of voltage gated potassium, sodium, and calcium channels (180; 205). The potency of volatile anesthetics is measured by the brain concentration required to produce immobility to surgical stimuli with a lower concentration being considered more potent. Since it is impractical to measure actual brain concentration, median end tidal alveolar concentration, or the concentration of anesthetic agent present during peak exhalation is utilized.

Volatile Anesthetic: Characteristics

Minimum alveolar concentration (MAC) is the median end tidal concentration of a volatile anesthetic that prevents movement in 50% of a population (human or animals) to surgical incision (69). In rodent models, the loss of righting reflex and response to tail clamp is utilized to determine MAC values (252). The MAC of isoflurane in adult male Sprague Dawley rats is 1.52% ± 0.12% (184). Lower anesthetic concentrations abolish explicit memory and the ability to respond to commands while increasing concentrations prevent movement to pain and blunt autonomic responses (252).

Volatile Anesthetics: Gene Alterations

Initially, volatile anesthetics were thought to be rapidly eliminated from the CNS upon discontinuation, allowing for gross evaluation of cognitive process following exposure (143; 144). However, recent evidence indicates that anesthesia exposure may have lingering effects. In adult Sprague Dawley rats, Rimipril noticed alterations in 269 unique genes for up to 6 hours following a single 15 minute exposure to 2% isoflurane

(198). Additionally, a 4 hour exposure to 1.2% isoflurane with 70% nitrous oxide altered 297 genes in the hippocampus of Fisher -344 rats for over 48 hours (52).

Volatile Anesthetics: Hippocampus

The hippocampus is a structure located in the temporal horn and plays a key role in the formation of new memories and retrieval of well learned information in both humans and animals (200; 260). Damage to the hippocampus results in the inability to form new autobiographical memories or to retrieve fact based memories such as ability to recall the what, when, and where of certain personal experiences (15; 46; 267). The hippocampus appears to be very sensitive to damage caused by exposure to anesthetics, especially volatile anesthetics (135).

Volatile Anesthetics: Drug Combinations

Typically, volatile anesthetics are not administered in isolation. Following a 6 hour exposure to the combination of midazolam, isoflurane, and nitrous oxide, infant Sprague-Dawley rats displayed widespread apoptosis, hippocampal synaptic dysfunction, and persistent learning and memory impairments (113). The evaluation of each anesthetic agent separately yielded mixed results. Increasing doses of midazolam or nitrous oxide showed no difference in level of apoptotic markers when compared to control animals. However, increasing concentrations of isoflurane (0.75%, 1%, or 1.5%) for 6 hours exhibited increasing amounts of degeneration in the cortex, hypothalamus, and hippocampus (113). The animals exposed to the combination of anesthetics as infants showed persistent deficits in learning and memory tasks into adulthood, indicating that even a simple exposure to anesthesia can have a long lasting effect (113). Additionally,

Lin and colleges noted that a single exposure to 1.2% isoflurane for 2 hours in adult rats displayed a decrease in hippocampal dependent memory for up to 2 weeks (135).

Volatile Anesthetics: Repeated Exposures

Compared to a single brief anesthesia exposure, prolonged exposures or multiple brief exposures display a greater amount of neuronal damage and memory impairment. A recent study by Amrock noted that a single 2 hour exposure to one MAC of sevoflurane did not alter synaptic density in the hippocampus. However, animals exposed to either a single 6 hour or 3 brief 2 hour exposures 72 hours apart displayed widespread synaptic loss in the hippocampus with multiple exposure group displaying the greatest decrease in mean density (10). Using the same repeated exposure paradigm, Murphy noted that infant rats exposed to 1.8% isoflurane for 2 hours a day on day 7, 10, and 13 displayed persistent memory lasting into adulthood (171). Conversely, the single exposure group paradoxically displayed an improvement in spatial memory function (171). Additionally, mice exposed to either low dose (1.5%) or high (2.5%) concentrations of sevoflurane for 1 hour every month for 5 months demonstrated increased hippocampal tau phosphorylation leading to persistent cognitive impairment whereas the single exposure failed to display an increase in tau proteins or alterations in learning or memory (125). Using a shorter time interval between anesthesia exposures, Shen noted that a 2 hour exposure to 1% sevoflurane 3 times a day led to alterations in learning and memory in both infant and adult Sprague Dawley rats and increasing the number of exposures exacerbated the effects (217). Furthermore, Shen noted that increasing the concentration of anesthesia while maintaining a stable exposure time could also lead to memory impairments (217). Taken together, these results indicate that a

single brief exposure to low concentrations of volatile anesthetics display minimal effects on hippocampal structure and function while increasing concentrations or exposure times can alter cognitive function and that multiple exposures can exacerbate these effects.

Volatile Anesthetics: Blood Brain Barrier

In addition to altering hippocampal function, recent evidence suggests that exposure to volatile anesthetics can also alter the structure and function of the BBB, especially in the hippocampus (101; 133). A simple study by Morrisroe showed that a simple 10 minute exposure to isoflurane in adult mice exhibited significant extravasation of Evans blue dye into the thalamus and hippocampus of adult mice (169). Evans blue dye (EBD) is an azo dye that readily and highly binds to serum albumin and under normal conditions cannot pass through the BBB to enter the brain parenchyma. Therefore, the presence of dye within the brain parenchyma indicates a compromise in the structure and function of the blood brain barrier. Increasing the exposure time to one hour significantly increased the amount of EBD in the amygdala and hypothalamus regions. However, within an hour of discontinuing the anesthetic, all the affected regions returned to baseline and were indistinguishable from control animals (12; 169). To better understand changes in the permeability of the BBB to both small and large molecular weight substances over time, aged Sprague Dawley rats were evaluated at 30 minutes, 1, 2, and 4 hours during a 1.5% isoflurane and then evaluated at 24, 48, and 72 hours following termination of anesthesia. (Ref) The content of NaFl, a small sodium fluorescent tracer, found in the hippocampus at 30 minutes, 1 hour, and 2 hours during anesthesia did not differ from control (30). However, at 4 hours, a significant amount of NaFl was noted in the hippocampus where it remained elevated for 24 hours before

returning to normal by 72 hours. The expression of immunoglobulin G (IgG) antibody in the hippocampus was utilized as a marker for permeability to large molecular weight substances (30). Under normal physiological conditions, an intact BBB prevents the passage of IgG antibodies (150 kDa) from the periphery into the CNS. However, if the BBB is damaged, IgG molecules can pass from the blood into the brain parenchyma. At the conclusion of the 4 hour anesthetic a significant number of IgG antibodies were noted in the hippocampus. By 24 hours, however, minimal amounts of IgG antibodies were noted in the hippocampus (30). In addition to increased duration of exposure, increasing concentration of volatile anesthetics has been shown to alter the permeability of the BBB in distinct brain regions. Utilizing a cat model of exposure, Tetrault noted that low doses of isoflurane (1%) increased the amount of EBD in the thalamus while high doses of isoflurane (3%) over the same period of time increased the expression of EBD into the cerebral cortex and thalamus (229).

In addition to permeability studies, transmission electron microscopy can be used to evaluate the ultrastructure of the BBB. A study by Cao examined the ultrastructure of the BBB in the hippocampus of aged rats immediately following either a 2 or 4 hour exposure to 1.5% isoflurane (30) Following a 2 hour exposure, minimal collapse of the basal lamina was noted. The basal lamina is an extracellular matrix that plays a key role in anchoring adjacent and regulating the expression of tight junction proteins. After a 4 hour exposure to 1.5% isoflurane, the basal lamina was completely collapses leading to angioedema, swollen astrocyte end feet, and a decrease in tight junction protein expression leading to a clear identifiable gap between adjacent cells. Over the next 48 to 72 hours, however, the basal lamina recovered and tight junctions reappeared (30).

Additionally, a separate study by He and colleagues noted the BBB remained open to large molecules for at least 24 hours following a single 2 hour exposure to 2% isoflurane (101).

A reduction in the expression of occludin is associated with increase permeability to both small and large molecular weight substances and new data indicates that exposure to isoflurane can alter the expression of occludin (263). To better understand the effects of different concentrations of isoflurane on the expression occludin, human brain vascular endothelial cells (HBVEC) were exposed to 0, 0.5, 1, 1.5, 2 or 2.5% isoflurane for either 3 or 6 hours. Cells exposed to 0, 0.5, or 1% displayed no changes in the mRNA or protein level of occludin while 2 and 2.5 % for 3 or 6 hours significantly decreased the mRNA levels of occludin (263). Additionally, the decrease in occludin expression was associated with an increase in permeability to fluorescein isothiocyanate (FITC) dextran at both 3 and 6 hours following the two hour exposure (263). However, the exact molecular mechanism by which isoflurane exposure decreases the expression of tight junction proteins remains unidentified.

To better understand if alterations in BBB structure and function was common to volatile anesthetics as a class, or only related to isoflurane exposure, Acharya exposed young (3-5 month), middle aged (10-12 month) and elderly (17-19 month) to either sevoflurane or isoflurane for 3 hours. Using scanning electron microscopy, control animals displayed distinct lines of tight junction folds, cytoplasmic protrusions parallel to long axis of vessel and microvilli along the luminal surface. However, following a single 3 hour exposure to either sevoflurane (1-3%) or isoflurane (1-3%) discrete holes in the tight junction folds, destruction of cytoplasmic protrusions, and loss of microvilli were

noted (6). To assess function integrity, extravasation of IgG antibodies into the brain parenchyma of the cerebral cortex was evaluated. In control animals, no IgG antibodies were noted in the brain tissue around cerebral vessels (6). On the other hand, animals exposed either sevoflurane or isoflurane for 3 hours, displayed extravasated IgG molecules around cerebral vessels. Additionally, it was noted, that older animals, and animals exposed to sevoflurane displayed greater extravasation than younger animals and animals exposed to isoflurane. Finally, it was shown that exposure to either sevoflurane or isoflurane can directly induce brain vascular endothelial cell death (6).

Volatile Anesthetics: Cellular Pathways and Blood Brain Barrier

In addition to altering protein expression, volatile anesthetics can modify extra and intracellular pathways that can arbitrate cellular function. Recently, isoflurane has been shown to active the extracellular kinase 1 and 2 (ERK1/2) pathway (131). The ERK1/2 signaling pathway plays a key role in cell proliferation, differentiation, and adaption through activation of intracellular kinases and phosphorylation of proteins altering protein-protein interactions (261). One of the protein-protein interaction regulated by ERK 1/2 is that of ZO-1 and occludin (36; 141). In human brain endothelial cells, increased levels of phosphorylated ERK 1/2 is associated with decreased expression of occludin and ZO-1 along with increased paracellular permeability to small (4 kDa) and medium (40 kDa) sized dextran's (141). Conversely, over-expression of ZO-1 and occludin, or down-regulation of the ERK 1/2 pathway reduced paracellular permeability to both small and medium weight dextran's. Comparing the loss of occludin to the loss of ZO-1 on paracellular permeability, it was noted that decreases or increases in the levels of ZO-1 exhibited a stronger effect than a similar increase or decrease of occludin

(141). In addition to decreasing the expression of occludin and ZO-1, activation of the ERK 1/2 pathway can alter the co-localization of occludin and ZO-1. Normal cells how co-localization of occludin and ZO-1 at cites of cell to cell contact. Following activation of the ERK 1/2 pathway, Calu-3 epithelial cells display a 15% reduction in the co-localization of occludin and ZO-1 compared to controls with this reduction resulting in increased paracellular conductance (189). Finally, activation of the ERK 1/2 pathway is associated with cognitive changes in adult mice. Young adult mice (C57BL/6) exposed to 1.4% isoflurane for 4 hours displayed alteration in hippocampal dependent learning and memory for up to 10 days (140).

Besides the ERK 1/2 pathway, isoflurane has recently been shown to up-regulate hypoxia inducible factor 1α (HIF-1α). In Hep3B cells exposed to varying concentrations of isoflurane for 6 hours, it was noted that low concentrations of isoflurane (0 – 1%) displayed minimal increases in HIF-1α protein while higher concentrations (2-4%) exhibited significant increases in HIF-1α protein accumulations (130). Since a 2% concentration showed a significant increase in HIF-1α, Hep3B cells were then exposed to 2% for increasing lengths of time. Stimulation for 0-2 hours displayed minimal increases in HIF-1α protein levels while exposure for 4, 6, or 8 hours revealed significant increases in HIF-1α protein levels (130). Additionally, since HIF-1α is a master transcription factor in response to hypoxia, down-stream targets were evaluated. A 2 hour exposure to 2% isoflurane revealed an increase in mRNA levels of vascular endothelial growth factor (VEGF), heme oxidase, and inducible nitrous oxide synthase which are important for energy metabolism and angiogenesis (130).

CONCLUSION

These results parallel the results of simple anesthesia exposure. Exposure to low levels of anesthesia is associated with minimal damage to the structure and function of the BBB, and what damage is done is rapidly repaired. However, exposure to one MAC of anesthesia, or above, leads increased BBB permeability by altering the expression or location of ZO-1. In regards to exposure, times up to 2 hours display minimal alteration in the structure and function of the BBB. However, exposure times greater than 3 hours are associated with alterations in the expression and location of occludin and ZO-1 leading to increased paracellular permeability to large molecular weight substances for 24 hours. Likewise, increasing concentration or prolonged exposure to isoflurane can lead to hippocampal dysfunction and cognitive impairment. Compared to a single anesthetic, multiple exposures can exacerbate the cognitive impairment leading to long lasting changes. There is little evidence on the effects of multiple exposures to isoflurane on the structure and function of the BBB. Therefore, the purpose of this dissertation is to evaluate the permeability of the BBB, as well as the expression of CL-5, occludin, and ZO-1 following multiple exposures to isoflurane.

CHAPTER 3: Methods

RESEARCH DESIGN

A randomized, posttest only, comparison group design will be utilized to accomplish this aim. A total of 81 animals were randomly divided into one of 4 different groups: 1) Non-exposure control (NEC); 2) 1 Prolonged Exposure (1PE); 3) 1 Brief Exposure (1BE); 4) 5 Brief Exposures (5BE). Each of the groups were then split into either a western blot/polymerase chain reaction (WB/PCR) or immunohistochemistry (IHC) section. Each of the sections were then further subdivide cohorts that were terminated either 4 or 24 hours following the last anesthesia exposure (Table 1).

Table 1: Animal groups, sections, and cohorts.

	SECTIONS			
	Western Blot/qPCR		***Immunohistochemistry***	
GROUPS	*4 HR Cohort*	*24 HR Cohort*	*4 HR Cohort*	*24 Cohort*
1. Control (n=15)	5		5	5
2. 1 PE (n=21)	5	5	5	6
3. 1 BE (n=21)	5	5	5	6
4. 5 BE (n=24)	5	5	6	8

Power Analysis

A sample size of 5 animals per section will have 80% power to detect a difference of two standard deviations among groups, based on a one-way ANOVA, with a 5% two sided significance level. This is based on the established effect size of 5% (SD = 10%) reduction in occludin expression in the hippocampus of elderly rates following a four hour exposure to 1.5% isoflurane. G*Power software (Brunsbutter, Germany) was used to calculate statistical power.

Animal Model

All experimental procedures were approved by the Uniformed Services University of the Health Sciences (USUHS) Institutional Animal Care and Use

Committee (GSN-15-958), and were in compliance with all Department of Defense directives for use of laboratory animals (DoD Directive 3216.1). Additionally, the Center for Laboratory Animal Medicine (LAM) at USUHS is fully accredited with the Association for the Assessment and Accreditation of Laboratory Animal Care (AAALAC).

Adult, male Sprague Dawley rats at 8-10 weeks of age (356 g ± 60.25 g) were purchased from Taconic Farms (Albany, New York) and used in all experiments. Upon arrival to LAM facility at USUHS, rats were pair housed in standard clear polycarbonate cages (22 x 12.5 x 8 inches) with Envigo Teklad Laboratory Aspen Bedding # 7093 (Frederick, MD) and a Bio-Serv nylabone (Flemington, NJ) for environmental enrichment. Animals were allowed free access to Envigo Teklad Global 18% protein diet (Frederick, MD) and fresh tap water. All animals were housed as cohorts in a single room under 12-hour light cycles (lights on 6AM - 6 PM) with constant temperature (22^{o}C ± 4^{o}C) and humidity (30-70%). Animals were allowed to acclimate to the LAM environment for 5 days prior to beginning any experiment.

ANESTHESIA EXPOSURE

Overview

Non-exposure control animals will be exposed to 100% oxygen for 5 minutes to simulate the experience of being placed into the anesthesia induction chamber. The 1PE group will receive a single 4-hour exposure to 1.5% isoflurane in 100% oxygen while 5BE group will receive a five 2-hour exposure to 1.5% isoflurane. Repeated exposures will occur about the same time each day with 24 hours between exposures (Table 2).

Table 2. Animal Exposure Timeline

Group	Acclimation					Exposure					Data Points	
	-5	-4	-3	-2	-1	1	2	3	4	5	4 HR	24 HR
Control (n=15)	X	X	X	X	X						10	5
1 PE (n=21)	X	X	X	X	X	X					10	11
1BE (n=21)	X	X	X	X	X	X					10	11
5BE (n=24)	X	X	X	X	X	X	X	X	X	X	10	14

Control Group

Animals were removed from their home cage and placed into a clear acrylic anesthesia induction chamber (3.75 x 9.00 x 3.75 inches; VetEquip, Livermore, CA) flushed with 100% oxygen at 5L/minute to simulate the stress of anesthesia induction. Following the exposure, animals were placed into a small polyacrylic mouse cage (11.5 X 7.5 X 5 inch) set on top of a K & H Small Animal Heating Pad (Colorado Springs, CO) for 15 minutes to simulate recovery from anesthesia before being returned to their home cage.

Single Exposure Groups

Animals were removed from their home cage and placed into a clear acrylic anesthesia induction chamber (3.75 x 9.00 x 3.75 inches; VetEquip, Livermore, CA) flushed with 5% isoflurane in 100% oxygen at 5L/minute to rapidly induce anesthesia. Upon loss of righting reflex, the concentration of isoflurane was decreased to 2% for 3 minutes to insure adequate induction of anesthesia. Animals were then moved from the induction chamber and placed on a Kent Scientific SurgiSuite System platform (Torrington, CT) where they were attached to a World Precision Instruments Anesthesia Facemask (Sarasota, FL). Placement into the anesthesia facemask constituted anesthesia start time. Once the animal was placed in the facemask, isoflurane concentration was decreased to 1.5% and the flow of 100% oxygen was reduced to 1L/min. At the

conclusion of the anesthetic, either 2 hours or 4 hours, the animal was placed in a small polyacrylic mouse cage (11.5 X 7.5 X 5 inch) set on top of a K & H Small Animal Heating Pad (Colorado Springs, CO) until fully recovered (return of righting reflexes).

Repeated Brief Exposures

The same anesthesia exposure procedures for the single prolonged and brief anesthesia groups applied to the multiple brief exposure groups. Repeated exposures were completed at about the same time each day with 24 hours between exposures. Animals that require multiple exposures will be returned to the LAM between exposures.

Monitoring Physiological Parameters

Isoflurane alters normal cerebral, cardiovascular, respiratory, and metabolic parameters. Understanding these changes in physiological parameters is essential in distinguishing between the pharmacological effects of isoflurane on the BBB from changes causes in physiological parameters.

Weight

Animals will be weighed immediately prior to any anesthesia exposure or procedure. A small lidded box was placed on a calibrated electronic scale (VWR, Randor, PA) and zeroed. Animals were then placed inside the small box and then onto the scale. Weight, to the nearest hundredth of a gram, was recorded.

Agent Monitoring

A Drager Vamos (Telford, PA) infrared anesthesia gas sensor was attached to the anesthesia facemask and was used to continuously monitor inspired and expired concentrations of isoflurane. Additionally, the fraction of inspired and expired oxygen

(O2) and carbon dioxide (CO2) was measured. Concentrations were recorded every 15 minutes throughout the anesthetic.

Vital Signs

A PhysioSuite MouseSTAT Pulse Oximeter (Torrington, CT) was attached to the hind paw to continuously monitor arterial oxygen saturation (Sa02), heart rate (HR), and respiratory rate (RR). Temperature was maintained between 36.5ºC and 37.5ºC with a PhysioSuite RightTemp (Torrington, CT) sensor connected to a servo controlled heating pad. Heart rate, RR, and temperature values were recorded on the anesthesia record every 15 minutes starting from placement into the anesthesia facemask.

Systolic, diastolic, and mean arterial blood pressure were measured every 30 minutes, starting at the 15-minute mark, with a CODA Non-Invasive Blood Pressure Monitor (Torrington, CT) system attached to the rodent tail. The CODA system uses a differential pressure transducer to measure return of tail blood flow and volume following occlusion. Tail blood flow and volume can vary greatly with temperature. Therefore, to ensure adequate tail temperature for accurate blood pressure measurements, the tail was placed between layers of a Medline Protection Plus Pad (Mundelein, IL) with a HotHands Hand Warmer (Dalton, GA) placed in the bottom layer. A ThermoWorks TW2 (America Fork, UT) infrared thermometer was used to ensure that the tail temperature was within 0.5ºC of the core body temperature.

The CODA system is comprised of an occlusion cuff and volume pressure recorder. The occlusion cuff is placed at the base of the tail and the volume pressure recorder is positioned just below occlusion cuff. For measurement, the occlusion cuff is inflated to suspend all tail blood flow and then slowly deflates over 15 seconds. As the

occlusion cuff is deflated, the increase in tail blood flow and volume is sensed by the volume pressure recorder and displayed as SBP, DBP, and MAP. Blood pressure values were recorded on the anesthesia record every 30 minutes starting at the 15 minute mark.

Arterial Blood Gas and Lactate

During the final 15 minutes of the anesthetic, an arterial blood gas sample was obtained from the ventral tail artery. The animal was placed in the dorsal recumbent position and the tail was cleansed with a 70% isopropyl alcohol swab (BD, Franklin Lakes, NJ). To prevent microclots from forming in the syringe, 200 µl of a 10 Unit/mL Heparin Lock Flush Solution (Fresenius Kabi, Schaumburg, IL) was aspirated into a BD 1 ml Luer-Lok syringe (Franklin Lakes, NJ) attached to a 25G, 1inch, Precision Glide needle (BD, Franklin Lakes, NJ) and then expectorated to leave just the needle full of the heparin solution. The 25G needle was advanced into the ventral tail artery to obtain about 150 µl of arterial blood with 95 µl being immediately transferred to an Abaxis VetScan CG4+ i-STAT cartridge (Union City, CA) to evaluate pH, PaC02 (mmHG), Pa02 mmHg), HCO3 (mmol/L), tCO2 (mmol/L), base-excess (mmol/L), Sa02 (%), and lactate (mmol/L) levels.

A VetScan i-STAT 1 handheld analyzer (Union City, CA) was utilized to read the CG4+ i-STAT cartridge. To evaluate internal function and quality control the i-STAT monitor, an i-STAT Electric Simulator check was conducted weekly. Additionally, to maintain consistency, the i-STAT system software was updated as required by the manufacture (Abaxis Vet Scan, Union City, CA).

Blood Glucose

Random plasma glucose was measured at the conclusion of the anesthetic. A 0.3 µl sample of arterial blood was placed on a FreeStyle Lite Glucose Test Strip (Abbot Park, IL) and placed into the FreeStyle Lite glucometer (Abbot Park, IL). Quality control checks utilizing FreeStyle High and Low Control Solution (Abbot Park, IL) were conducted monthly.

Hemoglobin

At the conclusion of the anesthetic, 0.2 µl sample of arterial tail blood was placed in a HemoCue Hemoglobin Microcuvette (Brea, CA) and analyzed by a HemoCue 201 Hemoglobin Meter (Brea, CA). The HemoCue 201 meter comes factory calibrated and does not require further calibration.

Dextran Injection

To evaluate BBB permeability, 40 Kd tetramethylrhodamine isothiocynate conjugated dextran (Sigma Aldrich, St. Louis, MO, #42874-1G) was injected into the lateral tail vein of immunohistochemistry section study animals. The powdered dextran was rehydrated in 10 ml 0.9% normal saline (Hospiria, Lake Forrest, IL), centrifuged at 12,000 x g for 5 minutes to remove insoluble particles, aliquoted into 2 ml syringes and placed into a -20^{o}C freezer until use.

At the conclusion of the anesthetic, a 22g intravenous catheter (BD, Franklin Lakes, New Jersey) was placed in the lateral tail vein and 0.5 ml of a 100mg/ml dextran solution (42874-1G, Sigma Aldrich, St. Louis, MO) was injected over 1 minute. To flush the catheter clear of dextran solution, 0.4 ml's of 0.9% normal saline was then

administered. The intravenous catheter was removed and hemostasis obtained prior to placement in the recovery cage.

TISSUE PREPARATION

Euthanasia and Hippocampal Dissection

A recent study by Rampil (1) indicates that even a single 15-minute exposure to 2% isoflurane can alter up to 269 genes for up to 6 hours. Therefore, animals undergoing Western Botting and quantitative polymerase chain reaction (qPCR) evaluation will be euthanized via rapid decapitation with a sharp guillotine. To accomplish this, animals were place DecapiCone (Braintree Scientific, Braintree MA) bag and then rapidly decapitated using a small animal guillotine (Harvard Apparatus, Holliston, MA). Their brain was quickly removed and placed into ice cold phosphate buffered saline (PBS) to remove gross contaminants. The brain was then removed and placed onto an ice cold metal plate where the hemispheres were bisected and the hippocampus dissected out. The right hippocampus was placed into a 2 ml Eppendorf tube containing 1.5 ml RNAlater solution (ThermoFischer Scientific, Waltham, MA), stored at 4^{o}C overnight and then moved into a -80^{o}C freezer the next morning for storage until use. The left hippocampus was placed into a new 1.5 ml Eppendorf tube and then snap frozen in 100% ethanol on dry ice before being stored at -80^{o}C.

Whole Animal Perfusion

Rats received an intraperitoneal injection of 60 mg/kg of body of Euthasol (pentobarbital sodium 390 mg/ml and phenytoin sodium 50 mg/ml). Once a surgical plane of anesthesia was confirmed by absence of response to toe pinch, each limb was secured to a dissecting board with an 18G needle. The distal end of the sternum was

grasped with a rat tooth forceps and a 5-6 cm lateral incision was made through the integumentum and abdominal wall just beneath the rib cage. The liver was then carefully separated from the diaphragm. Blunt scissors were then used to dissect the diaphragm away from the rib cage to expose the plural cavity. A thoracotomy was made along the far right and left side of the rib cage to reflect the sternum up over the head to expose the entire chest cavity. A 2 ml blood sample was collected and then placed into a sodium heparin vacutainer tube (Becton Dickinson, Franklin Lakes, NJ) via a direct cardiac puncture with a 25 gauge needle (Becton Dickinson, Franklin Lakes, NJ) attached to a 3 ml syringe (Becton Dickinson, Franklin Lakes, NJ). Following the blood draw, the thymus was retracted to expose the ascending aorta. A blunt, 20 gauge needle, primed with ice cold PBS, was advanced through the left ventricle into the ascending aorta. Next, a bulldog clamp was then applied across both ventricles to secure the needle in place. Upon verification of correct placement of the blunt needle in the ascending aorta, an infusion of ice cold PBS was started and a small incision to the right atrium was created as an outlet window. A Watson/Marlow (Wilmington, MA) benchtop peristaltic pump set at 20mL/min was used to infuse 1 ml/gram of ice cold PBS followed by 1 mL/gram of freshly prepared 4% paraformaldehyde. Following the perfusion, the head was decapitated and the brain was removed and placed in 4% paraformaldehyde overnight at 4^{o}C. The whole brain was then placed in increasing concentrations (10%, 20%, and 30%) of sucrose in PBS until it sank to the bottom of the container. The brain was then removed, placed in a cryomold filled with Tissue-Tek OCT (Sakura; Torrance, CA), frozen in a slurry of 100% ethanol and dry ice, wrapped in tinfoil, and stored at -80^{o}C until used.

WESTERN BLOT

Protein Extraction

The left hippocampal samples were weighed and placed into pre-chilled 1.5 ml Eppendorf tubes with an equal volumes of 0.5 mm glass beads (NextAdvanced, Averille Park, NY). Radioimmunoprecipitation assay buffer (RIPA) (20 nM Tris-HCL, 150 mM NaCl, 1 mM NaEDTA, 1 nM EGTA, 1% NP-40, 1% sodium deoxychocolate, 2.5 mM sodium pyrophosphate, 1mM β-glycerophosphate, 1nM Na_3VO_4, 1 μg/ml leuptin; ThermoScientific, Rockford, IL) with 1X Halt protease and phosphatase inhibitor cocktail added (sodium fluoride, sodium orthovanadate, β-glycerophosphate, sodium pyrophosphate, aprotinin, bestatin, E64, and leupeptin; ThermoScientific, Rockford, IL) at 8 times the volume of sample weight was added. Samples were then homogenized with the Bullet Blender (NextAdvanced, Averille Park, NY) on speed 6 for 3 minutes and then incubated in an ice bath on an orbital shaker for 30 mins. The lysate was centrifuging at 10,000 x g for 10 minutes at 4^{o}C to remove the glass beads and large cellular debris. Next, the protein isolates were placed in a clean Eppendorf tube and centrifuged at 20,000 x g for 15 minutes at 4^{o}C to remove the remaining cellular debris. The resulting supernatant was removed, assayed for total protein concentration using the bicinchoninic acid protein assay (BCA), aliquoted into smaller single use Eppendorf tubes, and stored at -80^{o}C until used.

Protein Quantification

A Pierce BCA Protein Assay Kit (Rockford, IL) was used for protein quantification. The working reagent was created by mixing 25 ml of bicinchoninic acid with 500 μl copper sulphate solution. Bovine serum standards (0-2000 μg/ml) were

prepared and 25 µl of each standard was placed in triplicate into a 96-well plate. The protein supernatant was diluted 10 fold in RIPA buffer (10 µl sample to 90 µl RIPA buffer), microcentrifuged for 30 seconds, and then 25 µl of each unknown sample was placed in triplicate into a 96-well plate. The BCA working reagent, 200 µl per standard and sample, were then added to each well and the plate was incubated at 37°C for 30 minutes. A BioTek (Winooski, VT) EL800 microplate reader was used to measure the absorbance at 570 nm. The data was then transferred to Microsoft Excel where a curvilinear regression logistics curve with an R^2 value > 0.95 and quadratic equation were generated. Absorbance values, minus background, of the unknown samples were then substituted for X the equation and concentration (µg/ml) were obtained.

Sodium Dodecyl Sulfate-Polyacrylamide Gel Electrophoresis (SDS-PAGE)

Rat brain lysates were mixed with NuPage 4x LDS Sample Buffer (2% lauryl dodecyl sulfate, 106 nM Tris HCL, 141 nM Tris base, 10% glycerol, 0.51 mM EDTA, 0.22 mM SERVA Blue G250, 0.175 nM phenol red; Life Technologies, Carlsbad, CA), NuPAGE 10X sample reducing agent (500 nM dithiothreitol, Life Technologies, Carlsbad, CA), and de-ionized water to a final concentration of 20 µg/15 µl. Samples were briefly sonicated and then heated to 70°C for 10 minutes. While the samples were being heated, a NuPage 4-12% Bis-Tris (occludin, claudin-5 and VEGF) or NuPage 3-8% Tris-Acetate (ZO-1) gel was loaded into XCell Sure Lock Mini-Cell Electrophoresis System with either 1X NuPage MOPS SDS running buffer (50 nM MOPS, 50 nM Tis base, 0.1% SDS, 1 nM ethylenediaminetetraacetic acid (EDTA), pH 7.7), Life Technologies, Carlsbad, CA) for the 4-12% Bis-Tris gel or 1X NuPage Tris-Acetate buffer (50 mM Tricine, 50 nM Tris Base, 0.1% SDS (pH 8.4) (Life Technologies,

Carlsbad, CA) for the 3-8% Tris-Acetate gel. To maintain samples in a reduced state while running, 500 µl NuPage Antioxidant (Proprietary Reagents, Life Technologies, Carlsbad, CA) was added to the inner XCell chamber. Following heating, the samples were briefly sonicated and loaded into the wells of the appropriate gel with Chameleon Duo Pre-Stained Protein ladder (10 µl/lane, #928-60000, Li-Cor Biosciences, Lincoln, NE) to estimate molecular weight. Electrophoresis was carried out at 40 Volts for 10 minutes to move samples into the stacking gel followed by 100 Volts for 150 minutes through the separating gel. Following electrophoresis, the gel was removed from the cassette and proteins transferred to a methanol activated polyvinylidene fluoride (PVDF) membrane over 10 minutes at 2.5 A utilizing the Trans-Blot Turbo Transfer System (Bio-Rad, Hercules, CA). To reduce background signature, the PVDF membrane was then blocked with Odyssey Blocking Buffer (Proprietary formula; Li-Cor, Lincoln, NE) in PBS for 60 minutes at room temperature. Next, the membrane was then incubated with one of the following primary antibodies from Invitrogen (Rockford, IL) or Abcam (Cambridge, MA) listed in Table 2 overnight at 4^{o}C. The next morning, the membrane was washed 3X's with PBST before being probed with one of the following IRD secondary antibodies from Li-Cor (Lincoln, NE) listed in Table 3 for 60 minutes at room temperature. Next, the membranes were washed 3X's for 5 minutes with PBS-T and for 10 minutes with PBS. Protein expression levels were then examined on the Odyssey CLx Imager (Li-Cor, Lincoln, NE) with band intensity determined by Image Studio Lite Software (Li-Cor, Lincoln, NE).

Table 3. Western blot primary and secondary Antibodies

Primary Antibody	**Supplier**	**Catalog Number**	**Concentration**
Rabbit anti-occludin	Invitrogen	71-1500	1:1,500
Mouse anti-claudin-5	Invitrogen	35-2500	1:500
Rabbit anti-ZO-1	Invitrogen	40-2200	1:500
Mouse anti-Beta Actin	Invitrogen	5-15739	1:5000
Rabbit anti VEGFA	Abcam	AB46154	1:1000
Secondary Antibodies	**Supplier**	**Catalog Number**	**Concentration**
Goat anti-rabbit (800)	Li-Cor	926-32211	1:15,000
Donkey anti-mouse (800)	Li-Cor	926-32212	1:1,000
Goat anti-rat (800)	Li-Cor	926-32211	1:10,000
Goat anti-mouse (680)	Li-Cor	925-68070	1:50,000
Goat anti-rabbit (800)	Li-Cor	926-32211	1:15,000

QUANTITATIVE REAL TIME POLYMERASE CHAIN REACTION

RNA Isolation

The right hippocampus sample was removed from -80^{o}C storage, allowed to gradually thaw on ice, and then placed into a PCR clean 1.5 ml Eppendorf tube containing 350 µl QIAzol Lysis Reagent (Qiagen, Germantown, MD). Hippocampal samples were dissected into tiny pieces prior to sonication (Diagenode Bioruptor; Denville, NJ) for two 30 second intervals with a 30 second pause between. After sitting at room temperature for 5 minutes, 70 µl trichloromethane (chloroform) (Sigma-Aldrich; St. Louis, MO) was added to each tube followed by vigorous shaking for 30 seconds. Samples were then centrifuged at 12,000 RMP for 15 minutes at 4^{o}C to phase separate the sample into RNA (clear upper layer), DNA (cloudy middle layer), and protein (red phenol lower layer). The RNA fraction was carefully removed and placed into a fresh PCR clean 1.5 ml Eppendorf where absolute ethanol (≥99.8%) (Sigma-Aldrich; St. Louis, MO), at 1.5 times the final volume of RNA, was added. Following a brief vortex and 5-minute incubation period, up to 700 µl of the RNA and ethanol mixture was added to a

RNeasy Mini Spin Column (Qiagen, Germantown, MD). The RNeasy Mini Spin Column was centrifuged briefly at room temperature to attach RNA to the spin column silica membrane. The membrane was then washed with RW1washbuffer to remove carbohydrates, proteins, and fatty acids. Following a brief centrifuge at room temperature (8000 rpm for 30 seconds), the silica membrane was rinsed with RPE wash buffer (to remove accumulated salts from the previous steps) and then centrifuged at room temperature for 30 seconds at 8000 RPM. Following a second washing and spin cycle with RPE Buffer, the spin column was moved into a clean Eppendorf tube and centrifuged for 1 minutes at maximum speed to remove any remaining wash buffer and other contaminants. The spin column was then placed in a clean collection tube and 37 µl of RNAse free water was placed on the silica membrane. To then elute the RNA from the silica membrane, the collection tube was centrifuged for 1 minute at 8,000 RPM. Samples were then placed in -80^{o}C freezer until use.

Determining RNA purity, quantification, & integrity

Spectrophotometer

To assess the purity of the RNA sample, a 1 µl sample was placed on a NanoDrop 1000 Spectrophotometer (ThermoScientific, Waltham, MA) for wavelength analysis. Only samples with a 260/280 ratio greater than 2.0 and a 260/230 ratio greater than 1.8 were used for qPCR analysis (Table 4).

Table 4: RNA Purity and Quantification

Sample	RNA Quant (µg/ml)	260/280	260/230	Group	RNA Quant (µg/ml)	260/280	260/230
4 Hours				24 Hours			
Control							
1	374.7	2.05	2.28	N/A			
6	419.3	2.03	2.27				

42	274.1	2.04	2.1				
62	209.2	2.11	2.13				
75	122.1	2.16	2.23				
1 Prolonged Exposure (1PE)							
5	230.4	2.03	2.03	**13**	241.3	2.05	2.05
41	230.5	2.07	2.11	**28**	177.9	2.09	2.05
86	64.9	2.07	1.85	**34**	100.8	2.09	2.02
133	152.7	2.15	2.25	**102**	134.4	2.14	2.19
135	254.6	2.08	2.16	**116**	170.7	2.08	2.03
1 Brief Exposure (1BE)							
3	239.8	2.04	2.1	**19**	90.7	2.08	2.01
10	78.8	2.03	1.8	**22**	109.5	2.10	2.09
30	213.4	2.05	1.9	**50**	161.8	2.10	1.82
81	168.6	2.07	1.9	**84**	91.9	2.18	2.08
134	103.8	2.09	2.0	**127**	240.8	2.09	2.15
5 Brief Exposures (5BE)							
11	130.8	2.12	2.02	**31**	327.8	2.06	2.12
94	108.0	2.06	1.85	**32**	75.8	2.07	1.93
105	197.9	2.10	2.12	**87**	130.8	2.10	1.92
112	169.8	2.07	2.13	**96**	164.4	2.10	2.08
120	206.6	2.07	2.02	**125**	231.1	2.04	1.95

Quant-iT Fluorescence Quantification

The Quant-iT RiboGreen RNA kit (ThermoFischer Scientific, Waltham, MA) was used to measure RNA concentration. Using the supplied 16S and 18S ribosomal RNA standards (2μg/ml), a high range (20 ng/ml to 1μg/ml) standard curve was prepared and placed in triplicate into a 96 well plate. Next, a 20 fold dilution (100 μl RiboGreen Quantitation Reagent to 19.9 ml's TE buffer) of the Quant-iT RiboGreen (ThermoFischer Scientific, Waltham, MA) assay was prepared. Each RNA sample was then diluted 100 fold (3uL RNA to 297 μl TE buffer) and placed in triplicate into a 96 well plate. A total of 100 μl of the RiboGreen Quantitation reagent was added to each standard and sample well. The plate was then covered, mixed well, incubated for 5 minutes, and then read on a SpectraMax plate reader (Molecular Devices, Sunnyvale, CA). SoftMax Pro software

version 5.4 was utilized to create a linear regression equation and sample values, minus background, were entered for quantification. Following quantification, listed in Table 5, RNA samples were stored at -80ºC until conversion into cDNA.

Table 5: Quant-iT Quantification Results

Sample	RNA Quant (µg/ml)	Sample	RNA Quant (µg/ml)
4 Hours		24 Hours	
Control			
1	595.4		
6	555.8		
42	365.5		
62	273.6		
75	257.4		
1 Prolonged Exposure (1PE)			
5	296.4	**13**	341.5
41	312.9	**28**	239.4
86	85.8	**34**	128.0
133	191.0	**102**	182.1
135	332.4	**116**	211.0
1 Brief Exposure (1BE)			
3	328.8	**19**	110.9
10	98.1	**22**	137.2
30	247.8	**50**	223.0
81	213	**84**	121.9
134	152.6	**127**	317.9
5 Brief Exposures (5BE)			
11	175.3	**31**	391.4
94	134.6	**32**	98.9
105	257.3	**87**	169.3
112	213.5	**96**	205.1
120	280.5	**125**	303.8

RNA Integrity

The integrity of RNA molecules is paramount for accurate PCR and RNA sequencing data. To analyze the integrity of RNA samples, the Advanced Analytical Fragment Analyzer (Advanced Analytical Technologies Inc.; Ankey, IA) and PROsize (2.0) data analysis software (Version 2.3) was used. Intercalating dye, 4 µl, was mixed

with 40 ml of RNA separation gel in a clean 250 ml conical centrifuge tube prior to loading into the Fragment Analyzer. A 1X capillary conditioning solution was made from the supplied 5X solution, placed into a 250 ml conical centrifuge tube, and then loaded into the Fragment Analyzer. For ladder preparation, 2 µl of the 25 ng/µl High Sensitivity RNA Ladder was placed into a fresh LoBind Eppendorf tube, heated to 70^{o}C for 2 minutes, and then placed on ice. Total RNA samples were removed from the freezer, thawed on ice, heated to 70^{o}C for 2 minutes, and then immediately placed on ice for 5 minutes. A RNase-free 96 well PCR plate was loaded with 2 µl of the denatured RNA ladder and total RNA sample, and then 22 µl of high sensitivity RNA diluent marker was added. Following thorough mixing of the solutions, the PCR plate centrifuged briefly to remove air bubbles and then placed into the sample drawer. PROsize software (Version 2.3) was used identify sample wells and design experimental separation method (DNF-471-33-SS) to identify total RNA. Results are reported in Table 6.

Table 6. RNA Quality Number: Sample number (RQN value)

Sample	RIN Numbers	Sample	RIN Numbers
4 Hours		24 Hours	
Control			
1	7.3		
6	5.4		
42	7.0		
62	4.5		
75	4.3		
1 Prolonged Exposure (1PE)			
5	5.1	**13**	5.7
41	4.5	**28**	4.0
86	2.9	**34**	6.5
133	5.9	**102**	6.8
135	5.4	**116**	6.7
1 Brief Exposure (1BE)			
3	7.2	**19**	6.2
10	6.9	**22**	6.9
30	6.6	**50**	6.3
81	10	**84**	10

134	5.4	**127**	5.2
5 Brief Exposures (5BE)			
11	6.9	**31**	6.7
94	6.9	**32**	10
105	5.0	**87**	6.6
112	4.8	**96**	6.3
120	5.5	**125**	5.2

Complementary DNA Synthesis (cDNA)

A master mix of 5x iScript advance (Bio-Rad, Hercules, CA) reaction mix (2µl/reaction), iScript advanced reverse transcriptase (0.5µl/reaction), and nuclease free water (1µl/reaction) was made and aliquoted (3.5 µl) to individual PCR strip tubes. Next, 500 ng RNA template material was added to the strip tubes. Finally, nuclease free water was added to bring the solution to 10 µl total volume. The solution was then heated at 46^{o}C for 20 minutes and then at 95^{o}C for 1 minute in a GeneAmp PCR System 9700 (Applied Biosystems, Foster City, CA). The cDNA was then stored at -80^{o}C till use.

Primer Design

Gene specific primers were designed using the Basic Local Alignment Search Tool (BLAST; National Center for Biotechnology Information) primer designing tool and then obtained from Integrated DNA Technologies (Skokie, IL). Primers were designed with the specific design parameters (Table 7). Efficiency was tested by creating a 10-fold dilution using rat brain lysate and specificity was verified by melt curve analysis.

Table 7. Primer Design Characteristics

Parameter	Range
Primer Length	18-24 bases
Melting Temperature (T_m)	59^{o}C
Difference in T_m	+/- 2^{o}C
GC Content	40-60%
Amplicon length	70-150 base pairs
Runs and repeats	Avoid runs > 4 repeats
Separation	Bind separate exons

Specific primers sequences for proteins of interest and oligodendrocyte markers are listed in Table 8.

Table 8. Forward and reverse primer sequences.

Gene	Forward (5'-3')	Reverse (5'-3')
Actin	CTGTGGTCTCTTTTTGGCAGA	AGAGAGAACAAGGCCACAGA
HPRT	AGACGTTCTAGTCCTGTGGC	GGACGCAGCAACAGACATTT
Occludin	TTAAGTACCCACCAGTGACCAG	ATGCGAACCTCCTTCTGGTTC
CL-5	CCTGGTCTCATTCCAGCAGTC	GGAGGAAGGCAACCCTTCTAA
ZO-1	TGTGATACAATGCTGTGCCCTA	AACAGAAATCGTGCTGATGTGC
MBP	TCCATCCCAAGGAAAGGGGA	TCTGCCTCCGTAGCCAAATC
MOBP	GCGAGACAAGCTGGGAATGA	CTGGTTCTTGGAGAGCCTGG
MAG	GACGATGGGGAGTACTGGTG	CTGCACAGTGCGATTCCAGA
CL-11	TCTCTACCACTGCAAGCCCC	TGAGGGCTCTACAAGCCTGC
SOX10	GCTGCTATCCAGGCTCCACTA	CCTTTTGGGATCTGCCTTGC

Quantitative Real Time Polymerase Chain Reaction (PCR)

For real-time quantitative reverse transcription PCR, SYBR-Green Amplification was performed using the Bio-Rad CFX384 real-time PCR Detection System and C1000 Touch Thermal Cycler (Hercules, CA). The PCR mixture contained SsoFast Eva Green Universal SYBR Green supermix, 300 nM forward and reverse primers, and 0.1 ul of cDNA template. The thermocycling conditions were as follows: initial denaturation at 95^{o}C for 10 minutes, followed by 40 cycles of 95^{o}C for 15 seconds, 60^{o}C for 30 seconds, and final extraction at 72^{o}C for 30 seconds. Each control sample and experimental sample was assayed using 4 replicates per primer. The expression of hypoxantine-guanine-phosphoribosyltransferase (HPRT) and beta-actin was used for internal control. The relative expression of occludin, CL-5, and ZO-1 was analyzed using the $2^{-\Delta\Delta CT}$ method.

RNA Sequencing

Total input of 500ng of RNA was used for library preparation using the TruSeq Standard mRNA Sample Preparation Kit (Illumina, San Diego, CA). The KAPA Library Quantification Kit for NGS (Kapa, Wilmington, MA) was utilized for PCR quantification of construction of libraries. The Fragment Analyzer Automated CE System (Advanced Analytical) was utilized to ensure library integrity and none of the libraries peaked around 120-130 bp which would indicate the presence adaptor dimers. Following pooling, libraries were sequenced on a NextSeq. 500 Desktop Sequencer (Illumina) using a NextSeq. 500 High Output Kit with paired-end reads at 75 base pair lengths according to manufactures' instructions. To convert the raw sequencing data file to FASTQ format, bcl2fastq2 conversion software (version 2.17) was utilized. TopHat Alignment (version 1.0) was utilized for sequence alignment and Cufflinks Assembly & DE (version 1.1.0) on BaseSpace Onsite (Illumina) was utilized for differential expression analysis. To identify a significance between control and 1PE anesthesia group, a threshold of 1.64 fold change and a q-value of at least 0.05 was considered biologically relevant. PANTHER classification analysis was utilized for functional enrichment analysis.

IMMUNOFLUORESCENCE

Tissue Sectioning

Rat brains were removed from the -80^{o}C freezer and placed in a -20^{o}C cryostat (Lecia Biosystems 3050S; Buffalo Grove, IL) for 30 minutes to equilibrate temperatures. Following equilibration, the sample was mounted to a tissue holder with OCT and then placed in the specimen rack. Serial coronal sections of the hippocampus were cut sequentially at 20 µm thickness using a Leica 3050s cryostat starting at Bregma -2.40 and

mounted on 75 X 25 mm positively charged glass slides (VWR; Randor, PA). Sectioned tissue were placed on slides in a 1 to 5 pattern (Figure 2) with 2 brain sections per slide. Slides were placed in a slide box wrapped in foil and placed in -80^{o}C freezer until needed.

Group Animal Slide Number Date/Initial	Group Animal Slide Number Date/Initial	Group Animal Slide Number Date/Initial	Group Animal Slide Number Date/Initial	Group Animal Slide Number Date/Initial

Figure 2. Slide pattern for immunofluorescence.

Immunofluorescence

Proteins of Interest (Occludin, CL-5, and ZO-1)

To evaluate for occludin, CL-5, and ZO-1 expression, 3 control and 3 experimental animals per groups were processed as a cohort. A total of 5 slides, approximately 200 µm apart, per animal were removed from the freezer and placed in a light proof humidity chamber. After warming to room temperature for 15 minutes, brain sections were hydrated with 1x PBS for 15 minutes. Slides were then placed into a vertical slide rack and then into a microwaveable glass dish were they were covered with sodium citrate buffer (10 nM sodium citrate; Sigma, St. Louis, MO) containing 0.05% Tween 20 (Sigma, St. Louis, MO) that was adjusted to pH 6.0 with 1N HCL (Sigma, St. Louis, MO). The microwaveable glass dish containing the slides and citrate buffer was then placed in an 850 watt microwave oven and microwaved for 5 minutes on high. Following a 2 minute rest period, the slides were again microwaved on high for 5

minutes. The microwaveable glass dish was removed from the microwave, covered with a glass lid, wrapped in aluminum tinfoil, and allowed to sit for 20 minutes at room temperature. The slides were then removed from the buffer, placed in a light proof humidification chamber, and washed three times in PBS for a total of 15 minutes. Brain sections were then outlined with a PAP pen (Vector Laboratories, Burlingame, CA) and covered with 300 µL's of 50 nM ammonium chloride (Sigma, St. Louis, MO) in PBS for 30 minutes at room temperature to help reduce background auto-fluorescence. Slides were then washed three times in PBS for a total of 15 minutes before being covered with 300 µl's of permeabilization buffer containing 0.3% Triton X-100 (Sigma, St. Louis, MO) diluted in PBS for 30 minutes. To prevent non-specific anti-body binding, the permeabilization buffer was removed and replaced with 300 µl of a blocking solution containing 1X animal free plant blocker (Vector Laboratories, Burlingame, CA) that was diluted in deionized water containing 0.03% Triton X-100 (Sigma, St. Louis, MO). After sitting at room temperature for 60 minutes, the blocking solution was gently removed and replaced with a primary antibody (listed in Table 9) solution containing a mixture of 1x animal free blocker diluted in deionizing water and 0.03% Triton X-100 (Sigma, St. Louis, MO). Samples were then taken to the Pharmacy Department 4^{o}C freezer where they stayed overnight (16 hours). In the morning, the primary antibody solution was removed and the sections were washed three times in PBS for a total of 15 minutes. After the final washing, the sections were incubated in the appropriate species specific secondary antibody (listed in Table 9) solution of 1x animal free blocker diluted in deionizing water and 0.03% Triton X-100 (Sigma, St. Louis, MO). After incubating for 2 hours at room temperature, the secondary antibody solution was removed and the

sections were washed three times in PBS for a total of 15 minutes. Following the final washing, the section were incubated with DyLight 594 labeled lycopersicon esculentum lectin (Vector Laboratories, Burlingame, CA) in order to mark cerebral blood vessels. After incubating for 2 hours at room temperature, the lectin solution was removed and the sections were washed three times in PBS for a total of 15 minutes. After drying the sections, a drop of ProLong Gold Anti-fade Mounting liquid containing the nuclear stain DAPI (4,6 diamidino-2-phenylindole; Invitrogen) was applied to each tissue section and then covered with a number 1.5 coverslip (40 x 60 mm; Corning, NY). Slides were then placed in a clean and dry humidification chamber where they were allowed to cure overnight in the dark before being placed in a microscope slide tray for long-term storage.

To evaluate for unspecific binding of the secondary antibody to the tissue, the same protocol was followed without the addition of the primary antibody in the antibody diluent. Additionally, to ensure specific binding of the primary to the secondary antibody, a secondary antibody from a different species (donkey anti-goat- 488; Jackson Laboratories; West Grove, PA) was placed into the secondary antibody solution.

Dextran Extravasation

To evaluate dextran extravasation from the blood vessels, 3 control and 3 experimental animals per group were processed as a cohort. In order to prevent the injected dextran from potentially being washed away, minimal washings with PBS was conducted(106) . A total of 5 slides, approximately 200 µm apart, per animal were removed from the freezer and placed in a light proof humidity chamber. After warming to room temperature for 15 minutes, brain sections were hydrated with 1x PBS for 10

minutes. Brain sections were then circled with a PAP pen (Vector Laboratories, Burlingame, CA) and covered with 100 µl of animal free plant blocker (Vector Laboratories, Burlingame, CA) diluted in deionized water containing 0.3% Triton X-100 (Sigma, St. Louis, MO) to prevent non-specific antibody binding. After sitting at room temperature for 60 minutes, the blocking solution was gently removed and replaced with a primary antibody (listed in Table 9) solution of 1x animal free blocker diluted in deionizing water and 0.03% Triton X-100 (Sigma, St. Louis, MO). Brain samples were then taken to the Pharmacy Department 4ºC freezer where they stayed overnight. In the morning, the primary antibody solution was removed and the sections were washed three times in PBS for a total of 15 minutes. After the final washing, the sections were incubated in the secondary antibody (listed in Table 9) of 1x animal free blocker diluted in deionizing water and 0.03% Triton X-100 (Sigma, St. Louis, MO). After incubating for 2 hours at room temperature, the secondary antibody solution was removed and the sections were washed three times in PBS for a total of 15 minutes. Following the final washing, the sections were incubated with DyLight 594 labeled lycopersicon esculentum lectin (Vector Laboratories, Burlingame, CA) to mark blood vessels. After incubating for 2 hours at room temperature, the lectin solution was removed and the sections were washed three times in PBS for a total of 15 minutes. After drying the sections, a drop of ProLong Gold Anti-fade Mounting liquid containing the nuclear stain DAPI (4,6 diamidino-2-phenylindole; Invitrogen) was applied to each tissue section and then covered with a number 1.5, 24 x 60 mm, coverslip. Slides were then placed in a clean and dry humidification chamber where they were allowed to cure overnight in the dark before being placed in a microscope slide tray for long-term storage.

To evaluate for unspecific binding of the secondary antibody to the tissue, the same protocol was followed without the addition of the primary antibody in the antibody diluent. Additionally, to ensure specific binding of the primary to the secondary antibody, a secondary antibody from a different species (donkey anti-goat- 488; Jackson Laboratories; West Grove, PA) was placed into the secondary antibody solution.

Table 9. Immunofluorescence primary and secondary antibodies.

Primary Antibody	**Supplier**	**Catalog Number**	**Concentration**
Rabbit anti-Claudin-5	Invitrogen	35-2500	1:100
Mouse anti-Occludin	Invitrogen	33-1500	1:100
Rabbit anti-ZO-1	Invitrogen	40-2200	1:100
Secondary Antibody	**Supplier**	**Catalog Number**	**Concentration**
Goat anti-mouse 488	Invitrogen	SA-11008	1:200
Goat anti-rabbit 488	Invitrogen	SA-11001	1:200
Donkey anti-goat 488	Invitrogen	SA-10086	1:200
Counterstain (Blood Vessel)	**Supplier**	**Catalog Number**	**Concentration**
DyLight 594 Lycopersicon Esculentum	Vector Laboratories	DL-1177	1:800

Image Acquisition

Images were acquired with a 12-bit monochrome digital camera (DS-Qi1, Nikon, Melville, New York) attached to a Nikon Eclipse 80i microscope (Melville, New York) with individual excitation and emission filters for DAPI (excitation at 345nm; emission at 458), fluorescein (FITC; excitation at 494; emission at 518) and Texas Red (excitation at 589; emission at 615). The same acquisition parameters were applied to all slides within a particular protein of interest (occludin, CL-5, ZO-1, dextran).

An individual blue, green, and red image of the hippocampus was obtained at 4x and 10x magnification before being combined into a single red/green/blue (RGB) image using NIS Elements Advanced Research Software (version 4.10.1; Nikon, Melville, New York). In order maintain optimal picture quality, and not lose any information about each

of the individual pictures, the combined RGB images were saved as a tagged image file format (TIFF). Additionally, 5 individual RGB phots at 20x magnification were taken sequentially through the lacunosum moleculare and radiatum layer of CA-1 and CA-2 portions of the hippocampus. The individual pictures were then combined into a single RGB image using NIS Elements Advanced Research Software and saved as a TIFF file.

IMAGE ANALYSIS

Immunohistochemistry

Quantitative image analysis for occludin, CL-5, and ZO-1 was performed on five non-overlapping fields through the hippocampus using ImageJ (National Institute of Health, Bethesda, MD; Version 1.51j8). In all images, the nucleus was stained blue, the protein of interest was stained green, and the blood vessels was stained red. A 20x TIFF image was opened in ImageJ and separated into the red, green, and blue photos. Background fluctuations were removed using a 50 pixel rolling ball algorithm. Thresholding, using the Triangle algorithm, was applied to the images to find the edges of the proteins of interest and the diameter of the blood vessel so they could be converted into black and white images. Next, the circumference of the blood vessels was measured using the analyze particles function. Finally, the percentage of the positively stained protein of interest was compared to the total area of the blood vessel.

A total of 3 control and 3 experimental animals per group was analyzed. For each animal, a total of 5 slides, approximately 200 μm apart, with a minimum of 5 blood vessel per slide were quantified and averaged to create a single percentage for that animal. Therefore, 25 vessels (5 slides X 5 vessels) was obtained. Data from each animal

was then averaged and then used for comparison. With 3 animals per group and 25 vessels per animal, quantification was based on 75 vessels (3 animals x 25 vessels).

Dextran Extravasation

Quantitative analysis of dextran extravasation was performed on five non-overlapping fields through the hippocampus using ImageJ (National Institute of Health, Bethesda, MD; Version 1.51j8). In all images, the nucleus was stained blue, the dextran was stained green, and the blood vessels was stained red. A 20x TIFF image was opened in ImageJ and separated into the red, green, and blue photos. In order to accurately quantify dextran extravasation, background, no background reduction was performed. Thresholding, using the Triangle algorithm, was applied to the images to identify the dextran and diameter of the blood vessel so they could be converted into black and white images. The amount of labeled dextran and the circumference of the blood vessel measured using analyze particles. Next, the circumference of the blood vessel was outlined and any labeled dextran particles within were removed and subtracted. Finally, the remaining amount of dextran fluorescence was measured and recorded.

A total of 3 control and 3 experimental animals per group was analyzed. For each animal, a total of 5 slides, approximately 200 µm apart, with a minimum of 5 blood vessel per slide were quantified and averaged to create a single percentage for that animal. Therefore, 25 vessels (5 slides X 5 vessels) was obtained. Data from each animal was then averaged and then used for comparison. With 3 animals per group and 25 vessels per animal, quantification was based on 75 vessels (3 animals x 25 vessels).

CHAPTER 4: Results

Results

PHYSIOLOGICAL PARAMETERS

Volatile anesthetics alter multiple different neuronal pathways to produce reversible loss of consciousness, amnesia, anesthesia, and immobility. Additionally, volatile anesthetics can alter normal cerebral, cardiovascular, respiratory, and metabolic parameters (67). Understanding these physiological changes is important for valid study results and animal welfare.

A one-way between groups ANOVA was conducted to explore the difference in weight at baseline and the impact of a single anesthesia exposure on HR, RR, SaO2, SBP, DBP, and MAP. For comparison, Exposure 1 in the 5 BE was used. To measure the same physiological parameters in control animals, they would have to be placed in rodent holders for extended periods of time (2 or 4 hours) putting them under undue stress and strain. Therefore, for physiological parameters, only weight was recorded in control animals. Between groups physiological parameters are listed in Table 10, and all values are listed as mean ± SEM.

Physiological Parameters: Between Groups

There was no statistical significance difference in baseline weight [$F(3,77) = 2.187$, $p = 0.096$], mean HR [$F(2,63) = 0.254$, $p = 0.777$], RR [$F(2,63) = 1.707$, $p = 0.190$], SBP [$F(2,63) = 0.354$, $p = 0.703$], DBP [$F(2,63) = 0.703$, $p = 0.207$], or MAP [$F(2,63) = 1.171$, $p = 0.317$] following a single exposure to anesthesia. The only statistically significant difference was in the mean SaO2 levels between the groups [$F(2,63) = 4.321$,

p = 0.017]. Post hoc comparison indicated that the mean SaO2 score in the 1BE group (96.97 ± 0.58) was significantly different from the 5BE group Exposure 1 (97.47 ± 0.54). The effect size, calculated using eta squared, was 0.12 and indicates a large effect. However, despite reaching statistical significance, the actual difference in mean SaO2 scores between the 1 BE group and Exposure 1 of the 5 BE group is not clinically relevant since all scores are above 90%, the normal accepted range.

Table 10. Physiological parameters by group listed as mean ± SEM.

	GROUP			
Parameter	Control	1 PE	1 BE	5 BE; Exp. 1
Weight	326.2 ± 16.3	359.8 ± 13.8	334.8 ± 12.1	367.1 ± 10.8
HR		366.8 ± 5.6	370.9 ± 4.0	366.2 ± 5.2
RR		65.2 ± 0.4	66.5 ± 0.6	65.7 ± 0.4
SaO2		97.2 ± 0.1	97.0 ± 0.1	**97.5 ± 0.1***
SBP		101.7 ± 0.9	100.5 ± 1.1	100.8 ± 1.1
DBP		74.4 ± 1	72.6 ± 0.9	74.7 ± 1
MAP		83.0 ± 0.9	81.4 ± 1	83.2 ± 0.8

* = p values < 0.05 compared to the 1 BE group.

Physiological Parameters: Between Repeated Exposures

To compare the effects of repeated anesthesia exposure on weight, HR, RR, SaO2, SBP, DBP, and MAP in the 5 BE group, a one-way repeated measures ANOVA was conducted. Repeated exposures physiological parameters are listed in Table 11. There was a significant effect of repeated anesthesia exposures on weight [Wilks' Lambda = 0.257, F (4,20) = 14.456, p < 0.001]. Post hoc testing revealed a significantly decreased the mean weight between Exposure 1 (367.1 ± 52.9) and Exposure 2 (362.6 ± 52.1, p < 0.001). There were additional decreases in weight between Exposure 2 (362.6 ± 52.1) and Exposure 3 (360.7 ± 51.6, p = 0.065), Exposure 3 (360.7 ± 51.6) and Exposure 4 (359.4 ± 57.0, p = 0.462), and Exposure 4 (359.4 ± 57.0) and Exposure 5 (359.9 ± 50.6, p = 0.99). However, these reductions in weight are not statistically significant.

There was no significant effect of repeated anesthesia exposures on HR [Wilks' Lambda = 0.657, F (4,20) = 2.613, p = 0.066], RR [Wilks' Lambda = 0.787, F (4,20) = 1.35, p = 0.285], DBP [Wilks' Lambda = 0.899, F (4,20) = 0.562, p = 0.693], or MAP [Wilks' Lambda = 0.905, F (4,20) = 0.523, p = 0.720].

There was a significant effect of repeated anesthesia exposures on SaO2 levels [Wilks' Lambda = 0.625, F(4,20) = 2.994, p < 0.043]. Post hoc tests revealed a significantly decreased SaO2 levels between Exposure 1 (97.49 ± 0.54) and Exposure 4 (97.09 ± 0.52, p < 0.035). These reductions in SaO2 levels are statistically significant, but not clinically relevant as all values are above 90%. Additionally, there was a significant effect of repeated anesthesia exposures on mean SBP values [Wilks' Lambda = 0.608, F(4,20) = 3.219, p = 0.034]. Post hoc tests revealed that there was a statistically significant increase in SBP between Exposure 1 (100.8 ± 5.5) and Exposure 4 (103.7 ± 4.2, p = 0.010). Despite reaching statistical significance, that actual difference (3 mmHg) in mean SBP is very small and not clinically relevant since both values are within the normal range (100-130 mmHg) (79).

Table 11. Physiological parameters by anesthesia exposure listed as mean ± SEM.

	EXPOSURE				
Parameter	1	2	3	4	5
Weight	367.1 ± 10.8	**362.6 ± 10.6***	360.7 ± 10.5	359.4 ± 10.4	359.9 ± 10.3
HR	366.2 ± 5.2	360.5 ± 3.8	365.5 ± 4.1	358.5 ± 4.0	359.5 ± 3.8
RR	65.7 ± 0.4	65.3 ± 0.5	65.5 ± 0.4	65.0 ± 0.3	65.7 ± 0.4
SaO2	97.5 ± 0.1	97.1 ± 0.1	97.3 ± 0.2	**97.1 ± 0.1†**	97.2 ± 0.1
SBP	100.8 ± 1.1	101.5 ± 1.3	101.6 ± 1.1	**103.7 ± .88#**	102.13 ± 1.0
DBP	74.7 ± 1	73.6 ± 1	73.55 ± 1.2	75.0 ± 1.1	74.02 ± 1.1
MAP	83.2 ± 0.8	82.5 ± 1.1	82.7 ± 1.2	84.0 ± 1	83.4 ± 1.1

* = p values < 0.05 compared to exposure 1; † = p value < 0.05 compared to exposure 1 & # = p values < 0.05 compared to exposure 1.

ARTERIAL BLOOD GAS

Even in trace amounts, isoflurane is a potent respiratory depressant that can lead to hypoxia and hypercarbia which increases with the length of exposure (66). This indicates that animals undergoing anesthesia with isoflurane may develop hypoxemia, hypercarbia, or respiratory acidosis. Therefore, understand the effects of isoflurane on arterial blood gas (ABG) parameters is essential for animal wellbeing and study outcomes. Since control animals were not exposed to isoflurane, they did not undergo ABG sampling.

Arterial Blood Gas: Between Groups

Arterial blood gas values by group are listed in Table 12. A one-way between groups ANOVA was conducted to compare the effects of a single anesthesia exposure on ABG values. For comparison, Exposure 1 in the 5 BE was used. There was no statistically significant difference in mean pH [$F(2,31) = 0.438$, $p = 0.649$], PaCO2 [$F(2,31) = 0.777$, $p = 0.468$], HCO3 [$F(2,31) = 0.236$, $p = 0.791$], BE [$F(2,31) = 0.185$, $p = 0.825$], or lactate [$F(2,31) = 2.64$, $p = 0.087$]. There was a statistically significant difference in mean PaO2 values between groups [$F(2,31) = 3.805$, $p = 0.033$]. Post hoc comparison indicated a significant decrease in the mean PaO2 values between the 1 PE (373.27 ± 53.0) and the 1 BE group (432.55 ± 52.1). The effect size, calculated eta squared, was 0.19 and indicates a large effect. However, despite reaching statistical significance, the actual difference in PaO2 levels is not clinically relevant since both are above 60 mmHg. Levels less than 60 mmHg indicate hypoxia.

Table 12. Arterial blood gas parameters by group, listed at mean ± SEM.

GROUP			
Parameter	1 PE	1 BE	5 BE; Exp. 1
pH	7.39 ± .00	7.40 ± .01	7.39 ± .01
PaCO2	38.4 ± 1.2	40.6 ± 1.5	40.0 ± 1.2
PaO2	373.3 ± 16.0	432.6 ± 15.7	**396.6 ± 13.7***
HCO3	23.7 ± .08	24.6 ± 1.0	24.2 ± 0.6
BE	-1.3 ± .7	-0.46 ± 0.9	-0.58 ± 0.8
Lactate	0.88 ± .09	1.16 ± .13	0.86 ± .08

* = p values < 0.05 compared to 1 PE group

Arterial Blood Gas: Between Exposures

Arterial blood gas parameters by exposure are listed in Table 13. To compare the effects of repeated anesthesia exposure on ABG results, a one-way repeated measures was conducted. There was no significant effect of repeated anesthesia exposure on mean PaCO2 [Wilks' Lambda = 0.539, F(2,8) = 3.423, p = 0.084], PaO2 [Wilks' Lambda = 0.792, F(2,8) = 1.05, p = 0.394], HCO3 [Wilks' Lambda = 0.991, F(2,8) = 0.037, p = 0.963], BE [Wilks' Lambda = 0.956, F(2,8) = 0.185, p = 0.835], or lactate [Wilks' Lambda = 0.991, F(2,8) = 0.350, p = 0.966]. There was a significant effect of repeated anesthesia exposures on pH values [Wilks' Lambda = 0.228, F(2,8) = 13.559, p = 0.003]. Post hoc testing revealed statistically significantly increase in pH levels between Exposure 1 (7.39 ± 0.03) and Exposure 3 (7.42 ± 0.02, p = 0.026), and between Exposure 1 (7.39 ± 0.03) and Exposure 5 (7.40 ± 0.02, p = .017). However, these changes in pH values are not clinically relevant since the values for each exposure fell within the normal range (7.35-7.45) for Sprague Dawley rats (224).

Table 13. Arterial blood gas parameters by exposure, listed by mean ± SEM.

	EXPOURE		
Parameter	1	3	5
pH	7.39 ± .01	**7.42 ± .01***	**7.40 ± .00†**
PaCO2	40.0 ± 1.2	37.7 ± 1.1	38.2 ± .8
PaO2	396.6 ± 13.7	400.3 ± 11.3	404.9 ± 17.7
HCO3	24.2 ± 0.6	24.1 ± 0.6	24.0 ± 0.5
BE	-0.58 ± 0.8	-0.25 ± 0.7	0.27 ± 0.1
Lactate	0.86 ± .08	0.83 ± .12	0.88 ± .07

* = p values < 0.05 compared to exposure 1; † = p value < 0.05 compared to exposure 1

GLUCOSE AND HEMOGLOBIN RESULTS

Isoflurane decreases the cerebral metabolic rate for glucose (CMRglu) leading to higher levels of plasma and cerebral glucose levels, or hyperglycemia (127). Hyperglycemia is associated with endothelial cell dysfunction; therefore, blood glucose values were measured at the end of each anesthetic. Since glucose measurements only require a small drop of blood, control animals were placed into a small animal holder and glucose measurement were obtained from the rat tail.

Additionally, since animals in the 5 BE group were undergoing multiple blood draws, hemoglobin levels were measured following each ABG measurement to ensure study animals did not become anemic. Anemia can lead to inadequate oxygen delivery to tissue beds causing tissue hypoxia. Additionally, while trying to deliver more oxygen to the various tissue beds, the heart rate increases. Since measuring hemoglobin levels only required a small sample of blood, hemoglobin levels in control animals were measure the same time as glucose measurements were.

Glucose and Hemoglobin Results: Between Groups

Glucose and hemoglobin results by group are listed in Table 14. A one-way between groups ANOVA was conducted to compare the effects of a single anesthesia exposure on

glucose and hemoglobin values. There was a statistical difference in mean glucose levels between groups [F(3,11) = 2.975, p = 0.041]. Post hoc testing indicated that there was a significant the mean glucose increased between control (118.0 ± 20.4) and the 1PE (137.5 ± 22.5, p = 0.012) group, 1 BE (139.4 ± 15.4, p = 0.026) group, and the 5 BE- Exposure 1 (136.1 ± 20.9, p = 0.021). There was no significant difference in mean HGB levels between groups [F (3,11) = .310, p = .818].

Table 14. Glucose and hemoglobin results by group, listed as mean ± SEM.

	GROUP			
Parameter	Control	1 PE	1 BE	5 BE; Exp. 1
Glucose	118.0 ± 5.9	**137.5 ± 6.5***	**139.4 ± 4.4†**	**136.1 ± 5.6#**
Hemoglobin	14.6 ± .22	14.4 ± .29	14.3 ± .18	14.4 ± .20

* = p values < 0.05 compared to control; † = p value < 0.05 compared to control & # = p value < 0.05 compared to control.

Glucose and Hemoglobin: Between Exposures

Glucose and hemoglobin values listed by exposure are listed in Table 15. To compare the effects of repeated anesthesia exposure on glucose and hemoglobin values, a one-way repeated measures ANOVA was conducted. There was no significant effect of repeated anesthesia exposures on mean glucose levels [Wilks' Lambda = 0.714, F(2,11) = 2.21, p = 0.156]. There was a significant effect of repeated anesthesia exposures on hemoglobin levels [Wilks' Lambda = 0.400, F(2,11) = 8.236, p = 0.007]. Post hoc tests revealed that anesthesia exposure significantly increased hemoglobin levels between Exposure 1 (14.3 ± 0.63) and Exposure 5 (15.0 ± 0.36, p = 0.003), but not Exposure 3 (14.8 ± 0.74, p = 0.056). The effect size, measured by Partial Eta squared, is 0.60 indicates a large effect. However, this difference is not clinically relevant as both values are within normal parameters (13.2- 16.7).

Table 15. Glucose and hemoglobin values by exposure, listed as mean ± SEM.

EXPOURE			
Parameter	1	3	5
Glucose	136.1 ± 5.6	133.9 ± 5.0	122.9 ± 4.3
Hemoglobin	14.4 ± .1	14.8 ± .2	**15.0 ± .1***

* = p values < 0.05 compared to control

QUANTITATIVE REAL TIME POLYMERASE CHAIN REACTION RESULTS

To explore mRNA expression levels of CL-5, occludin, and ZO-1 at 4 and 24 hours following 1 PE, 1 BE, or 5 BE's to 1.5% isoflurane, hippocampal tissue was analyzed by qRT-PCR with results displayed in Table 16.

At 4 hours following 1 PE to 1.5% isoflurane, there were no significant changes in CL-5 (FC: 1; p = 0.999), occludin (FC: -1.1, p = 0.481), or ZO-1 (FC: 1.27; p = 0.205) levels (Figure 2). Additionally, there were no change in CL-5 (FC: 1, p = 0.875), occludin (FC: -1.25; p = 0.085), or ZO-1 (FC: 1; p =0.649) levels at 24 hours following 1 PE to isoflurane (Figure 3).

In the 1 BE group, there were no significant changes in mRNA levels at either 4 hours [(CL-5- FC: 1; p = 0.929) (occludin – FC: 1; p = 0.951) (ZO-1 – FC: 1.1; p = 0.555)] or 24 hours [(CL-5 – FC: 1; p = 0.932) (occludin- FC: -1.1; p =0.496) (ZO-1 – FC: 1.1; p = 0.220)] following a isoflurane exposure (Figure 4).

At 4 hour following 5 BE's to 1.5% isoflurane, there were no significant changes in CL-5 (FC: -1.1; p = 0.267), occludin (FC: 1; p = 0.898), or ZO-1 (FC: 1; p = 0.993) mRNA levels (Figure 5). Additionally, there was no changes in CL-5 (FC: -1.1; p = .0.413), occludin (FC: -1.25; p = 0.276), and ZO-1 (FC: 1; p = 0.431) mRNA levels at 24 hours following 5 BE's to isoflurane (Figure 5).

Table 16. RT-qPCR mean ΔΔCt values, fold change, and p-values for study proteins.

EXPOSURE GROUP						
	1 PE- 4 Hours (n=4)			**1 PE – 24 Hours (n=4)**		
Gene	ΔΔCt	Fold Change	p value	ΔΔCt	Fold Change	p value
CL-5	0.00 ± 0.05	1	0.999	0.17 ± 0.15	1	0.875
Occludin	0.12 ± 0.15	-1.1	0.481	0.34 ± 0.09	-1.25	0.085
ZO-1	-.11 ± 0.13	1.27	0.205	-0.04 ± 0.09	1	0.649
	1 BE– 4 Hours (n=4)			**1 BE– 24 Hours (n=3)**		
CL-5	-0.02 ± 0.21	1	0.929	0.01 ± 0.11	1	0.932
Occludin	-0.01 ± 0.09	1	0.951	0.11 ± 0.14	-1.1	0.496
ZO-1	-0.06 ± 0.09	1.1	0.555	-.13 ± 0.10	1.1	0.220
	5 BE– 4 Hours (n=4)			**5 BE– 24 (n=4)**		
CL-5	0.15 ± 0.13	-1.1	0.267	0.12 ± 0.03	-1.1	0.413
Occludin	-0.02 ± 0.08	1	0.898	0.19 ± 0.19	-1.25	0.276
ZO-1	-0.01 ± 0.03	1	0.993	0.02 ± 0.04	1	0.431

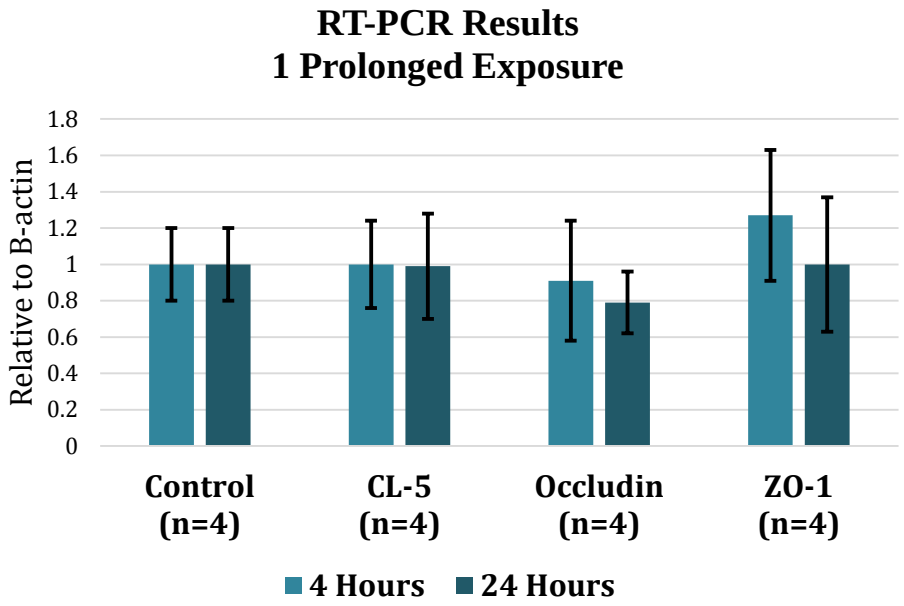

Figure 3. Real-time RT-PCR analysis of CL-5, occludin, and ZO-1 mRNA levels following a 1 Prolonged Exposure (4 hour) to 1.5% isoflurane.

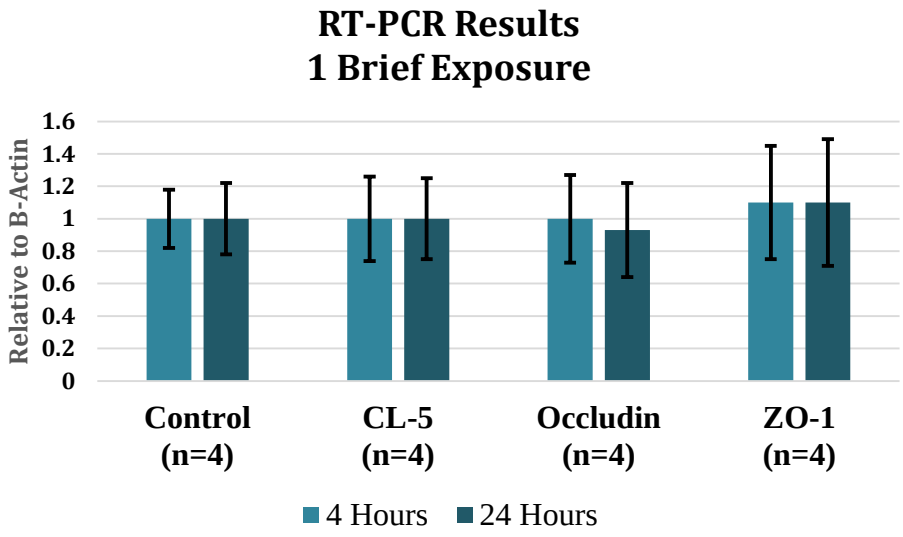

Figure 4. RT-PCR analysis of CL-5, occludin, and ZO-1 mRNA levels following 1 Brief Exposure (2 Hours) to 1.5% isoflurane.

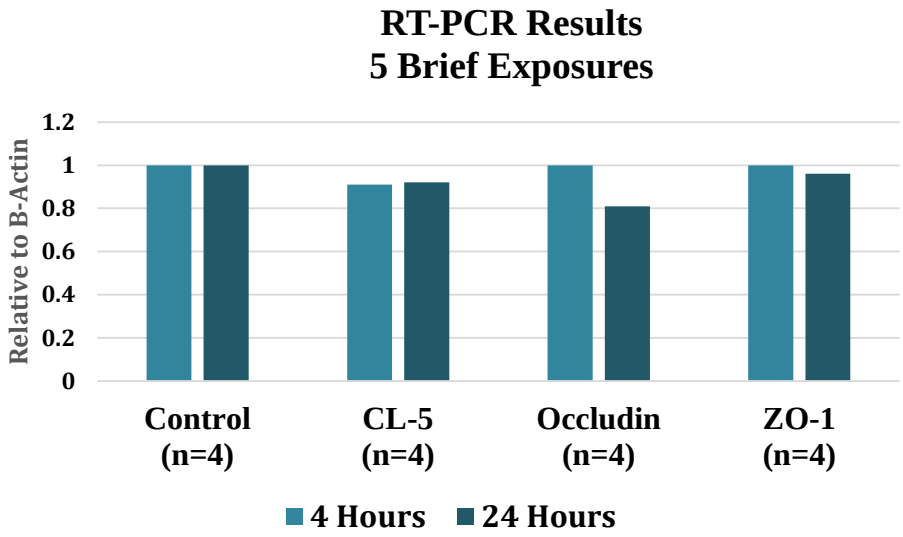

Figure 5. RT-PCR analysis of CL-5, occludin, and ZO-1 mRNA levels following 5 Brief (2 Hour) exposures to 1.5% isoflurane on consecutive days.

RNA SEQUENCING RESULTS

Overview

Since there were minimal changes in the specific proteins of interest (CL-5, occludin, & ZO-1), the expression profile of protein encoding genes in the hippocampus of control (n=4) and 1 PE4 (n=4) was explored. After quality control checks were completed, 2 animals in the control group and 1 animal in the 1 PE group were removed from analysis. Following alignment and quantification, 17,031 genes underwent differential expression analysis with 1,553 genes showing a significant ($p < 0.05$) change between C4 and 1 PE4 animals. From these 1,553 genes, transcripts were narrowed down to those genes that showed a greater/less than 1.64 fold change from control animals. Applying this criteria led to the identification of 207 up-regulated and 333 down regulated genes. The top 15 up and down regulated genes are listed in Table 17.

Table 17. Top 15 up and down regulated genes following 1 PE to 1.5% isoflurane.

UP REGULATED GENES			DOWN REGULATED GENE		
Gene	**Log_2 Fold Change**	**Absolute Change**	**Gene**	**Fold Change**	**Absolute Change**
Ntrk1	3.91	15.04	Htra4	-2.99	-7.95
Ccdc27	3.45	10.92	S100a9	-2.98	-7.90
Hdc	3.37	10.36	Odf311	-2.74	-6.73
Cd3e	2.74	6.68	Trhr2	-2.52	-5.74
Cyp1b1	2.63	6.21	Cbln4	-2.33	-5.06
Fam111a	2.35	5.12	Epcam	-2.28	-4.87
Ppl	2.33	5.04	Prph	-2.25	-4.77
Nmb	2.11	4.33	Cbln1	-2.21	-4.64
Mltia	2.10	4.30	Plagl1	-2.20	-4.59
Car3	2.10	4.28	Rxrg	-2.08	-4.25
Spata18	1.95	3.88	Fam129c	-2.01	-4.06
Cyp4b1	1.94	3.86	Kcnfl	-2.00	-4.04
Tnnt1	1.94	3.85	Trhr	-1.99	-3.97
Sulta1	1.92	3.78	Ovol2	-1.99	-3.97
Pex11a	1.88	3.68	Dntt	-1.98	-3.89

Gene Ontology Biological Process Analysis

To search for gene combinations with particular cellular or physiological role, the 207 up and 333 down regulated genes were analyzed with GATHER for gene ontology analysis (35). The top 10 statistically significant biological functions are listed in Table 18. The significant pathways included processes such as communication, metabolism, neurogenesis, nerve/synaptic transmission, transport, and cell to cell signaling. Volatile anesthetics cause a dose dependent decrease in cerebral metabolic requirement for oxygen (CMRO2) and glucose (CMROl) by potentiating the inhibitory effects of GABA and glycine receptors and inhibiting the excitatory effects of glutamate, acetylcholine, and histamine (28).

Table 18. Top 10 Gene Ontology Processes.

Gene Ontology Number	Gene Ontology Name	Number of Gene	p Value
1. 0007154	Cell Communications	103	p< 0.0001
2. 0008152	Metabolism	97	p< 0.0001
3. 0007399	Neurogenesis	24	p< 0.0001
4. 0007268	Synaptic Transmission	18	p< 0.0001
5. 0019226	Nerve Transmission	18	p< 0.0001
6. 0044238	Primary Metabolism	87	p< 0.0001
7. 0030001	Metal Ion Transport	21	p< 0.0001
8. 0044237	Cellular Metabolism	34	p< 0.0001
9. 0007267	Cell-cell signaling	27	p< 0.0001
10. 0006813	Potassium Ion Transport	13	p< 0.0001

RNA-Seq: Study Proteins

The expression of transcripts for CL-5, occludin, and ZO-1 were compared between C4 and 1 PE4 animals with values listed in Table 19. Although there was a decrease in both transmembrane protein values, CL-5 (21.3 vs 16.8) and occludin (4.6 vs. 3.5), they did not reach statistical significance (CL-5: $p = 0.07$; occludin: $p = 0.07$). There was a statistically significant increase in ZO-1 transcripts in 1 PE4 animals (62.9)

compared to control (49.4; p = 0.02). However, this only resulted in a 1.27 fold increase and was not considered significant (FC ± 1.64).

Table 19. RNA Seq values for study proteins (Cl-5, occludin, & ZO-1)

Gene	Control Value	1PE4 Value	Log2 Fold Change	Absolute Fold Change	p-value
Cldn5	21.3	16.8	-0.33	-1.26	0.07
Occludin	4.6	3.5	-0.37	-1.29	0.07
ZO-1	**49.4**	**62.6**	**0.34**	**1.27**	**0.02***

*p values < 0.05 compared to control animals

RNA-Seq: BBB Accessory Proteins

In addition to CL-5, occludin, and ZO-1, special attention was paid to other transmembrane molecules and cytoplasmic adaptor proteins involved in BBB structure and function (55). Results for these transcripts are listed in Table 20. A heat map these additional transmembrane and cytoplasmic adaptor proteins, along with study proteins is provided in Figure 6.

There was a significant increase in JAM3 transcripts in the 1 PE4 (25.2) animals compared to C4 (19.2; p = 0.02) animals; however, it did not reach significance by fold change (1.31). Additionally, there was a statistically significant increase in TJP2 (p = 0.05), Magi2 (p = 0.03), MPP7 (p = 0.01), Pard3 (p = 0.008), Lin7c (p = 0.007), and Dlg1 (p = 0.002) in the 1 PE4 group compared to control. However, none of the fold changes was considered significant (± 1.64). Finally, there was a significant decrease in Clgn1 transcripts in 1 PE4 animals (5.3) compared control animals (9.7) by both p-value (p = 0.005) and fold change (-1.85).

Table 20. Differently expressed BBB transcripts including fold changes and p-value.

Gene	Control Value	1PE4 Value	Log2 Fold Change	Absolute Fold Change	p-value	Significance
Transmembrane Proteins						
Cldn1	2.3	1.8	-0.35	-1.27	0.195	No
Cldn10	23.8	21.6	-0.13	-1.09	0.47	No
Cldn12	15.8	16.7	0.08	1.06	0.63	No
Jam2	19.9	21.2	0.1	1.07	0.64	No
Jam3	19.2	25.2	0.39	1.31	**0.02***	No
Marveld1	1.59	1.57	-0.02	-1.1	0.94	No
Marveld2	1.56	1.82	0.21	1.01	0.53	No
Cytoplasmic Adaptors						
TJP2 (ZO-2)	13.9	17.1	0.30	1.23	**0.05***	No
TJP3 (ZO-3)	2.5	3.0	0.03	1.02	0.42	No
Magi2	54.1	68.0	0.33	1.25	**0.03***	No
Magi3	17.6	14.9	-0.23	-1.17	0.13	No
MPP7	5.6	8.2	0.55	1.46	**0.01***	No
Dlgap4	49.8	43.4	-0.19	-1.14	0.18	No
Cgnl1	**9.7**	**5.3**	**-0.87**	**-1.82†**	**0.005***	**Yes**
Dlg1	45.9	33.2	-0.47	-1.39	**0.002***	No
Pard6g	3.0	2.6	-0.18	-1.13	0.63	No
Pard3	9.6	13.0	0.43	1.34	**0.008***	No
Lin7c	147.2	198.3	0.42	1.33	**0.007***	No

* p-value < 0.05 compared to control. † Fold Change ± 1.64

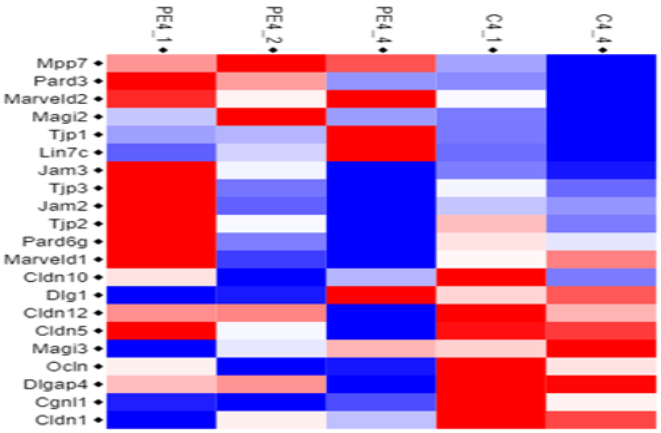

Figure 6. Heat map of study genes (CL-5, occludin, & ZO-1) and accessory transmembrane and cytoplasmic proteins.

RNA-Seq: Specific Brain Cell Markers

Exposure to volatile anesthetics creates a complex state of reversible loss of consciousness, amnesia, analgesia, and immobility. To accomplish such a complex state, multiple different cellular targets on a variety of different glial cells in diverse brain regions are involved (27). Therefore, the effects of 1 PE to isoflurane on specific brain cell markers was compared to control animals and is listed in Table 21 with a heat map provided as Figure 7.

There was no significant difference by either p-value or fold change between 1 PE4 animals compared to control in any neuronal, microglia, or pericyte specific marker. In exploring astrocyte specific markers, there was a statistically increase in GJB6 transcripts in 1 PE4 animals (54.6) compared to control (30.0; $p = 0.005$; FC = 1.82). Gap junction beta 6 (GJB6), or connexin 30, form channels between adjoining cells and allow for the passive flow of potassium or sodium between their cytoplasm's. In astrocytes, these channels allow for the flow of sodium between and vascular endothelial cells and are important for neurometabolic coupling (75).

For specific endothelial cell markers, there was a statistically significant decrease in Vwa1 (8.9) transcripts in 1 PE4 animals compared to control (6.6) by p-value ($p = 0.04$), but not by fold change (-1.35). Conversely, there was a significant increase in Ahnak transcripts in 1 PE4 animals (21.65) compared to control animals (17.39) by p-value ($p = 0.03$), but not by fold change (1.24). The endothelial cell markers Rgs4 and Zic1 were significantly alter by p-value and fold change. Compared to control animals (92.92), there was a statistically significant decrease in Rgs4 transcripts (34.79) in 1 PE4 animals ($p = 0.02$; FC: -2.68). In the 1 PE4 animals (8.11), there was a significant increase in Zic1 transcripts compared to control (3.65) at both p-value ($p = 0.001$) and

fold change (2.22). Regulator of G-proteins signaling, or Rgs4, is an important GTPase regulator of inhibitory G-protein subunits and aids in the termination of signals at the Mu opioid receptor while ZIC family member 1 is a transcription factor that is important for neurogenesis (210; 211). Volatile anesthetics have been shown to modulate the binding of ligands, such as naloxone, on opioid receptor and cause neurogenesis, especially in developing neurons (47; 227).

There was a statistically significant increase in the oligodendrocyte markers Mag ($p = 0.005$), Mog ($p = 0.008$), Cldn-11 ($p = 0.005$), and Sox10 ($p = 0.005$) in the 1 PE4 group compared to control animals by p-values, but not by fold change [(Mag - FC: 1.62) (Mog - FC: 1.49) (Cldn-11 – FC 1.05) (Sox10 - FC: 1.38)]. However, in comparing 1 PE4 animals to control animals, there was a statistically significant increase in the Mbp and Mobp transcripts by p-vale (Mbp: $p = 0.0015$; Mobp: $p = 0.0005$) and fold change (Mbp - FC: 1.67; Mobp – FC: 1.77). Myelin basic protein (MBP) is a major constituent of the myelin sheath for oligodendrocytes and is responsible for the formation and stabilization of the myelin sheath (22). In addition to myelin sheaths, Mbp is found in the bone marrow and immune cells (152). Myelin-associated oligodendrocyte basic protein (Mobp) is essential for compacting and stabilizing the myelin sheath and degradation is implicated in substance abuse disorders and Multiple Sclerosis (166). In the developing brain, a 5 hour exposure to isoflurane showed widespread apoptosis of oligodendrocytes (24; 177; 212).

Table 21. RNA-Seq results for brain specific markers listed by cell type.

Gene_ID	Control Value	Anesthesia value	Log2 Fold Change	Absolute Fold Change	p_value	Significance by p < 0.05 & fold ± 1.64
	Neurons					
Syp	444.4	403.7	-0.13	-1.09	0.35	No
KCC2	90.3	80.7	-0.16	-1.1	0.27	No
SNAP25	1065.8	1094.2	0.03	1.02	0.82	No
NEFL	311.3	343.7	0.14	1.1	0.34	No
NEFH	59.7	62.4	0.06	1.04	0.67	No
	Astrocyte					
Gfap	317.5	347.1	0.13	1.09	0.41	No
S100b	851.1	806.5	-0.07	-1.05	0.62	No
Aqp4	240.7	231.3	-0.10	-1.07	0.50	No
GLT-1	46.7	56.8	0.29	1.22	0.06	No
FGFR3	23.7	22.3	-0.09	-1.06	0.58	No
GJB6	**30.0**	**54.6**	**0.86**	**1.82†**	**0.0005***	**Yes**
	Microglia					
Tmem119	4.2	3.7	-0.18	-1.13	0.49	No
Aif1	16.9	17.3	0.03	1.02	0.89	No
CD68	0.87	1.1	0.43	1.34	0.25	No
CD86	0.82	1.3	0.82	1.76	0.16	No
CD80	0.46	0.46	0.00	1	0.98	No
ITGAM	5.2	4.4	-0.22	-1.16	0.27	No
	Pericyte					
Abcc9	4.8	3.9	-0.28	-1.21	0.13	No
PdgfrB	10.2	9.8	-0.06	-1.04	0.70	No
Kcnj8	1.4	1.9	0.41	1.32	0.29	No
Acta2	6.4	7.7	0.27	1.21	0.28	No
Gnas	952.7	892.9	-0.09	-1.06	0.55	No
	Oligodendrocyte					
Mbp	**1086.9**	**3021.5**	**0.74**	**1.67†**	**0.0015***	**Yes**
Mobp	**96.6**	**170.7**	**0.82**	**1.77†**	**0.005***	**Yes**
Mag	89.5	141.4	0.70	1.62	**0.005***	No
Mog	93.9	140.4	0.58	1.49	**0.008***	No
Cldn11	111.2	184.5	0.73	1.05	**0.005***	No
Sox10	16.9	23.4	0.47	1.38	**0.005***	No
	Endothelial					
Tie2	8.34	8.1	-0.04	-1.02	0.81	No
Rgs4	**92.92**	**34.79**	**-1.42**	**-2.68†**	**0.001**	**Yes**
Zic1	**3.65**	**8.11**	**1.15**	**2.22†**	**0.001**	**Yes**
Vwa1	8.9	6.6	-0.44	-1.35	**0.04***	No
Ahnak	17.39	21.65	0.32	1.24	**0.03***	No

* p-value < 0.05 compared to control; † Fold change ± 1.64

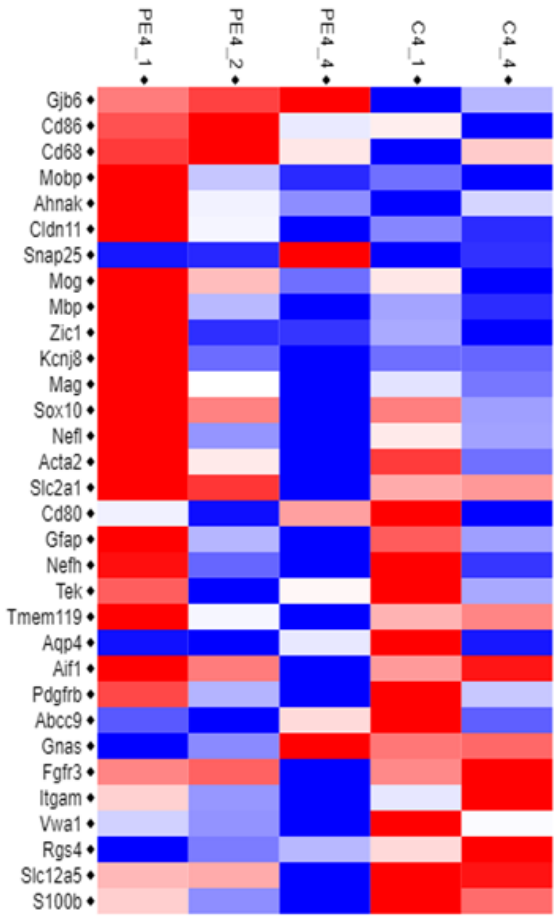

Figure 7. Heat map of specific brain cell markers.

Oligodendrocyte RT-PCR

Since there was a statistically significant increase in the 6 different oligodendrocytes markers, PCR primers were designed, ordered, and underwent RT-qPCR analysis. Oligodendrocyte RT-qPCR results are listed in Table 22. For each oligodendrocyte gene of interest, an independent samples t-test was conducted to compare the ΔΔCt values between control and 1 PE4 animals. There was a statistically significant difference in Mbp ΔΔCt values between control (1.0 ± 0.10) and 1 PE4 animals (1.40 ± 0.14, $t(4) = -3.8$, $p = 0.03$). The magnitude of difference in means is very large (Cohen's $d = 3.3$) between the 1 PE4 and control group. Additionally, there was a significant difference in Mobp ΔΔCt values between control (1.0 ± 0.17) and 1 PE4 animals (1.55 ± 0.21, $t(4) = -3.22$, $p = 0.05$). The magnitude of the difference in means is very large (Cohen's $d = 2.9$). Although there was a significant increase in Mag, Cldn-11, and Sox10 ΔΔCt values, they did not reach statistical significance.

Table 22. Oligodendrocyte PCR values and fold change.

Gene	ΔΔ CT Values	PCR p-values	PCR Fold Change	RNA Sequence Fold Change
MBP	**1.40 ± 0.10**	**0.03***	**1.38**	**1.67†**
MOBP	**1.55 ± 0.21**	**0.05***	**1.56**	**1.77†**
MAG	1.41 ± 0.14	0.09	1.42	1.62
CLDN-11	1.50 ± 0.28	0.06	1.51	1.50
SOX10	1.40 ± 0.01	0.21	1.43	1.38

*p-values < 0.05 compared to control; † Fold change ± 1.64

RNA-Seq: Volatile Anesthetic Targets

Volatile anesthetics have been show to enhance inhibitory neurotransmitters (GABA & glycine) and diminish excitatory neurotransmitters (glutamate, acetylcholine, serotonin, and histamine) (28). Additionally, multiple different ion channels (potassium & sodium) and opioid receptors may also be affected. Results for anesthesia specific

markers are presented as inhibitory, excitatory (glutamate, acetylcholine & histamine/serotonin), opioid, and ion channels (83; 102). A heat map of anesthesia targets is presented in Figure 8.

RNA-Seq: Volatile Anesthesia Targets: Inhibitory

Inhibitory anesthesia targets are listed in Table 23. In 1 PE4 animals, there was a significant decrease in GabrA1 and GabrB2 transcripts compared to control animals by p-value (GabrA1- p = 0.009; Gabrb2 0.01) but not fold change (GabrA1- FC: -1.31; GabrB2 – FC: -1.32). Additionally, there was a significant increase in GabrB3 transcripts in 1 PE4 animals compared to control by p-value (0.02) but not by fold change (1.27). There was a statistically significant decrease in GabaB3 and Glra1 transcripts in 1 PE4 animals compared to control by both p-values (GabaB3: p = 0.001; Glra1: p = 0.001) and fold change (GabaB3: -1.92; Glra1: -2.07). The gamma-aminobutyric acid receptor subunit A3 (GabrB3) is highly expressed in the hippocampus and is associated with Prader-Willi and Angelman Syndrome, both of which display intellectual disabilities (65). The glycine receptor alpha 1 (Glra1) helps mediate post-synaptic inhibition and is associated with hyperkplexia, or startle syndrome (162).

Table 23. Inhibitory Anesthesia Targets (GABA & Glycine)

Gene_ID	Control Value	Anesthesia Value	Log2 Fold Change	Absolute Fold Change	p-value	Significance
GabrA1	151.9	115.5	-0.39	-1.31	**0.009***	No
GabrA2	130.4	124.7	-0.06	-1.04	0.66	No
GabrA3	**29.43**	**15.32**	**-0.94**	**-1.92†**	**0.001***	**Yes**
GabrA4	53.9	64.0	0.24	1.18	0.12	No
GabrA5	97.1	107.3	0.14	1.01	0.33	No
GabrA6	0.27	0.28	0.01	1.00	0.89	No
GabrB1	94.5	96.0	0.02	1.01	0.88	No
GabrB2	59.9	45.1	-0.41	-1.32	**0.01***	No
GabrB3	141.2	178.9	0.34	1.27	**0.02***	No
Glra1	**0.37**	**0.18**	**-1.05**	**-2.07†**	**0.001***	**Yes**
Glra2	5.3	6.6	0.33	1.26	0.10	No
Glra3	1.6	0.9	-0.81	-1.7	0.11	No
Gla4	0.34	0.35	0.03	1.02	0.89	No

* p-values < 0.05 compared to control animals; † Fold Change ± 1.64

RNA-Seq: Volatile Anesthetics - Excitatory

RNA-Seq: Excitatory - Glutamate receptors

In the central nervous syndrome (CNS), glutamate is the primary excitatory neurotransmitter and binds to either metabotropic receptors (mGluR) or inotropic (AMPA, kinate, or NMDA) receptors. Results for glutamate receptors are listed in Table 24. Compared to control animals, there was a significant increase in Grin2a, Gria1, and Grik4 transcripts in 1 PE4 animals by p-value (Grin2a: p = 0.01; Gria1: p = 0.01; Grik4: p = 0.01), but not by fold change (Grin2a: 1.46; Gria1: 1.27; Grik4: 1.31). Conversely, there was a significant decrease in Grin2c, Grik1, and Grm2 transcripts in 1 PE4 animals compared to control by p-values (Grin2c: p = 0.02; Grik1: p = 0.02; Grm2: p = 0.007), but not by fold change (Grin2c: -1.30; Grik1: -1.37; Grm2: -1.51). Finally, there was a significant decrease in Grin2d, Grin3a, Grik3, Grm4, and Grm8 in 1 PE4 animals

compared to control by both p-values (Grin2d: p = 0.01; Grin3a: p = 0.01; Grik3: p = 0.05; Grm4: p = 0.005; Grm8: p = 0.005) and by fold change (Grind2d: -1.65; Grin3a: -2.07; Grik3: -2.14; Grm4: -1.83; Grm8: -2.64). Grin2d helps mediate synaptic transmission in hippocampal interneurons while Gin3a is important for interactions between neurons and glial cells (119; 188). Both Grik3 and Grm8 may play a role in depressive disorders and alcoholism while Grm4 may protect the brain against hypoxic damage (132; 213).

Table 24. Volatile anesthetics: Excitatory glutamate receptor subunits.

Gene_ID	Control Value	Anesthesia Value	Log2 Fold Change	Absolute Fold Change	p-value	Significance
Glutamate Receptors						
Grin1	127.44	135.16	0.08	1.06	0.56	No
Grin2A	115.49	169.10	0.55	1.46	**0.001***	No
Grin2B	147.20	149.99	0.03	1.02	0.86	No
Grin2C	20.13	15.43	-0.38	-1.30	**0.02***	No
Grin2D	**2.11**	**1.28**	**-0.72**	**-1.65†**	**0.01***	**Yes**
Grin3A	**10.86**	**5.23**	**-1.05**	**-2.07†**	**0.01***	**Yes**
Grin3B	0.55	0.61	0.14	1.1	0.99	No
Gria1	199.9	255.2	0.35	1.27	**0.01***	No
Gria2	247.6	292.8	0.24	1.18	0.14	No
Gria3	87.3	95.4	-0.12	-1.09	0.38	No
Gria4	57.0	47.5	-0.26	-1.20	0.09	No
Grik1	12.4	9.1	-0.45	-1.37	**0.02***	No
Grik2	52.1	48.2	-0.11	-1.08	0.44	No
Grik3	**15.2**	**7.0**	**-1.1**	**-2.14†**	**0.005***	**Yes**
Grik4	26.2	34.3	0.39	1.31	**0.01***	No
Grik5	35.5	37.4	0.06	1.04	0.66	No
Grm1	17.7	23.6	0.41	1.02	0.07	No
Grm2	12.5	8.3	-0.60	-1.51	**0.007***	Yes
Grm3	83.1	74.0	-0.16	-1.11	0.26	No
Grm4	**4.7**	**2.5**	**-0.87**	**-1.83†**	**0.05***	**Yes**
Grm5	80.2	76.6	-0.06	-1.04	0.66	No
Grm6	1.3	1.2	-0.10	-1.07	0.70	No
Grm7	53.2	47.8	0.21	1.16	0.10	No
Grm8	**13.4**	**5.0**	**-1.4**	**-2.64†**	**0.005***	**Yes**

* p-values < 0.05 compared to control; † Fold change ± 1.64

RNA-Seq: Excitatory - Acetylcholine Receptors

In addition to inhibiting glutamate receptors, volatile anesthetics also alter the firing of neuronal acetylcholine receptors. In the brain acetylcholine plays an important part in pain interpretation, learning, memory, and attention. The effects of 1 PE to isoflurane on neuronal nicotinic receptor subunits (Chrna) is listed in Table 25. There was a significant increase in Chrna1 values in 1 PE animals compared to control by both p-value (0.05) and fold change (1.68). Additionally, there was a significant decrease in Chran3, Chrna4, and Chrna5 transcripts in 1 PE4 animals compared to control by p values (Chrna3: p = 0.02; Chrna4: p = 0.02; & Chrna5: p = 0.002) and fold change (Chran3 – FC: -3.03; Chrna4 – FC: -3.18 & Chrna5 – FC: -2.00). The cholinergic receptor family (Chrna1-5) play an important role in nicotine dependency, frontal lobe epilepsy, synaptic transmission, and attention (219).

Table 25. Excitatory volatile anesthesia targets: Acetylcholine

Gene_ID	Control Value	Anesthesia Value	Log2 Fold Change	Absolute Fold Change	p-value	Significance
Chrna1	**1.1**	**1.9**	**0.75**	**1.68**	**0.05***	**Yes**
Chrna2	2.2	3.5	0.66	1.59	0.03	Yes
Chrna3	**1.3**	**0.4**	**-1.60**	**-3.03**	**0.02***	**Yes**
Chran4	**14.7**	**4.6**	**-1.67**	**-3.18**	**0.005***	**Yes**
Chrna5	**9.0**	**4.3**	**-1.0**	**-2.00**	**0.005***	**Yes**

*****p-values < 0.05 compared to control; † Fold change ± 1.64

RNA-Seq: Excitatory - Histamine Receptors

Histamine receptors play an important role in promoting wakefulness, feeding behaviors, motivation and acquiring and maintaining both short and long term memories. Since amnesia is an important component of anesthesia, the effects of 1 PE to isoflurane on histamine receptors was evaluated and listed in table 26. There was a significant

reduction in Hrh3 transcripts in 1 PE group compared to control by both p-value (0.005) and fold change (-1.83). The histamine 3 receptor is important for cognitive process in the hippocampus and helps regulate oligodendrocyte differentiation and regulation (39; 145).

Table 26. Excitatory volatile anesthetics: Histamine

Gene_ID	Control Value	Anesthesia Values	Log2 Fold Change	Absolute Fold Change	p-value	Significance
Hrh1	4.6	6.1	0.40	1.32	0.13	No
Hrh2	6.5	4.8	-0.43	-1.35	0.14	No
Hrh3	**27.6**	**12.3**	**-0.87**	**-1.83†**	**0.005***	**Yes**

*p = < 0.05 compared to control; † Fold change ± 1.64

RNA-Seq: Opioid Receptors

Isoflurane may alter the binding of ligands to the opioid receptors in the brain. Therefore, the effects of isoflurane on the different opioid receptors was evaluated with results listed in Table 27. There was a significant decrease in Oprd1 and Oprl1 transcripts in 1 PE4 animals compared to control animals by both p-value (Oprd1 – p = 0.03; Oprl1 – p = 0.005) and by fold change (Oprd1- FC: -1.99; Oprl1 – FC: -1.73). The delta type opioid receptor (Oprd1) is important for pain perception and opiate facilitated analgesia while the opioid related nociception receptor (Oprl1) are involved in learning, memory, stress response, inflammation, and immune response (11; 104).

Table 27: Volatile anesthesia targets: Opioid receptors.

Opioid Receptors						
Oprm1	6.7	5.2	-0.37	-1.29	0.17	No
Oprk1	0.63	0.27	-1.2	-2.29	No Test#	No
Oprd1	**2.2**	**1.1**	**-0.99**	**-1.99†**	**0.03***	**Yes**
Oprl1	**17.2**	**9.9**	**-0.79**	**-1.73†**	**0.005***	**Yes**

* p-values <0.05 compared to control; † Fold change ± 1.64; # Insufficient read depth for accurate analysis.

RNA-Seq: Ion Channels

In addition to altering inhibitory and excitatory receptors, volatile anesthetics have also been shown to alter different neuronal ion channels that can potentially alter resting membrane potential and neurotransmitter release. Calcium (Ca+) and potassium (+) ion channel receptor subunits that are important for neuronal signaling are listed in Table 28. There was a significant increase in Cacna1a and Cacna1h values in 1 PE4 animals compared to control animals by p-value (Cacna1a: $p = 0.01$; Cacna1g: $p = 0.02$), but not by fold change (Cacna1a – 1.30; Cacna1g – 1.27). Conversely, there was a significant decrease in Cacna1i and Kcnk10 values in 1 PE4 animals compared to control by p-value (Cacna1i: $p = 0.01$; Kcnk10: $p = 0.02$), but not by fold change (Cacna1i: -1.31; Kcnk10: -1.41). In Cacna1g, Kcnk9, and Kcnk12, there was a significant decrease in transcript amounts in the 1 PE4 animals compared to control animals by both p-value (Cacna1g: $p = 0.001$; Kcnk9: $p = 0.001$; Kcnk12: $p = 0.001$) and by fold change (Cacna1g: -2.01; Kcnk9: -2.60; Kcnk12: -2.32). The A1g subunit of voltage gated neuronal calcium channels (Cacna1g) plays an important role in baseline neuronal oscillation and modulations in central pain syndromes (42; 43). In addition to playing a role in cognition, Kcnk9 channels play a role in protecting neurons from oxygen-glucose depravation (139). The tandem pore domain halothane inhibited potassium channel (Thik-2 or Kcnk12) are found throughout the brain and dorsal root ganglion and may play a role in inflammation signaling and pain transmission (90; 236).

Table 28. Volatile anesthesia targets: Ion channels

Gene_ID	Control Value	Anesthesia Value	Log2 Fold Change	Anesthesia Fold Change	p-value	Significance
Calcium Channels						
Cacna1a	39.11	51.00	0.38	1.30	**0.01***	No
Cacna1b	33.24	32.36	-0.04	-1.03	0.79	No
Cacna1c	24.37	28.90	0.25	1.19	0.10	No
Cacna1d	19.63	23.13	0.24	1.19	0.12	No
Cacna1e	104.38	117.83	0.17	1.13	0.25	No
Cacna1g	**17.73**	**8.8**	**-1.01**	**-2.01**	**0.001***	**Yes**
Cacna1h	18.71	23.82	0.35	1.27	**0.02***	No
Cacna1i	24.62	18.72	-0.39	-1.31	**0.01***	No
Cacnb1	36.12	31.96	-0.18	-1.13	0.26	No
Cacnb2	30.21	46.85	0.63	1.54	**0.001***	No
Cacnb3	50.31	47.78	-0.07	-1.05	0.063	No
Cacnb4	61.60	42.85	-0.52	-1.43	**0.001***	No
Potassium Channels						
Kcnk1	18.68	18.68	0	-1.00	0.98	No
Kcnk2	9.99	7.52	-0.41	-1.32	0.06	No
Kcnk3	0.92	0.50	-0.87	-1.83	0.88	No
Kcnk4	17.36	10.99	-0.66	-1.58	0.88	No
Kcnk5	0.49	0.39	-0.33	-1.26	0.98	No
Kcnk9	**15.75**	**6.05**	**-1.38**	**-2.60†**	**0.0001***	**Yes**
Kcnk10	5.90	4.18	-0.50	**-1.41**	**0.02***	No
Kcnk12	**4.66**	**2.00**	**-1.22**	**-2.32†**	**0.001***	**Yes**
Kcnk13	0.71	0.70	0.02	1.01	0.99	No

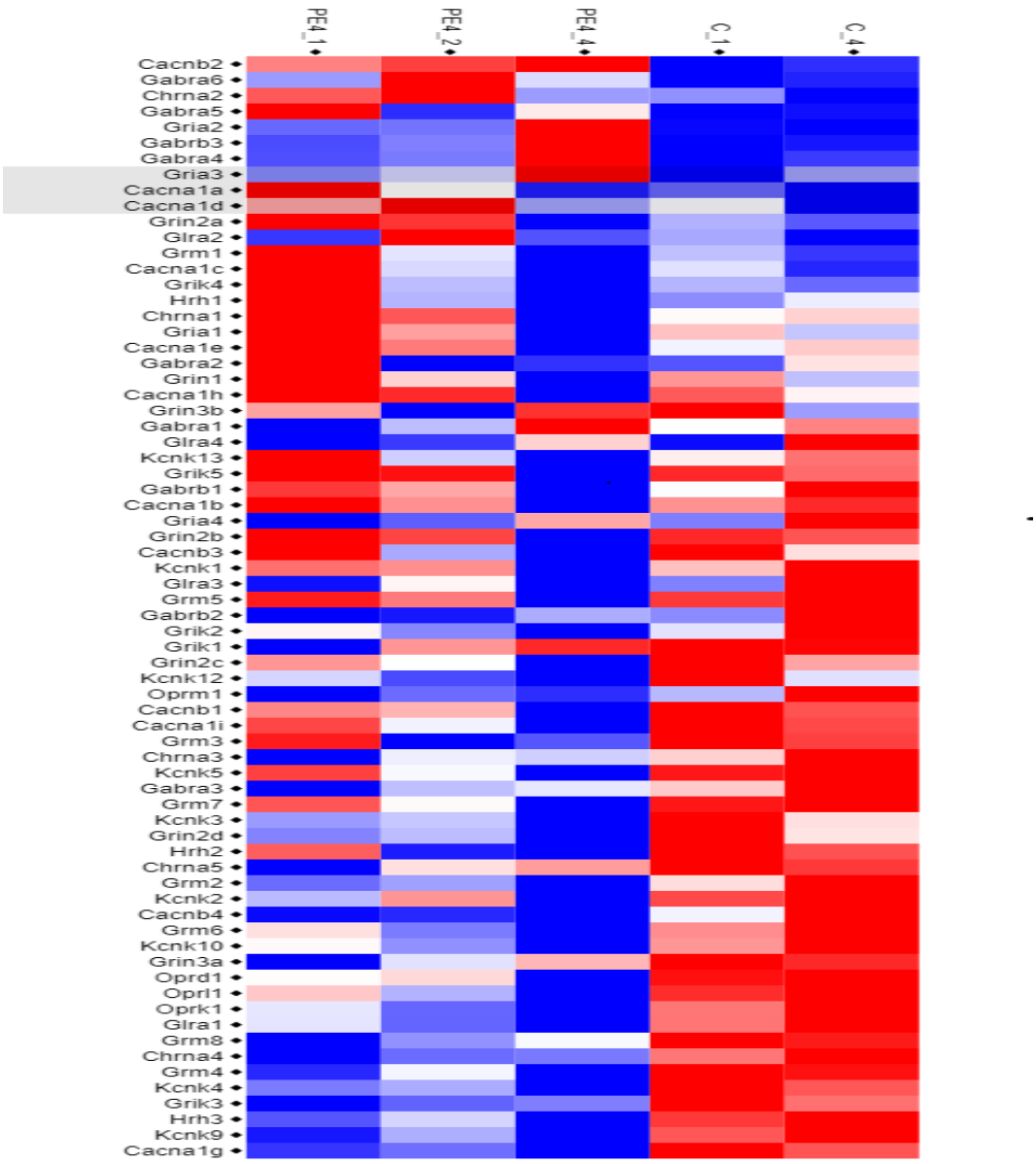

Figure 8. Heap map of inhibitory and excitatory anesthesia targets, and ion channels.

WESTERN BLOT

Immunoblotting, or Western Blotting, analysis was conducted to separate, identify, and quantify protein levels of CL-5, occludin, and ZO-1 in hippocampal tissue. Samples from 3 control animals, 5 animals from each of the cohorts (4-hour & 24-hour), and 2 ladders was loaded onto each gel with relative expression being normalized to B-actin. Each experiment was repeated at least 3 times.

Single Prolonged Exposure

Following 1 PE to 1.5% isoflurane, there was a significant difference in CL-5 [$F(2,9) = 7.951$; $p = 0.010$], occludin [$F(2,9) = 40.449$; $p = 0.001$], and ZO-1 [$F(2,9) = 47.903$; $p = 0.001$]. In looking at CL-5, post hoc testing revealed a significant CL-5 value in the 4-hour cohort (307.17 ± 11.28; $p = 0.030$) but not the 24-hour cohort (353.83 ± 8.03) when compared to the control cohort (352.03 ± 7.92) (Figure 9A). Additionally, when comparing CL-5 values in the 4-hour cohort (307.17 ± 11.28) to 24-hour cohort values (353.83 ± 8.03), a statistically significant increase ($p = 0.012$) back to control values was noted. Following 1 PE, there was a statistically significant decrease in occludin values in both the 4-hour cohort (217 ± 6.11; 0.001) and 24-hour cohort (254.65 ± 9.82; $p = 0.001$) compared to control values (320.83 ± 7.55) (Figure 9B). Additionally, there was a statistically significant increase in occludin values in the 24-hour cohort (254.65 ± 9.82) compared to the 4-hour cohort (217 ± 6.11; p = 0.-16). There was a statistically significant increase in ZO-1 values in both the 4-hour cohort (374.73 ± 14.61; $p = 0.010$) and 24-cohort (468.30 ± 8.40; $p = 0.001$) compared to control values (307.63 ± 8.34) (Figure 9C). Furthermore, there was statistically significant increase in ZO-1

values between the 4=hour cohort (374.73 ± 14.61; p = 0.001) and the 24-hour cohort (468.30 ± 8.40).

Single Brief Exposure

Following a single brief exposure to 1.5% isoflurane, there was no significant difference in the expression of CL-5 [F(2,9) = 3.095; p = 0.101], occludin [F(2,10) = 0.143; p = 0.868], ZO-1 [F(2,10) = 3.237; p = 0.0.82] in either the 4-hour cohort (CL-5: p = 0.088; occludin: p = 0.966; ZO-1: p = 0.301) or the 24-hour cohort (CL-5: p = 0.0492; occludin: p = 0.976; ZO-1: p = 0.089). Additionally, there was no significant difference in CL-5 (p = 0.391), occludin (p = 0.857), or ZO-1 (p = 0.482) levels between the 4-hour cohort and 24 hour cohort.

5 Brief Exposures

Following 5 BE's to 1.5% isoflurane, there was no significant difference in the expression of CL-5 [F(2,9) = 1.495; p = 0.275] (Figure 10A) or ZO-1 [F(2,9) = 2.123; p = 0.128] (Figure 10C) at in either the 4-hour cohort (CL-5: p = 0.440; ZO-1: p = 0.440) or the 24-hour cohort (CL-5: p = 0.985; ZO-1: 0.189). However, there was a significant decrease in occludin levels [F(2,9) = 28.865; p = 0.001] (Figure 10B) in both the 4-hour (263.34 ± 11.69; p = 0.001) and 24-hour cohort (344.62 ± 16.65; p 0.029) compared to control (409.38 ± 8.80). Additionally, there was a significant recovery of occludin levels between the 4-hour (263.34 ± 11.69) and 24-hour cohort (344.62 ± 16.65; p = 0.004).

Figure 9A

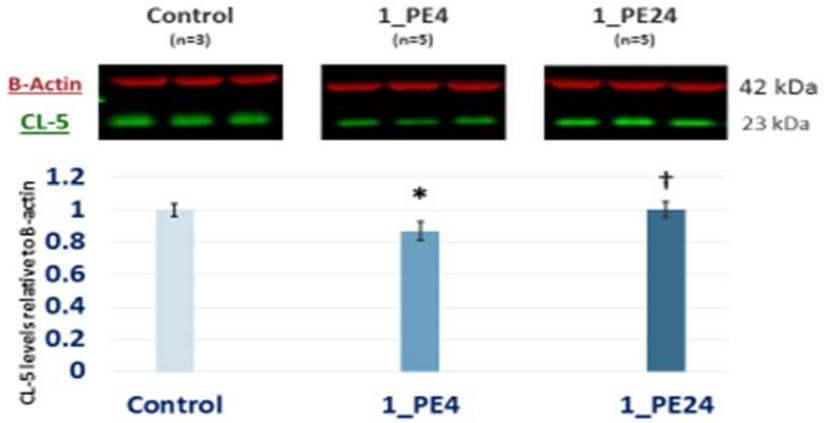

Figure 9B

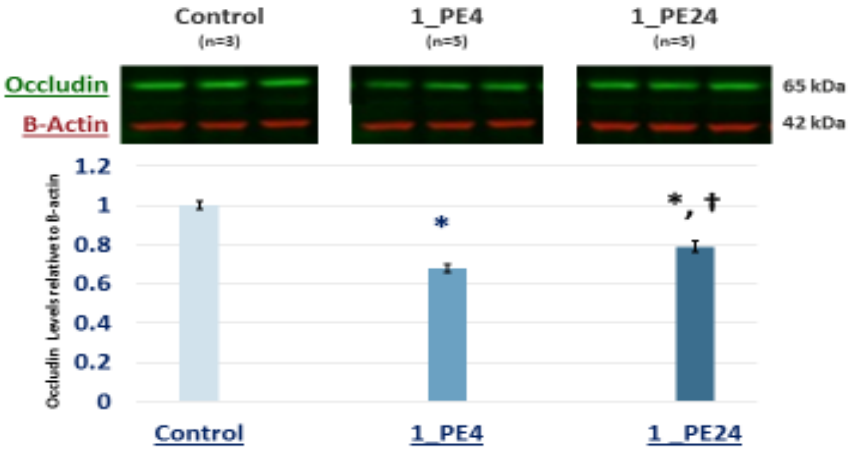

Figure 9C

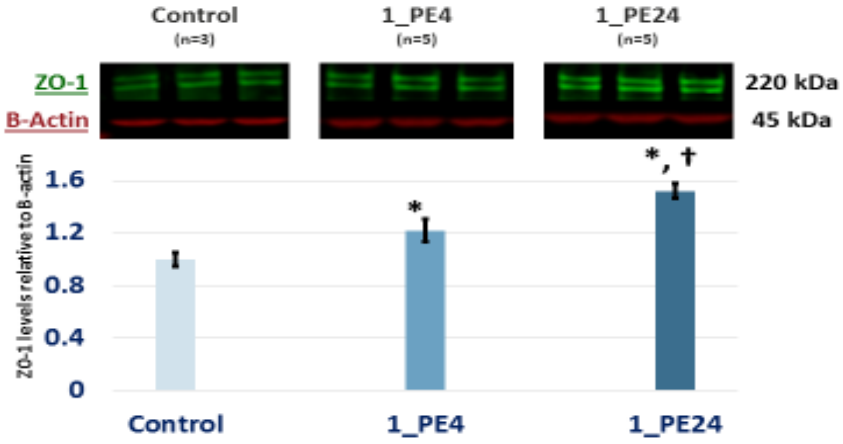

Figure 9. Western blot analysis of CL-5 (9A), occludin (9B), and ZO-1 (9C) protein levels following 1 PE to 1.5% isoflurane. * $p < 0.05$ compared to control group; † $p < 0.05$ compared to 1_PE4 group

Figure 10A

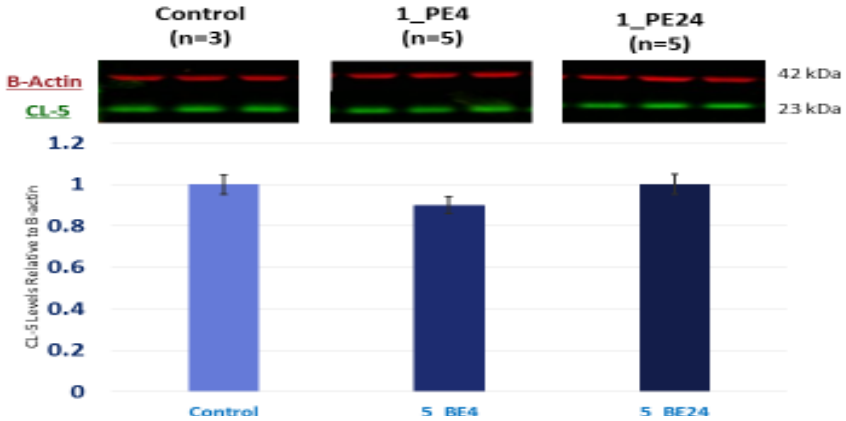

Figure 10B

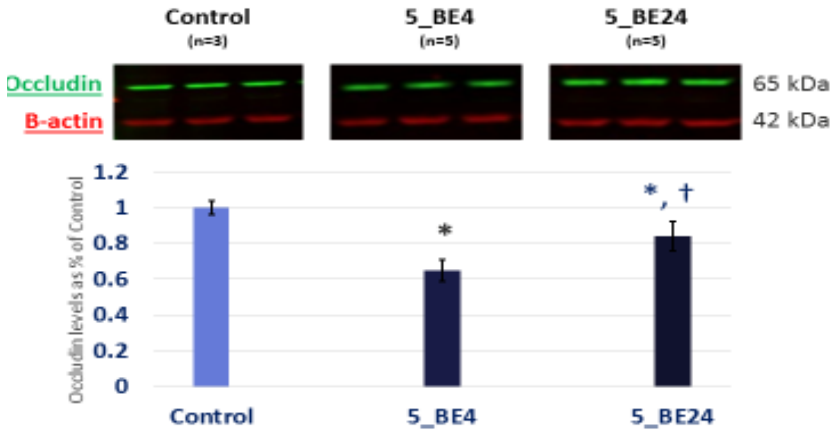

Figure 10C

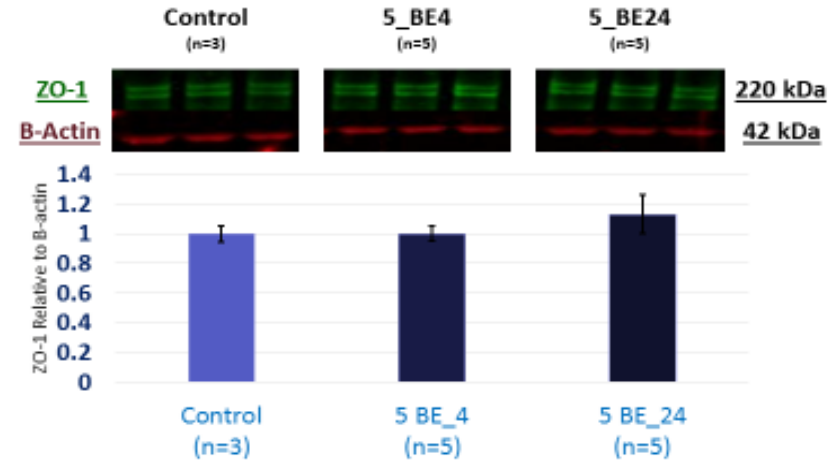

Figure 10. Western blot analysis of CL-5 (10A), occludin (10B), and ZO-1 (10C) protein levels following 5 BE's to 1.5% isoflurane. * $p < 0.05$ compared to control group; † $p < 0.05$ compared to 1_PE4 group

IMMUNOHISTOCHEMISTRY

To analyze the percentage of CL-5, occludin, and ZO-1 levels in hippocampal blood vessels compared to lectin staining at 4 and 24 hours following 1 PE, 1 BE, or 5 BE's exposures to 1.5% isoflurane, 5 equivalent sections from each animal underwent immunofluorescent staining and microscopic analysis. Sections started at Bregma -2.40 mm and were 200 microns apart. In each of the 5 hippocampal section, 5 vessels (5 sections x's 5 vessels = 25 vessels/animal) were analyzed and then averaged together to obtain 1 value per animal. The proteins of interest (CL-5, occludin, and ZO-1) were stained green, the lumen of the blood vessel was stained red (lectin), and the cell nuclei was stained blue (DAPI).

Single Prolonged Exposure

Immunohistochemistry results for CL-5 (Figure 11A), occludin (Figure 11B) and ZO-1 (Figure 11C) following 1 PE to isoflurane can be found in Figure 10. Following 1 PE to 1.5% isoflurane, there was a significant decrease in the percentage of CL-5 [$F(3,10) = 19.67$; $p = 0.001$], occludin [$F(3,10) = 36.429$; $p = 0.001$], and ZO-1 [$F(3,10) = 18.077$; $p = 0.001$] expression in hippocampal blood vessels compared to control (Figure 11). There was a significant decrease in expression of CL-5 in the 4 hour cohort (8.54 ± 0.25; $p = 0.001$), but not the 24 hour cohort (10.03 ± 0.17; $p = 0.823$) compared to control (10.22 ± 0.16) animals (Figure 11A). Additionally, the decrease in CL-5 levels seen in the 4 hour cohort significantly recoved back to baseline levels in control 24 hour (10.01 ± 0.07; $p = 0.001$) animals. There was a significant decrease in occludin expression in both the 4 hour cohort (5.62 ± 0.12; $p = 0.001$) and the 24 hour cohort (7.00 ± 0.10) compared to the control animals (8.10 ± 0.10) (Figure 11B). Additionally, there

was a significant increase in occludin levels between the 4 hour cohort (5.62 ± 0.12) and the 24 hour cohort (7.00 ± 0.10; p = 0.005), but not back to control values (8.10 ± 0.10) though (Figure 11B). In looking at ZO-1, there was a significant decrease in ZO-1 levels in the 4 hour cohort (11.30 ± 0.14; p = 0.001) compared to control animals (14.71 ± .050), but not in the 24 hour cohort (14.43 ± 0.20; p = 0.952) (Figure 11C). There was a significant recover of ZO-1 levels between 4 hour cohort (11.30 ± 0.14) and 24 hour cohort (14.43 ± 0.20; p = 0.001) (Figure 11C).

Figure 11A

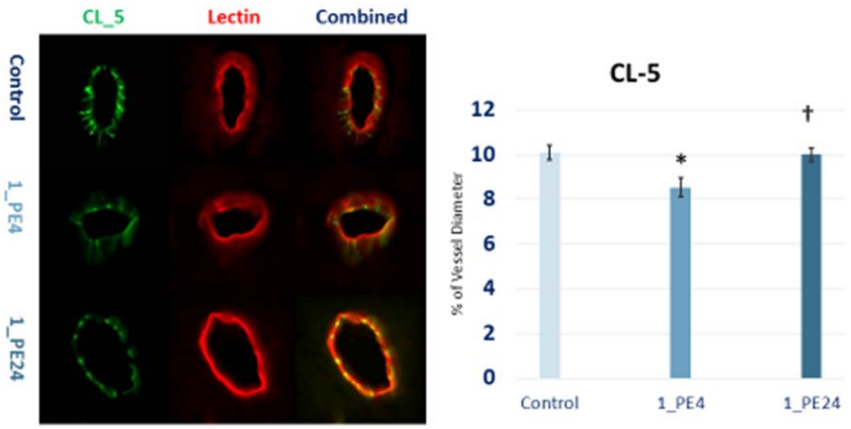

Figure 11B

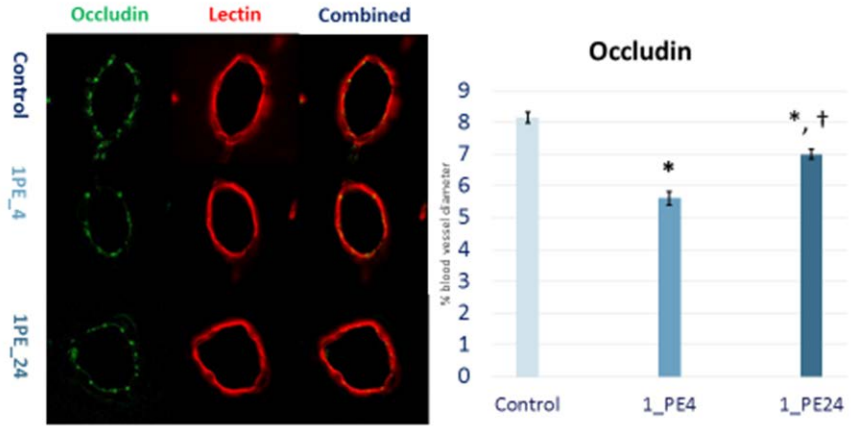

Figure 11C

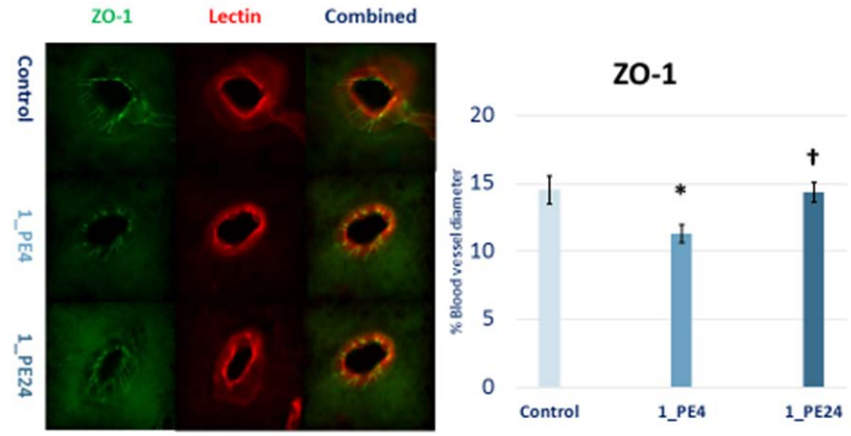

Figure 11. Immunofluorescence microscopy results for CL-5 (Figure 11A), occludin (Figure 11B), and ZO-1 (Figure 11C) in the 1 Prolonged Exposure group.
* $p < 0.05$ compared to control group; † $p < 0.05$ compared to 1_PE4 group

Single Brief Exposure

Following 1 BE to 1.5% isoflurane, there was no significant changes in CL-5 [$F(3,9) = 0.922$; $p = 0.496$] (Figure 12A), occludin [$F(3,9) = 0.153$; $p = 0.925$] (Figure 12B), or ZO-1 [$F(3,9) = 1.279$; $p = 0.334$] (Figure 12C) levels compared to control animals (Figure 12) at either 4 hours (CL-5: $p = 0.649$; occludin: $p = 0.999$; ZO-1: $p = 0.983$) or 24 hours (CL-5: $p = 0.451$; occludin: $p = 0.990$; ZO-1: $p = 0.490$).

5 Brief Exposures

Following 5 BE's to 1.5% isoflurane there, were no significant changes in CL-5 [$F(3,9) = 0.833$; $p = 0.509$] (Figure 13A) or occludin [$F(3,9) = 0.234$; p 0.870] (Figure 13B) levels at either 4 hours (CL-5: $p = 0.759$; occludin: $p = 0.999$) or 24 hours (Cl-5: $p = 0.895$; occludin: $p = 0.899$). However, there was a significant decrease in ZO-1 levels [$F(3,9) = 21.182$; $p = 0.001$] (Figure 13C). Post hoc testing revealed a significant decrease in ZO-1 levels in the 4 hour cohort (13.03 ± 0.31; $p = 0.044$) and 24 hour cohort (10.90 ± 0.42; $p = 0.001$) compared to control (14.75 ± 0.66) (Figure 13C). Additionally, there was a significant decrease in ZO-1 levels between the 4 hour cohort (13.03 ± 0.31) and the 24 hour cohort (10.90 ± 0.42; $p = 0.017$) (Figure 13C).

Figure 12A

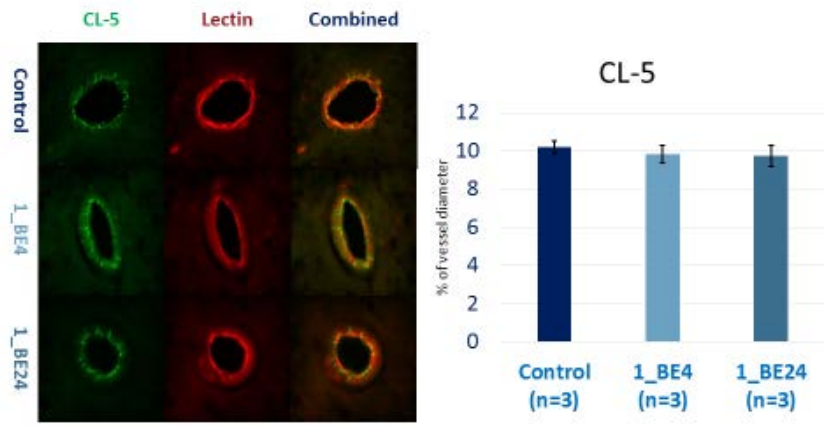

Figure 12B

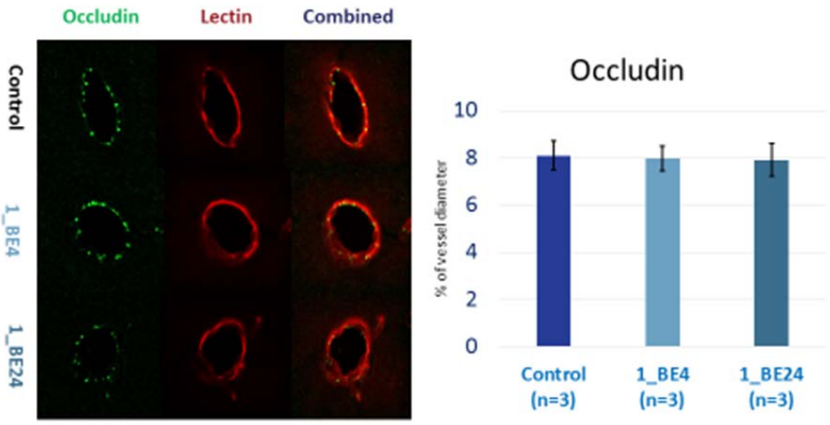

Figure 12C

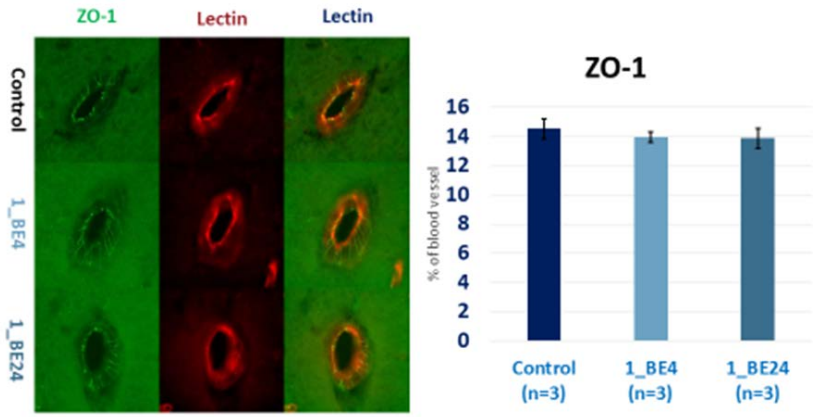

Figure 12. Immunofluorescence microscopy results for CL-5 (Figure 12A), occludin (Figure 12B), and ZO-1 (Figure 12C) in the 1 Brief Exposure Group. *$p < 0.05$ compared to control; † $p < 0.05$ compared to 1_BE4 cohort.

Figure 13A

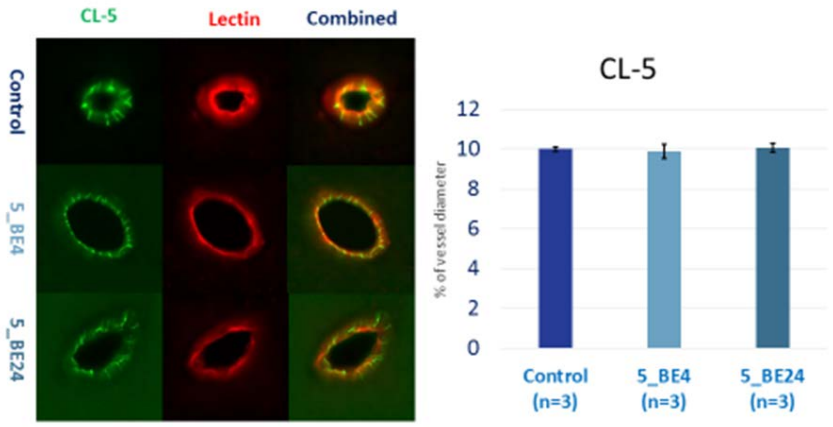

Figure 13B

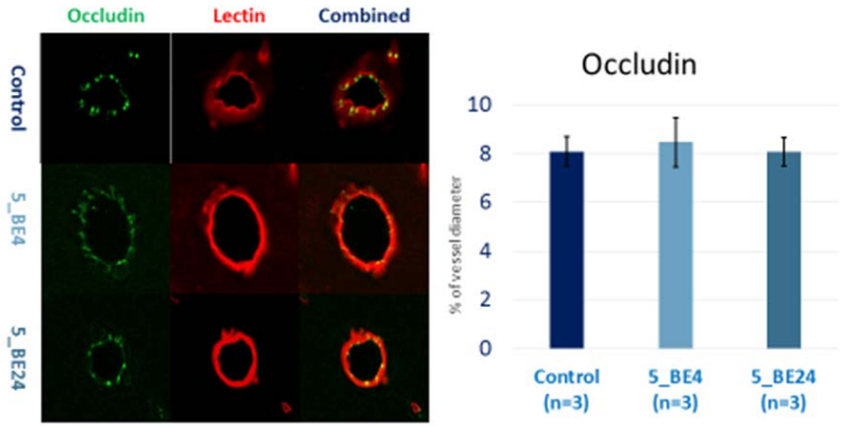

Figure 13C

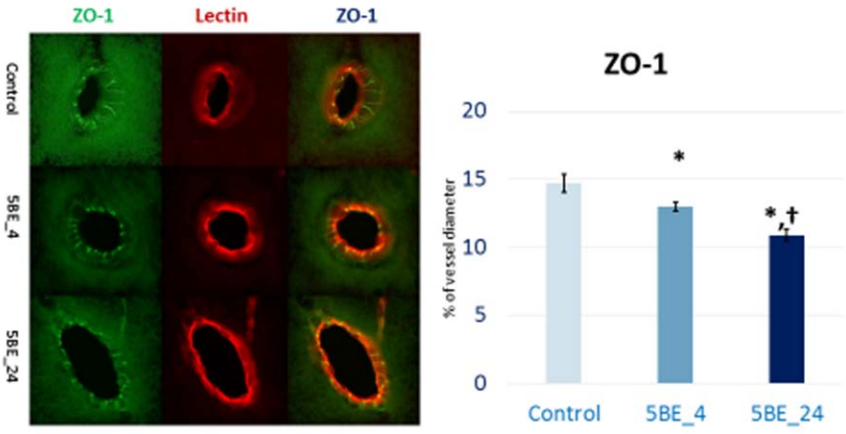

Figure 13. Immunofluorescence microscopy results for CL-5 (Figure 13A), occludin (Figure 13B), and ZO-1 (Figure 13C) in the 5 Brief Exposure Group.
*$p < 0.05$ compared to control; † $p < 0.05$ compared to 5 BE4 cohort.

DEXTRAN EXTRAVASATION

Extravasation of FITC-dextran was used as a measure of alteration in BBB permeability (106). Following 1 PE to 1.5% there was a significant increase in dextran extravasation [$F(2,8) = 294.40$; $p = 0.001$] (Figure 14). Post hoc testing revealed that there was a significant increase in dextran extravasation in the 4- hour (0.214 ± 0.005) cohort compared to the C4 (0.06 ± 0.003; $p = 0.001$) cohort and between the 24- hour (0.132 ± 0.006) cohort and the C24 (0.06 ± 0.002) cohort (Figure 14A). Additionally, there was partial recovery of the BBB permeability because a significant decrease in dextran extravasation was noted in the 24- hour (0.132 ± 0.006) cohort when compared to the 4-hour (0.214 ± 0.005; $p = 0.001$) cohort (Figure 14A).

Following 1 BE to 1.5% isoflurane, there was no statistically significant difference in dextran extravasation levels [$F(3,8) = 0.771$, $p = 0.542$] between C4 (0.061 ± 0.003) cohort and the 4 -hour (0.074 ± 0.012; $p = 0.561$) cohort or between the C24 (0.061 ± 0.002) cohort and the 24- hour (0.066 ± 0.006; $p = 0.970$) cohort (Figure 14B). Additionally, there was no difference in dextran extravasation values between the 1 BE4 (0.074 ± 0.012) cohort and the 1 BE24 (0.066 ± 0.006; $p = 0.833$) cohort.

There was a statically significant difference in dextran extravasation values following 5 BE's to 1.5% isoflurane [$F(3,8) = 11.633$, $p = 0.003$] (Figure 14C). Post hoc testing indicated a significant increase in dextran extravasation values between the C4 (0.061 ± 0.006) cohort and the 5 BE4 (0.120 ± 0.026; $p = 0.004$) cohort (Figure 14C). There was no difference in dextran extravasation values between the C24 (0.061 ± 0.004) cohort and the 5 BE24 (0.076 ± 0.009; $p = 0.574$) cohort. Additionally, there was a significant decrease in the amount of dextran extravasation between the 5 BE4 (0.120 ± 0.026) cohort and the 5 BE24 (0.076 ± 0.009; $p = 0.022$) cohort.

Figure 14A

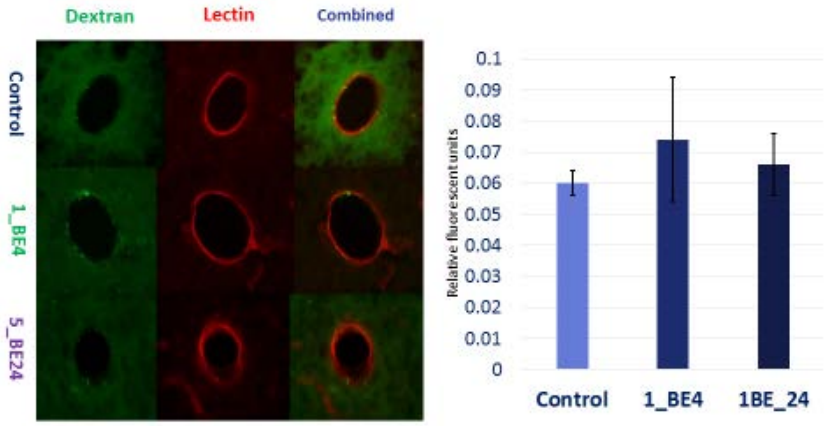

Figure 14B

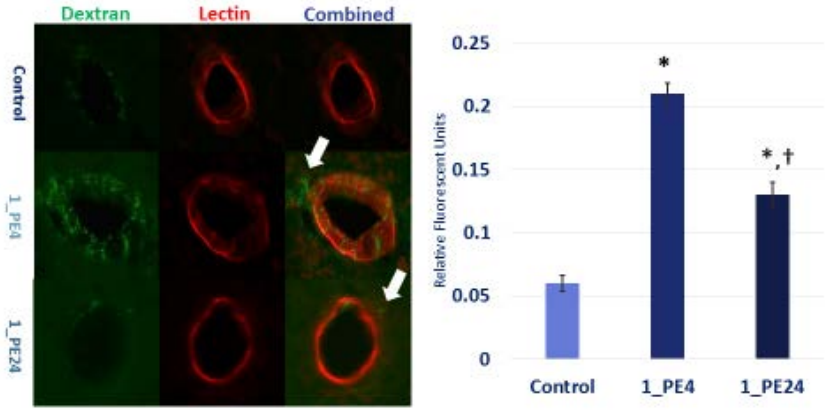

Figure 14C

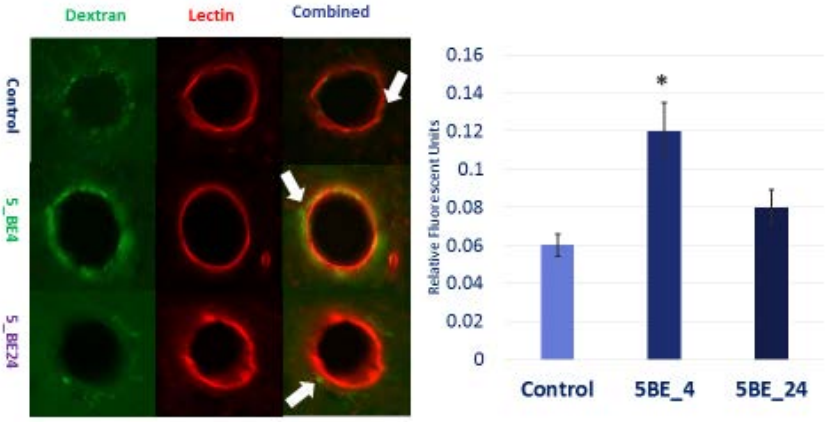

Figure 14. Dextran results following 1 PE (14A), 1 BE (14B) or 5 BE's (14C) to isoflurane. *p< 0.05 compared to control; † p < 0.05 compared to 4 hour cohort.

CHAPTER 5: Discussion

Isoflurane is a commonly used anesthetic in both animal research and human surgery. A single prolonged exposure to isoflurane has been shown to alter the structure and function of the blood brain barrier leading to cognitive impairment in multiple different animal models (30; 108). Complex trauma patients, however, may undergo multiple brief operations prior to definitive repair. The effects of multiple brief exposures to isoflurane on the structure and function of the BBB remains undetermined. Therefore, the goal of our study was to evaluate the effects of multiple brief exposures to isoflurane on the structure and function of the BBB. Additionally, since isoflurane exposure can alter other physiological parameters, cardiorespiratory, arterial blood gas, and metabolic parameters were measured.

PHYSIOLOGICAL PARAMETERS

Cardiorespiratory Parameters

Volatile anesthetics can alter multiple different cellular pathways in the brain and spinal cord to produce the general anesthesia characteristics of reversible loss of consciousness, amnesia, analgesia, and immobility (28). However, volatile anesthetics display several non-anesthetic properties that can alter normal cardiovascular, respiratory, and metabolic parameters (66). Understanding these changes in physiological parameters on study animals is essential to distinguish between the primary pharmacological effects of the isoflurane from the secondary effects cause by hemodynamic derangements.

In rodents, isoflurane exposure can alter HR, BP, and depress cardiac systolic function (259). Acute hypertension, through reduction in CL-5 expression, and hypotension, through alterations in neurovascular coupling and decreased cortical

activity, can lead to BBB damage and cognitive changes (163). Therefore, HR and BP measurements were evaluated every 15 minutes while under anesthesia.

Under isoflurane anesthesia, HR values can vary by end tidal concentration and range from 235-399 beats per minute (199; 259). In our study, mean HR values, by exposure group, ranged from 360-371 BPM and were well within normal reference ranges. Additionally, our mean HR values of 350-380 BPM over the 5 repeated exposures, were within normal reference ranges and were comparable to adult male Wistar rats undergoing 6 exposures to isoflurane over a 3 week period (7).

Blood pressure is an important measure of cardiac function and is an indicator to how well organs are being perfused. Blood pressure is made up of the SPB (pressure during contraction), DBP (pressure when the heart is at rest between beats) and MAP (average BP during a single cardiac cycle) with MAP being the best indicator of cardiovascular function (233). Normally, MAP ranges from 70-110 mmHg with MAP's < 60 mmHG indicating inadequate pressure to deliver oxygen to the tissue and remove metabolic waste produces. A recent study by Yamamoto et al. indicates that isoflurane induced hypo-perfusion, a MAP < 60 mmHg for 2 hours, significantly increased microglia activation, β-amyloid protein deposition, and axonal damage of hippocampal neurons (256). Additionally, MAPs > 110 for an extended period of time can lead to heart failure and BBB dysfunction (86; 183). The mean MAP in each exposure group, and across each repetitive exposure, in our study animals was > 80 mmHg and < 110 indicating adequate tissue perfusion. Additionally, our mean SBP was > 100 mmHg and mean DBP was > 70 mmHg for each group and exposure. These values are well within

normal reference ranges and are comparable to results obtained in previous studies by Albrecht et al. and Yang et al. (7; 259)

In addition to altering cardiovascular functions, isoflurane is a potent respiratory system depressant leading to a reduction in RR, hypoventilation, and a decreased ventilator response to hypoxia and hypercapnia (67). Both hypoxia ($PaO_2 < 60$ mmHg) and hypercapnia ($PaCO_2 > 45$ mmHg) are associated with BBB dysfunction and changes in cognition (73). Therefore, a pulse oximeter was used continuously throughout the anesthetic period to measure arterial oxygen saturation (SaO_2) and blood gas analysis was conducted at the conclusion of the anesthetic to monitor oxygenation and ventilation.

An oxygen saturation (SaO_2) > 90% is desired and correlates to a $PaO_2 > 60$ mmHg (86). If the SaO_2 is < 90%, action needs to be taken to ensure adequate oxygenation is achieved. The exposure group and repetitive exposures mean SaO_2 values were > 97% and SaO_2 levels never fell below 90% at any time point during any of the anesthetic exposures. This limits the chance that our study animals were hypoxic for any period of time.

Arterial Blood Gas Parameters

In addition to measuring oxygenation, arterial blood gas analysis allows for measurement of ventilation status ($PaCO_2$) and acid-base balance (pH and HCO_3). Normal $PaCO_2$ values range from 35-45 mmHg (224). With hypoventilation, CO_2 is unable to be eliminated by the lungs and values increase making the blood more acidic while with hyperventilation, more CO_2 is eliminated and the blood becomes alkalemic. In our study, $PaCO_2$ values ranged between 38 and 41 mmHg and mirror results obtained

in adult or aged Sprague-Dawley rats spontaneously breathing 1.5 - 2% isoflurane for either 2 or 4 hours (41; 218).

The kidneys play a crucial role in acid/base balance by excreting or retaining hydrogen ions based on HCO3 ion levels. If the kidneys are unable to exchange enough hydrogen ions for HCO3 ions, metabolic acidosis ensues. Conversely, if the kidneys are unable to maintain enough hydrogen ions in relation to HCO3 ions, metabolic alkalosis ensues. Normal HCO3 ion blood levels are 22 – 27 mmol/L (86). In the present study, our HCO3 values ranged from 23-25 mmol/L and are similar to values (22.7 mmol/L) obtained by Luo et al. in adult Sprague-Dawley rats spontaneously breathing 1.4% isoflurane for 2 hours (145).

The partial pressure of oxygen dissolved in blood, or PaO2, ranges from 80 – 100 mmHg and varies with the fraction of inspired oxygen concentration (FiO2), barometric pressure, and PaCO2 level (86). With administration of 100% oxygen, PaO2 values should be about 500 mmHg (253). Our mean PaO2 values, however, ranged from 373 – 430 mmHg indicating relative hypoxemia, or PaO2 values lower than expected for a given FiO2 concentration.

The partial pressure of oxygen present in the alveolar, or PAO2, is the main determinant of oxygen diffusion through the alveolar membrane into the blood. Under normal conditions, the difference in PAO2 (alveolar) and PaO2 (arterial) concentration is less than 20 mmHg (220). However, under pathological conditions, a larger gradient may develop indicating a problem with oxygen diffusion across the alveolar membrane, a large area of the lungs that receive adequate oxygenation, but inadequate blood flow (dead space ventilation), an area of adequate blood flow, but poor ventilation (pulmonary

shunt) or defect in the heart that allows de-oxygenated blood to mix with oxygenated blood (right to left shunt) or hypoventilation (86).

The alveolar –arterial gradient, or A-a gradient, can be used to quantify the difference between oxygen concentrations and aid in the diagnosis and proper treatment. The lowest PaO2 in our study was 373.3 ± 16.0 in the 1 PE group. Imputing this value into the A-a formula (PA02 – PaO2), an A-a gradient of 292 mmHg is obtained indicating an obstacle in the transfer of oxygen from the alveoli to the arterial blood. A recent study by Wilding et al. indicates that the delivery of 100% oxygen in rats can collapse the alveoli leading to absorption atelectasis (253). Normally, room air contain a mixture of oxygen (21%) and nitrogen (78%), and since nitrogen does not readily diffuse from the alveoli into the blood, a small amount remains keeping the alveoli open. When breathing 100% oxygen for an extended period of time, however, all the nitrogen is replaced with oxygen. Since oxygen is readily diffusible into the blood, no oxygen remains in the alveoli leading to alveolar collapse. A collapsed alveoli with adequate perfusion leads to a pulmonary shunting and a lower PaO2 values. Our study animals, however, did not display any signs of hypoxia (PaO2 > 60 mmHg and SaO2 > 97%) or low tissue oxygenation (lactate < 2 mmol/L) levels and therefore believe that the relative hypoxia noted by arterial blood gas measurement had minimal impact on study results.

Metabolic Parameters

In our study, there was a statistically significant decrease in mean weight between exposure 1 (367.1 ± 10.8 g) and exposure 2 (362.6 ± 10.6 g) in the 5 BE group with an additional minor decrease in mean weight noted between exposure 2 (362.6 ± 10.6) and exposure 3 (360.7 ± 10.5 g) before leveling off between exposure 4 (359.4 ± 10.4 g) and

exposure 5 (359.9 ± 13.0 g). Overall, however, the decrease in mean weight was only 7g or about 2% of the total body weight and is not clinically relevant nor did it meet the criteria for animal welfare concerns set by the Institutional Animal Care and Use Committee at Uniformed Services University (193).

In addition to weight, we monitored glucose and lactate concentrations. Hyperglycemia (> 200 mg/dL) and hypoglycemia (< 60 mg/dL) can alter BBB transporter mechanisms and tight junction protein expression leading to BBB dysfunction (192). Normal fasting blood glucose in rodent is 70 – 110 mg/dL with values < 60 mg/dL indicating hypoglycemia and values > 190 mg/dL indicating hyperglycemia (249). Compared to controls values, isoflurane exposure significantly increased arterial glucose concentrations in both the different exposure groups and with each exposures in the 5 BE group. The increase in arterial blood glucose concentrations maybe partially explained by stress induced release of cortisol, a decrease in the release of insulin, or changes in the metabolic requirements for glucose (127; 147). The maximum mean glucose value in study animals was 139.4 ± 4.4 mg/dL in the 1 BE group. Although this values is elevated, it did not reach hyperglycemic levels; therefore, limiting the possibility that changes in glucose values alter study outcomes.

Besides being a waste product of metabolism, lactate is an important fuel for many cells. In the brain, lactate is released by astrocytes and used by neurons as an energy substrate. Additionally, lactate has been shown to be an important signaling molecule involved in learning, memory, and neuroprotection (194). Serum lactate levels are typically < 1 mmol/L with lactate levels > 2 mmol/L being considered abnormal and indicating tissue hypo-perfusion or hypoxia (86). Serum lactate levels in our study

animals were all < 2 mmol/L demonstrating adequate tissue oxygenation reducing the probability of tissue hypo-perfusion altering study results.

RNA-SEQUENCING

Volatile anesthetics alter multiple different cellular targets within the CNS to create a complex state of reversible loss of consciousness, amnesia, analgesia, and immobility. Recent evidence indicates that alterations in cellular process may persist longer than functional responses (52). To better understand the cellular process and pathways involved, we described the changes in hippocampal gene expression following a single prolonged exposure to isoflurane. Using the inclusion criteria of $p < 0.05$ and absolute fold change of 1.64, 504 genes (207 up-regulated & 333 down regulated) underwent large scale biological process using GATHER analysis tool. Large scale functional analysis indicated that prolonged isoflurane exposure altered multiple pathways involved in cellular communication, metabolism, and transmission. The biological pathways altered in our study are similar to those observed by Wang et al. (247) They describe changes in cell-cell signaling, synaptic transmission, and transmission of nerve impulses biological pathways in adult rats following a single exposure to 2% isoflurane for 15 minutes. However, following differential expression analysis, only 368 genes were noted to be altered. The difference in number of significantly altered genes may be related to differences in duration of the anesthetic (15 min vs. 4 hours) or inclusion criteria (absolute fold change of 2 vs. 1.64).

Since isoflurane ubiquitously affects all CNS cells, specific cellular markers for neurons, astrocytes, microglia, pericytes, oligodendrocytes, and endothelial cells were evaluated. There were no significant changes in any neuronal, microglia, or pericytes

markers. There was a single astrocyte marker, gap junction beta 6 (GJB6) or connexin 30, that was significant up regulated by both p value and fold change. Gap junctions are specialized structures that form small junctions between adjacent cells and are important for tissue homeostasis and response to pathological stress. They are distributed in a tissue specific manner with GJB6 found in the inner ear, on pericytes, astrocyte end feet (124; 157; 175) . In astrocytes, connexin 30 is responsible for rapid sodium signaling between astrocytes, neurovascular coupling, BBB maintenance, and myelin maintenance through coupling with oligodendrocytes (234). Deletion of GJB6 leads to alterations in neurovascular coupling, loss of BBB integrity under increased vascular pressure, and vacuolation and myelin defects in hippocampal oligodendrocytes that result in balance impairments and changes in spatial memory (146; 234).

In addition to alternating gap junction that link astrocytes to oligodendrocytes, prolonged exposure to isoflurane upregulated all 5 oligodendrocyte protein markers. However, only two, MBP (myelin basic protein) and MOBP (myelin associated oligodendrocyte basic protein) were up regulated by both p values ($p < 0.05$) and fold change ($\pm$ 1.64). Myelin basic protein is major component of the myelin sheath while MOBP is important for stabilizing the tight junction proteins located within the myelin sheath. Oligodendrocyte are highly specialized cells within the CNS that insulate axonal segments of neurons by wrapping them in myelin sheaths (23). These wrapping reduce capacitance and increasing resistance along the axon thereby increasing the speed of conduction between neurons. In addition to insulating neurons, oligodendrocytes provide trophic support to both neurons and vascular endothelial cell of the BBB, and help regulate the extracellular environment (159).

The myelin sheath is comprised of 80% lipids and 20% proteins, with MBP and MOBP playing key roles (22; 23). Demyelination, or loss of myelin sheaths, play a key role in multiple sclerosis, Alzheimer's disease, traumatic brain injury, and recently schizophrenia (159; 166). In order to continuously synthesize components for the membrane sheath, oligodendrocytes are highly metabolically active and highly susceptible to oxidative damage, glutamate excitotoxicity, and pro-inflammatory cytokine (159). Changes in oligodendrocyte structure and function lead to alterations in movement, sensation, cognition, and emotions(23).

Oligodendrocytes, especially immature ones, seem to be highly susceptible to the effects of isoflurane. Gestational, neonatal, or infant rhesus macaque monkeys exposed to 0.7 – 1.5% isoflurane for 5 hours showed a significant increase in neuronal and oligodendrocyte cell death especially in the cerebral cortex, cerebellum, and striatum (24; 51; 212). Additionally, gestational and fetal rhesus macaque brains exposed to propofol, another commonly used anesthetic for procedural sedation or general anesthesia, for 5 hours showed a significant increase in neuronal and oligodendrocyte apoptosis (51).

Volatile anesthetics enhance the inhibitory effects of GABA and glycine, and reduce the excitatory effects of serotonin, acetylcholine, and glutamate (28). Oligodendrocytes contain receptors for GABA, glycine, serotonin, and multiple different glutamate receptors (115). Changes in these neurotransmitter signaling patterns is associated with alterations in proliferation, differentiation, and myelination causing alterations in CNS functions. Under pathological conditions such as ischemia, stoke, spinal cord injury, or MS excess glutamate predominates. In oligodendrocytes, excess glutamate levels lead to a rise in intracellular calcium leading to deformed myelin sheaths

and reduced action potentials (115). Since isoflurane attenuates glutamate signaling, isoflurane exposure, in this context, may prove therapeutic. Conversely, both isoflurane and propofol active $GABA_A$ receptors leading to increased chloride conductance and hyperpolarization in neurons. In oligodendrocytes, though, $GABA_A$ activation has been shown to reduce the number of oligodendrocyte precursor cells and myelin internodes lengths and to increase myelin sheath size all of which alter the conduction speed of neurons (99). Therefore, the effects of isoflurane exposure on oligodendrocytes is complex. However, since propofol has no effects on glutamate levels, the effects on $GABA_A$ receptors may predominate (246; 251).

In addition to operating at the BBB, claudins, especially claudin-11 (CL-11), play an important role oligodendrocyte physiology (159). Normally, oligodendrocytes form flat sheets of myelin that wrap around the axon multiple times in order to increase nerve conduction (23). The wrapping of myelin sheaths are anchored together by complexes of CL-11 and MOBP (166). In claudin-11 deficient mice, the myelin sheaths appear structurally normal; however, they display a very specific phenotype characterized by mild tremors, gait problems, and a significant reduction in membrane excitability and conduction velocity (61). Compared to large axons with thicker myelin sheaths, small axons seem to be particularly affected (60). In the present study, a prolonged exposure to isoflurane reversibly altered the protein expression of CL-5. Additionally, RNA-Seq analysis indicated a significant increase in mRNA values in 1 PE (184.5) compared to control animals (111.2). Hence, it is possible that a prolonged exposure to isoflurane may also alter the protein expression of CL-11 leading to conduction delays.

Tight Junctions: Accessory Proteins

In addition to study proteins, (CL-5, occludin, and ZO-1) multiple other transmembrane and cytoplasmic tight junction proteins were evaluated by RNA-Seq. Of the 20 different proteins evaluated, only cingulin was significantly altered by p-value (< 0.05) and fold change (-1.82). Cingulin is a dimer of two subunits with a globular head and tail connected by a coiled rod domain that helps regulate BBB function by binding to both the actin cytoskeleton and cytoplasmic plaque protein like ZO-1 (49; 54).

In MDCK lacking cingulin, the location, structure, and function of tight junctions were not altered. However, there was a significant increase in gene expression of claudin-2, claudin-6, claudin-7 and occludin, the protein expression of ZO-1, ZO-2, claudin-6, and occludin (44; 95). These changes in gene and protein expression appear to be mediated through the Ras homolog gene family, member A (RhoA) signaling pathway with high levels of cingulin correlating to low RhoA activity and low cingulin levels correlates to high RhoA activity (44). Besides regulating TJP expression, cingulin mediates the effects of transcription factors such as apoptosis-inducing factor (AIF) and ZO-1 associated nucleic acid binding protein (ZONAB) (45). ZO-1 associated nucleic acid binding (ZONAB) communicates the health status of the TJP to the cell nucleus playing a key role in regulate cell proliferation and density (16). Therefore, it appears that the cytoplasmic plaque protein cingulin plays key role in the regulation and maintenance of TJP by communicating the condition of tissue barrier to the nucleus and regulating multiple cell signaling pathways. Despite this importance, a search of PubMed using the search terms “cingulin, blood brain barrier, and volatile anesthetics” returned zero documents. Hence, future studies evaluating the structure and function of the BBB

following isoflurane exposure also need to explore the effects on tight junction accessory proteins and known signaling pathways.

Blood Brain Barrier

The BBB is a highly regulated system that is essential for the maintenance of brain allostasis. Anatomically, cerebral vascular endothelial cells form the anatomical basis of the BBB and differ significantly from peripheral endothelial cells. In contrast to peripheral endothelial cells, cerebral vascular endothelial cells display low pinocytic activity, increased mitochondria, specialized transporters, lack fenestrations, and contain tight junctions that link adjacent endothelial cells together severely limiting paracellular diffusion of molecules into the brain (100). However, cerebral vascular endothelial cells do not act in isolation, they are intimately connected to astrocytes, pericytes, microglia, oligodendrocytes, extracellular matrix and neurons. This intimate relationship between cerebral vascular endothelial cells and other glial cells is termed the neurovascular unit and allows the cerebral vascular system to rapidly respond to increased neuronal activity (170) .

Under normal physiological conditions, the BBB severely limits the passage of substances from the blood into the brain. To enter the brain, most substances must cross the BBB via transmembrane diffusion and those with low molecular weights and high lipid solubility, such as isoflurane, predominate (185). Additionally, substances such as amino acids, vitamins, glucose, and hormones are active transported from the blood into the brain parenchyma via saturable transport systems (100) . Due to the presence of tight junction proteins, paracellular, or diffusion between endothelial cells, is severely limited to very small hydrophilic molecules and ions.

Under pathological conditions, however, BBB permeability can increase modifying brain function in a region specific manner. Blood brain barrier dysfunction plays a significant role in Alzheimer's, Parkinson's, multiple sclerosis, epilepsy, traumatic brain injury, stroke, and normal aging disease progression (111). Conversely, artificially producing temporary BBB dysfunction can be an effective way to deliver medication into the brain to treat malignant brain tumors (186). The underlying mechanism, in either case, is disruption of the tight junction protein complexes thereby allowing for the increased paracellular passages of substances into the brain parenchyma. In our present study, we demonstrate that both a single prolonged exposure or multiple brief exposures to isoflurane exposure can alter the expression of tight junction proteins leading to increased permeability to large molecular weight substances. This agrees with studies by Zhao et al. and Cao et al. that indicate isoflurane exposure can induce reversible alter the expression of tight junction proteins leading to BBB dysfunction (30; 263).

TIGHT JUNCTION PROTEINS

Tight junction protein complexes bind two adjacent cells together preventing the paracellular passage of substances between them. These tight junction complexes are formed by the intricate interactions of over 40 different transmembrane proteins and cytoplasmic plaque proteins (1). Claudins and occludins are the two most important transmembrane proteins while ZO-1 is the most important cytoplasmic plaque protein. Claudins are a family of 24 different proteins with CL-5 being important for sealing the BBB. Loss of CL-5 results in size selective loosening of the BBB and neonatal death (176). Occludin, on the other hand, plays a prominent role in structural integrity and

regulation of barrier properties. Tight junction can form without occludin; however, they exhibit a unique phenotype characterized by chronic inflammation and brain calcification (209). The C -terminus of both CL-5 and occludin bind to cytoplasmic plaque protein ZO-1. Zonula occludens-1 is responsible for tissue organization, tight junction formation, cytoskeletal dynamics, and intracellular signaling. During development, ZO-1 loss leads to embryonic lethality while downregulation, following development, is associated with tight junction breakdown and increased BBB permeability (116).

Transmembrane Proteins

In the present study, either 1 PE or 5 BE's to 1.5% isoflurane induced multiple changes in the protein expression of CL-5, occludin, and ZO-1. At 4 hours following 1 PE, there was a significant decrease in the protein expression and immunostaining of both CL-5 and occludin. By 24 hours, though, CL-5 protein expression and immunostaining were fully recovered to normal while occludin expression and immunostaining were only partially recovered, but still significantly decreased compared to controls. In response to 5 BE's, there was no change in the protein expression or immunostaining of CL-5 at either 4 or 24 hours following the final exposure. The protein expression of occludin was significantly decreased at 4 and 24 hours while immunostaining revealed a disrupted staining patter that did not reach significance. These results indicate that 1 PE to isoflurane had a more prominent effect on transmembrane proteins that multiple brief exposures did.

Here, we show multiple changes in transmembrane proteins expression following isoflurane exposure. Our results are consistent with those obtained in previous studies using both cellular and animal models of isoflurane exposure (29; 263). Using human

brain vascular endothelial cells, Zhao et al. noted that exposure to 1.5-2% isoflurane for 4 hours increased the expression hypoxia induction factor 1α, reduced expression of occludin and increased BBB permeability to small molecules for 24 hours (263). Additionally, aged rats exposed to 1.5% isoflurane for 4 hours displayed increased levels of HIF-1α, decreased occludin and altered the structure and function of the BBB for at least 24 hours (29).

Our results for CL-5, however, are dissimilar to those previously reported. A study by Cao et al. reported that CL-5 expression was not significantly decreased immediately following and 72 hours following a 4-hour exposure to 1.5% isoflurane (30). The different effects of Isoflurane exposure on CL-5 expression may be due to differing evaluation time points. We chose to measure the effects of isoflurane at 4 and 24 hours following the exposure because these time point correlate with opening and closing of the BBB to large substances while Cao et al. chose to measure the effects immediately following and again at 72 hours (29). Our results indicate that changes in CL-5 expression may develop shortly after exposure, but once developed can rapidly be reversed.

Cytoplasmic Proteins

The protein expression and immunostaining pattern of ZO-1 displayed a complex response to either 1 PE or 5 BE's to isoflurane. Following 1 PE, there was a significant increase in the protein expression of ZO-1 at both 4 and 24 hours. However, after 5 BE's to isoflurane, our results indicate no change in the protein expression of ZO-1. In non-exposed control animals, a continuous staining pattern along the cell membrane was noted. At 4 hours following either 1 PE or 5 BE's, the ZO-1 staining intensity was

reduced and clear opening in the staining pattern were noted. By 24 hours, only a partial recovery was noted as both groups continued to display a discontinuous staining pattern along the cell membrane.

DEXTRAN EXTRAVASATION

To evaluate the function of the BBB, we evaluated the extravasation of dextran in the hippocampus of isoflurane exposed rats compared to control animals. Increased BBB permeability can be evaluated with both endogenous markers such as albumin, fibrinogen, or IgG, or exogenously injected substances such as Evans Blue dye, horseradish peroxidase, sodium fluorescein, or conjugated dextrans. Typically, these molecules are large enough and do not readily pass through an intact BBB, but easily pass through under pathological conditions. In this present study, a 40 kDa FITC conjugated dextran was injected via the tail vein at the end of the anesthetic. Recent evidence suggests that anesthesia and the combination of anesthesia and surgery can increase the amount damage associated molecular patterns (DAMPs) such high mobility group box-1 and S100 calcium binding protein B which can trigger an innate immune system response. This activated immune system response triggers a pro-inflammatory cytokine (IL-1B, IL-6, & TNF-a) response from monocytes and macrophages leading to neuroinflammation and hippocampus dysfunction. Since the molecular weight of these DAMPS and pro-inflammatory cytokines range from 15 -40 kDa, a 40 kDa dextran was selected (Akidus).

At 4 or 24 hours following 1 BE, minimal changes in the permeability of the BBB were noted. However, following either a 1 PE or 5 BE's exposures to isoflurane, we observed a substantial increase in the amount of extravasated dextran with the amount in

the 1 PE group being significantly more than that the amount the 5 BE group. At the 24-hour mark though, the amount of dextran extravasated returned to normal in the 5 BE group but was still significantly elevated in the 1 PE group. These results indicate that both 1 PE and 5 BE's can reversibly alter the permeability of the BBB with 1 PE being more destructive than 5 BE's.

Our results are consistent with previous studies that show increased BBB permeability to both small and large molecular weight substances at 4 hours following a single exposure to 1.5% isoflurane for 4 hours, but only to large molecular weight substances at 24 hours (Cao). In addition to isoflurane, sevoflurane, a different volatile anesthetic, has also been shown to alter the structure and function of the BBB. In fact, exposure to 1-3% sevoflurane for 3 hours demonstrated a greater influx of IgG into the cerebral cortex compared to isoflurane. Moreover, the extent of IgG extravasation increased with age and use of sevoflurane, another volatile anesthetic (Acharya).

LIMITATIONS AND FUTURE WORK

Our study has some limitations. First, we did not explore the precise mechanism by which isoflurane alters the structure and function of the BBB. Recently, isoflurane exposure has been shown to alter the expression of the pattern recognition receptor, receptor for advanced glycation endpoints (RAGE), transcription factors high mobility group box-1 (HMGB-1), nuclear factor kappa-light-chain enhancer of activated B-cells (NF-kB) and the Wnt signaling pathway. Additionally, isoflurane exposure has be shown to increase the expression of the pro-inflammatory cytokines interleukin (IL) -1B and IL-6, and matrix metalloproteinase-2 (MMP-2). In future studies, we plan on evaluating the response of HMGB-1, IL-1B, IL-6, and MMP-2 to repeated exposures to isoflurane along

with the ability of anti-inflammatory medication like lidocaine, aspirin, and HMG-CoA reductase inhibitors to limit these inflammatory responses.

Traditionally, anesthesia, especially repeated exposures to general anesthesia with a volatile anesthetic, is not conducted without some form of surgical insult. Therefore, lack of an appropriate surgical model is another limitation of the present study. Since the majority of combat wounded suffer orthopedic trauma from IED blasts, we plan implementing a tibial fracture procedure into our repetitive anesthesia exposure model. In rodents, this model has been shown to induce a stress and inflammatory response marked by increased pro-inflammatory cytokines [Interleukin- 1β (IL-1B), IL-6, and tumor necrosis factor-α (TNF-α) level, BBB dysfunction, and microglia activation leading to neuroinflammation and subsequent cognitive decline.

Finally, our study focused on the molecular and cellular aspects of repeated anesthesia exposure and not any behavioral or cognitive effects. The cognitive and behavioral effects of repeated anesthesia exposures are highly variable and depend on the age of the animal used, choice of anesthetic agent (isoflurane vs. sevoflurane), duration of the anesthetic, time between exposures, and the cognitive and behavioral tests employed. Traditionally, tests that evaluate hippocampal functioning (learning and memory), such as the Barnes maze, Morris water maze, fear conditioning, Y-maze, and novel object recognition, have been used to evaluate the effects anesthesia exposure. However, POCD has also been shown to alter complex attention, emotion, and executive function. Therefore, future studies will incorporate a battery of behavioral and cognitive testing to evaluate attention and executive function as well as learning and memory.

Conclusion

The results of this study suggest that either a single prolonged or multiple brief exposures to isoflurane can alter tight junction expression and increase BBB permeability for up to 24 hours. These findings are clinically relevant as trauma patients, especially poly-trauma patients, may undergo either a prolonged exposure or multiple brief exposures to anesthesia during their course of treatment.

1. Abbott NJ, Patabendige AA, Dolman DE, Yusof SR, Begley DJ. 2010. Structure and function of the blood-brain barrier. *Neurobiology of disease* 37:13-25
2. Abbott NJ, Ronnback L, Hansson E. 2006. Astrocyte-endothelial interactions at the blood-brain barrier. *Nature reviews. Neuroscience* 7:41-53
3. Abbruscato TJ, Davis TP. 1999. Combination of hypoxia/aglycemia compromises in vitro blood-brain barrier integrity. *The Journal of pharmacology and experimental therapeutics* 289:668-75
4. Abildstrom H, Rasmussen LS, Rentowl P, Hanning CD, Rasmussen H, et al. 2000. Cognitive dysfunction 1-2 years after non-cardiac surgery in the elderly. ISPOCD group. International Study of Post-Operative Cognitive Dysfunction. *Acta anaesthesiologica Scandinavica* 44:1246-51
5. Abrahamson DR. 1986. Recent studies on the structure and pathology of basement membranes. *The Journal of pathology* 149:257-78
6. Acharya NK, Goldwaser EL, Forsberg MM, Godsey GA, Johnson CA, et al. 2015. Sevoflurane and Isoflurane induce structural changes in brain vascular endothelial cells and increase blood-brain barrier permeability: Possible link to postoperative delirium and cognitive decline. *Brain research* 1620:29-41
7. Albrecht M, Henke J, Tacke S, Markert M, Guth B. 2014. Influence of repeated anaesthesia on physiological parameters in male Wistar rats: a telemetric study about isoflurane, ketamine-xylazine and a combination of medetomidine, midazolam and fentanyl. *BMC veterinary research* 10:310
8. Altholtz LY, Fowler KA, Badura LL, Kovacs MS. 2006. Comparison of the stress response in rats to repeated isoflurane or CO2:O2 anesthesia used for restraint during serial blood collection via the jugular vein. *Journal of the American Association for Laboratory Animal Science : JAALAS* 45:17-22
9. Amasheh S, Schmidt T, Mahn M, Florian P, Mankertz J, et al. 2005. Contribution of claudin-5 to barrier properties in tight junctions of epithelial cells. *Cell and tissue research* 321:89-96
10. Amrock LG, Starner ML, Murphy KL, Baxter MG. 2015. Long-term effects of single or multiple neonatal sevoflurane exposures on rat hippocampal ultrastructure. *Anesthesiology* 122:87-95
11. Andero R. 2015. Nociceptin and the nociceptin receptor in learning and memory. *Progress in neuro-psychopharmacology & biological psychiatry* 62:45-50
12. AR P, S R. The Effects of Midazolam and Sevoflurane Anesthesia on the Permeability of the Blood Brain Barrier in Mice. *Proc. Australian Cognitive Neuroscience Conference, Brisbane, Australia 2012*:
13. Argaw AT, Gurfein BT, Zhang Y, Zameer A, John GR. 2009. VEGF-mediated disruption of endothelial CLN-5 promotes blood-brain barrier breakdown. *Proceedings of the National Academy of Sciences of the United States of America* 106:1977-82
14. Armulik A, Genove G, Mae M, Nisancioglu MH, Wallgard E, et al. 2010. Pericytes regulate the blood-brain barrier. *Nature* 468:557-61
15. Babb SJ, Crystal JD. 2006. Discrimination of what, when, and where is not based on time of day. *Learning & behavior* 34:124-30

16. Balda MS, Garrett MD, Matter K. 2003. The ZO-1-associated Y-box factor ZONAB regulates epithelial cell proliferation and cell density. *The Journal of cell biology* 160:423-32
17. Balda MS, Whitney JA, Flores C, Gonzalez S, Cereijido M, Matter K. 1996. Functional dissociation of paracellular permeability and transepithelial electrical resistance and disruption of the apical-basolateral intramembrane diffusion barrier by expression of a mutant tight junction membrane protein. *The Journal of cell biology* 134:1031-49
18. Bauer H, Zweimueller-Mayer J, Steinbacher P, Lametschwandtner A, Bauer HC. 2010. The dual role of zonula occludens (ZO) proteins. *Journal of biomedicine & biotechnology* 2010:402593
19. Bazzoni G, Martinez-Estrada OM, Orsenigo F, Cordenonsi M, Citi S, Dejana E. 2000. Interaction of junctional adhesion molecule with the tight junction components ZO-1, cingulin, and occludin. *The Journal of biological chemistry* 275:20520-6
20. Beeman N, Webb PG, Baumgartner HK. 2012. Occludin is required for apoptosis when claudin-claudin interactions are disrupted. *Cell death & disease* 3:e273
21. Berger M, Nadler JW, Browndyke J, Terrando N, Ponnusamy V, et al. 2015. Postoperative Cognitive Dysfunction: Minding the Gaps in Our Knowledge of a Common Postoperative Complication in the Elderly. *Anesthesiology clinics* 33:517-50
22. Boggs JM. 2006. Myelin basic protein: a multifunctional protein. *Cellular and molecular life sciences : CMLS* 63:1945-61
23. Bradl M, Lassmann H. 2010. Oligodendrocytes: biology and pathology. *Acta neuropathologica* 119:37-53
24. Brambrink AM, Evers AS, Avidan MS, Farber NB, Smith DJ, et al. 2010. Isoflurane-induced neuroapoptosis in the neonatal rhesus macaque brain. *Anesthesiology* 112:834-41
25. Brightman MW, Reese TS. 1969. Junctions between intimately apposed cell membranes in the vertebrate brain. *The Journal of cell biology* 40:648-77
26. Brooks TA, Hawkins BT, Huber JD, Egleton RD, Davis TP. 2005. Chronic inflammatory pain leads to increased blood-brain barrier permeability and tight junction protein alterations. *American journal of physiology. Heart and circulatory physiology* 289:H738-43
27. Brown EN, Lydic R, Schiff ND. 2010. General anesthesia, sleep, and coma. *The New England journal of medicine* 363:2638-50
28. Campagna JA, Miller KW, Forman SA. 2003. Mechanisms of actions of inhaled anesthetics. *The New England journal of medicine* 348:2110-24
29. Cao Y, Li Z, Li H, Ni C, Li L, et al. 2018. Hypoxia-inducible factor-1alpha is involved in isoflurane-induced blood-brain barrier disruption in aged rats model of POCD. *Behavioural brain research* 339:39-46
30. Cao Y, Ni C, Li Z, Li L, Liu Y, et al. 2015. Isoflurane anesthesia results in reversible ultrastructure and occludin tight junction protein expression changes in hippocampal blood-brain barrier in aged rats. *Neuroscience letters* 587:51-6

31. Card E, Pandharipande P, Tomes C, Lee C, Wood J, et al. 2015. Emergence from general anaesthesia and evolution of delirium signs in the post-anaesthesia care unit. *British journal of anaesthesia* 115:411-7
32. Cardoso FL, Brites D, Brito MA. 2010. Looking at the blood-brain barrier: molecular anatomy and possible investigation approaches. *Brain research reviews* 64:328-63
33. Carmeliet P. 2003. Angiogenesis in health and disease. *Nature medicine* 9:653-60
34. Carvey PM, Hendey B, Monahan AJ. 2009. The blood-brain barrier in neurodegenerative disease: a rhetorical perspective. *Journal of neurochemistry* 111:291-314
35. Chang JT, Nevins JR. 2006. GATHER: a systems approach to interpreting genomic signatures. *Bioinformatics (Oxford, England)* 22:2926-33
36. Chen L, Liu W, Wang P, Xue Y, Su Q, et al. 2015. Endophilin-1 regulates blood-brain barrier permeability via EGFR-JNK signaling pathway. *Brain research* 1606:44-53
37. Chen SW, Zhu J, Zuo S, Zhang JL, Chen ZY, et al. 2015. Protective effect of hydrogen sulfide on TNF-alpha and IFN-gamma-induced injury of intestinal epithelial barrier function in Caco-2 monolayers. *Inflammation research : official journal of the European Histamine Research Society ... [et al.]* 64:789-97
38. Chen Y, Merzdorf C, Paul DL, Goodenough DA. 1997. COOH terminus of occludin is required for tight junction barrier function in early Xenopus embryos. *The Journal of cell biology* 138:891-9
39. Chen Y, Zhen W, Guo T, Zhao Y, Liu A, et al. 2017. Histamine Receptor 3 negatively regulates oligodendrocyte differentiation and remyelination. *PloS one* 12:e0189380
40. Cherry JD, Olschowka JA, O'Banion MK. 2014. Neuroinflammation and M2 microglia: the good, the bad, and the inflamed. *Journal of neuroinflammation* 11:98
41. Chi OZ, Mellender SJ, Kiss GK, Liu X, Weiss HR. 2017. Blood -brain barrier disruption was less under isoflurane than pentobarbital anesthesia via a PI3K/Akt pathway in early cerebral ischemia. *Brain research bulletin* 131:1-6
42. Choi S, Yu E, Hwang E, Llinas RR. 2016. Pathophysiological implication of CaV3.1 T-type Ca2+ channels in trigeminal neuropathic pain. *Proceedings of the National Academy of Sciences of the United States of America* 113:2270-5
43. Choi S, Yu E, Lee S, Llinas RR. 2015. Altered thalamocortical rhythmicity and connectivity in mice lacking CaV3.1 T-type Ca2+ channels in unconsciousness. *Proceedings of the National Academy of Sciences of the United States of America* 112:7839-44
44. Citi S, Paschoud S, Pulimeno P, Timolati F, De Robertis F, et al. 2009. The tight junction protein cingulin regulates gene expression and RhoA signaling. *Annals of the New York Academy of Sciences* 1165:88-98
45. Citi S, Pulimeno P, Paschoud S. 2012. Cingulin, paracingulin, and PLEKHA7: signaling and cytoskeletal adaptors at the apical junctional complex. *Annals of the New York Academy of Sciences* 1257:125-32

46. Clark RE, Zola SM, Squire LR. 2000. Impaired recognition memory in rats after damage to the hippocampus. *The Journal of neuroscience : the official journal of the Society for Neuroscience* 20:8853-60
47. Cominski TP, Ansonoff MA, Turchin CE, Pintar JE. 2014. Loss of the mu opioid receptor induces strain-specific alterations in hippocampal neurogenesis and spatial learning. *Neuroscience* 278:11-9
48. Conway EM, Carmeliet P. 2004. The diversity of endothelial cells: a challenge for therapeutic angiogenesis. *Genome biology* 5:207
49. Cordenonsi M, D'Atri F, Hammar E, Parry DA, Kendrick-Jones J, et al. 1999. Cingulin contains globular and coiled-coil domains and interacts with ZO-1, ZO-2, ZO-3, and myosin. *The Journal of cell biology* 147:1569-82
50. Cotran RS, Karnovsky MJ. 1968. Ultrastructural studies on the permeability of the mesothelium to horseradish peroxidase. *The Journal of cell biology* 37:123-37
51. Creeley C, Dikranian K, Dissen G, Martin L, Olney J, Brambrink A. 2013. Propofol-induced apoptosis of neurones and oligodendrocytes in fetal and neonatal rhesus macaque brain. *British journal of anaesthesia* 110 Suppl 1:i29-38
52. Culley DJ, Yukhananov RY, Xie Z, Gali RR, Tanzi RE, Crosby G. 2006. Altered hippocampal gene expression 2 days after general anesthesia in rats. *European journal of pharmacology* 549:71-8
53. Cummins PM. 2012. Occludin: one protein, many forms. *Molecular and cellular biology* 32:242-50
54. D'Atri F, Nadalutti F, Citi S. 2002. Evidence for a functional interaction between cingulin and ZO-1 in cultured cells. *The Journal of biological chemistry* 277:27757-64
55. Daneman R, Zhou L, Agalliu D, Cahoy JD, Kaushal A, Barres BA. 2010. The mouse blood-brain barrier transcriptome: a new resource for understanding the development and function of brain endothelial cells. *PloS one* 5:e13741
56. Daneman R, Zhou L, Kebede AA, Barres BA. 2010. Pericytes are required for blood-brain barrier integrity during embryogenesis. *Nature* 468:562-6
57. Deckardt K, Weber I, Kaspers U, Hellwig J, Tennekes H, van Ravenzwaay B. 2007. The effects of inhalation anaesthetics on common clinical pathology parameters in laboratory rats. *Food and chemical toxicology : an international journal published for the British Industrial Biological Research Association* 45:1709-18
58. Deiner S, Silverstein JH. 2009. Postoperative delirium and cognitive dysfunction. *British journal of anaesthesia* 103 Suppl 1:i41-6
59. DePalma RG, Burris DG, Champion HR, Hodgson MJ. 2005. Blast injuries. *The New England journal of medicine* 352:1335-42
60. Devaux J, Fykkolodziej B, Gow A. 2010. Claudin Proteins And Neuronal Function. *Current topics in membranes* 65:229-53
61. Devaux J, Gow A. 2008. Tight junctions potentiate the insulative properties of small CNS myelinated axons. *The Journal of cell biology* 183:909-21
62. Dobrogowska DH, Vorbrodt AW. 2004. Immunogold localization of tight junctional proteins in normal and osmotically-affected rat blood-brain barrier. *Journal of molecular histology* 35:529-39

63. Dougherty AL, Mohrle CR, Galarneau MR, Woodruff SI, Dye JL, Quinn KH. 2009. Battlefield extremity injuries in Operation Iraqi Freedom. *Injury* 40:772-7
64. Duvernoy H, Delon S, Vannson JL. 1983. The vascularization of the human cerebellar cortex. *Brain research bulletin* 11:419-80
65. Ebert MH, Schmidt DE, Thompson T, Butler MG. 1997. Elevated plasma gamma-aminobutyric acid (GABA) levels in individuals with either Prader-Willi syndrome or Angelman syndrome. *The Journal of neuropsychiatry and clinical neurosciences* 9:75-80
66. Eger EI, 2nd. 1981. Isoflurane: a review. *Anesthesiology* 55:559-76
67. Eger EI, 2nd. 1984. The pharmacology of isoflurane. *British journal of anaesthesia* 56 Suppl 1:71s-99s
68. Eger EI, 2nd. 2004. Characteristics of anesthetic agents used for induction and maintenance of general anesthesia. *American journal of health-system pharmacy : AJHP : official journal of the American Society of Health-System Pharmacists* 61 Suppl 4:S3-10
69. Eger EI, 2nd, Saidman LJ, Brandstater B. 1965. Minimum alveolar anesthetic concentration: a standard of anesthetic potency. *Anesthesiology* 26:756-63
70. Ehrlich P. 1885. *Das Sauerstorffbedurfins des Organismus*. Hirschwals, Berlin
71. Emsley JG, Macklis JD. 2006. Astroglial heterogeneity closely reflects the neuronal-defined anatomy of the adult murine CNS. *Neuron glia biology* 2:175-86
72. Engelhardt B. 2003. Development of the blood-brain barrier. *Cell and tissue research* 314:119-29
73. Engelhardt S, Patkar S, Ogunshola OO. 2014. Cell-specific blood-brain barrier regulation in health and disease: a focus on hypoxia. *British journal of pharmacology* 171:1210-30
74. Errede M, Girolamo F, Ferrara G, Strippoli M, Morando S, et al. 2012. Blood-brain barrier alterations in the cerebral cortex in experimental autoimmune encephalomyelitis. *Journal of neuropathology and experimental neurology* 71:840-54
75. Escartin C, Rouach N. 2013. Astroglial networking contributes to neurometabolic coupling. *Frontiers in neuroenergetics* 5:4
76. Eskridge SL, Macera CA, Galarneau MR, Holbrook TL, Woodruff SI, et al. 2012. Injuries from combat explosions in Iraq: injury type, location, and severity. *Injury* 43:1678-82
77. Fanning AS, Anderson JM. 2009. Zonula occludens-1 and -2 are cytosolic scaffolds that regulate the assembly of cellular junctions. *Annals of the New York Academy of Sciences* 1165:113-20
78. Feldman GJ, Mullin JM, Ryan MP. 2005. Occludin: structure, function and regulation. *Advanced drug delivery reviews* 57:883-917
79. Feng M, Whitesall S, Zhang Y, Beibel M, D'Alecy L, DiPetrillo K. 2008. Validation of volume-pressure recording tail-cuff blood pressure measurements. *American journal of hypertension* 21:1288-91
80. Fenstermacher J, Gross P, Sposito N, Acuff V, Pettersen S, Gruber K. 1988. Structural and functional variations in capillary systems within the brain. *Annals of the New York Academy of Sciences* 529:21-30

81. Fischer S, Wobben M, Marti HH, Renz D, Schaper W. 2002. Hypoxia-induced hyperpermeability in brain microvessel endothelial cells involves VEGF-mediated changes in the expression of zonula occludens-1. *Microvascular research* 63:70-80
82. Frank RN, Dutta S, Mancini MA. 1987. Pericyte coverage is greater in the retinal than in the cerebral capillaries of the rat. *Investigative ophthalmology & visual science* 28:1086-91
83. Franks NP. 2008. General anaesthesia: from molecular targets to neuronal pathways of sleep and arousal. *Nature reviews. Neuroscience* 9:370-86
84. Furuse M, Hirase T, Itoh M, Nagafuchi A, Yonemura S, et al. 1993. Occludin: a novel integral membrane protein localizing at tight junctions. *The Journal of cell biology* 123:1777-88
85. Furuse M, Sasaki H, Tsukita S. 1999. Manner of interaction of heterogeneous claudin species within and between tight junction strands. *The Journal of cell biology* 147:891-903
86. Ganong WF. 2003. Review of Medical Physiology. United States: McGaw-Hill Companies
87. Gawande A. 2004. Casualties of war--military care for the wounded from Iraq and Afghanistan. *The New England journal of medicine* 351:2471-5
88. Geiger S, McCormick F, Chou R, Wandel AG. 2008. War wounds: lessons learned from Operation Iraqi Freedom. *Plastic and reconstructive surgery* 122:146-53
89. Goldman EE. 1909. die auseere und innere Sekretion des gesunden kranken Organismus im Lichte der "vitalen garbung.". *Beitrag Klinische Chirurgie*:192-265
90. Goldstein SA, Bockenhauer D, O'Kelly I, Zilberberg N. 2001. Potassium leak channels and the KCNK family of two-P-domain subunits. *Nature reviews. Neuroscience* 2:175-84
91. Gomez-Gonzalez B, Huratado-Alvarado G, Velazquez-Moctezuma J. 2012. Local and Temporal Regulation of the Blood Brain Barrier During Normal and Altered Physiological States. In *The Blood Brain Barrier: New Research*, ed. PA Montenegro, SM Juarez. New York: Nova Science Publishers. Number of.
92. Gonzalez-Mariscal L, Betanzos A, Avila-Flores A. 2000. MAGUK proteins: structure and role in the tight junction. *Seminars in cell & developmental biology* 11:315-24
93. Gottardi CJ, Arpin M, Fanning AS, Louvard D. 1996. The junction-associated protein, zonula occludens-1, localizes to the nucleus before the maturation and during the remodeling of cell-cell contacts. *Proceedings of the National Academy of Sciences of the United States of America* 93:10779-84
94. Grape S, Grape S, Ravussin P, Rossi A, Kern C. 2012. Postoperative cognitive dysfunction. *Trends in anaesthesia & critical care* 2:98-103
95. Guillemot L, Hammar E, Kaister C, Ritz J, Caille D, et al. 2004. Disruption of the cingulin gene does not prevent tight junction formation but alters gene expression. *Journal of cell science* 117:5245-56
96. Gunzel D, Yu AS. 2013. Claudins and the modulation of tight junction permeability. *Physiological reviews* 93:525-69

97. Halfter W, Oertle P, Monnier CA, Camenzind L, Reyes-Lua M, et al. 2015. New concepts in basement membrane biology. *The FEBS journal* 282:4466-79
98. Hamilton NB, Attwell D, Hall CN. 2010. Pericyte-mediated regulation of capillary diameter: a component of neurovascular coupling in health and disease. *Frontiers in neuroenergetics* 2
99. Hamilton NB, Clarke LE, Arancibia-Carcamo IL, Kougioumtzidou E, Matthey M, et al. 2017. Endogenous GABA controls oligodendrocyte lineage cell number, myelination, and CNS internode length. *Glia* 65:309-21
100. Hawkins BT, Davis TP. 2005. The blood-brain barrier/neurovascular unit in health and disease. *Pharmacological reviews* 57:173-85
101. He HJ, Wang Y, Le Y, Duan KM, Yan XB, et al. 2012. Surgery upregulates high mobility group box-1 and disrupts the blood-brain barrier causing cognitive dysfunction in aged rats. *CNS neuroscience & therapeutics* 18:994-1002
102. Hemmings HC, Jr., Akabas MH, Goldstein PA, Trudell JR, Orser BA, Harrison NL. 2005. Emerging molecular mechanisms of general anesthetic action. *Trends in pharmacological sciences* 26:503-10
103. Hildebrand F, Giannoudis P, Kretteck C, Pape HC. 2004. Damage control: extremities. *Injury* 35:678-89
104. Hilgemeier AT, Serna DM, Patel TP, Rambaran KA, Amin ZM, et al. 2018. Pain Perception and the Opioid Receptor Delta 1. *Cureus* 10:e2149
105. Hirase T, Staddon JM, Saitou M, Ando-Akatsuka Y, Itoh M, et al. 1997. Occludin as a possible determinant of tight junction permeability in endothelial cells. *Journal of cell science* 110 (Pt 14):1603-13
106. Hoffmann A, Bredno J, Wendland M, Derugin N, Ohara P, Wintermark M. 2011. High and Low Molecular Weight Fluorescein Isothiocyanate (FITC)-Dextrans to Assess Blood-Brain Barrier Disruption: Technical Considerations. *Translational stroke research* 2:106-11
107. Hovens IB, Schoemaker RG, van der Zee EA, Heineman E, Izaks GJ, van Leeuwen BL. 2012. Thinking through postoperative cognitive dysfunction: How to bridge the gap between clinical and pre-clinical perspectives. *Brain, behavior, and immunity* 26:1169-79
108. Hu N, Guo D, Wang H, Xie K, Wang C, et al. 2014. Involvement of the blood-brain barrier opening in cognitive decline in aged rats following orthopedic surgery and high concentration of sevoflurane inhalation. *Brain research* 1551:13-24
109. Huber JD, Witt KA, Hom S, Egleton RD, Mark KS, Davis TP. 2001. Inflammatory pain alters blood-brain barrier permeability and tight junctional protein expression. *American journal of physiology. Heart and circulatory physiology* 280:H1241-8
110. Hynes RO, Lander AD. 1992. Contact and adhesive specificities in the associations, migrations, and targeting of cells and axons. *Cell* 68:303-22
111. Iadecola C. 2017. The Neurovascular Unit Coming of Age: A Journey through Neurovascular Coupling in Health and Disease. *Neuron* 96:17-42
112. Itoh M, Furuse M, Morita K, Kubota K, Saitou M, Tsukita S. 1999. Direct binding of three tight junction-associated MAGUKs, ZO-1, ZO-2, and ZO-3, with the COOH termini of claudins. *The Journal of cell biology* 147:1351-63

113. Jevtovic-Todorovic V, Hartman RE, Izumi Y, Benshoff ND, Dikranian K, et al. 2003. Early exposure to common anesthetic agents causes widespread neurodegeneration in the developing rat brain and persistent learning deficits. *The Journal of neuroscience : the official journal of the Society for Neuroscience* 23:876-82
114. Johnson T, Monk T, Rasmussen LS, Abildstrom H, Houx P, et al. 2002. Postoperative cognitive dysfunction in middle-aged patients. *Anesthesiology* 96:1351-7
115. Karadottir R, Attwell D. 2007. Neurotransmitter receptors in the life and death of oligodendrocytes. *Neuroscience* 145:1426-38
116. Katsuno T, Umeda K, Matsui T, Hata M, Tamura A, et al. 2008. Deficiency of zonula occludens-1 causes embryonic lethal phenotype associated with defected yolk sac angiogenesis and apoptosis of embryonic cells. *Molecular biology of the cell* 19:2465-75
117. Kaufman RD. 1977. Biophysical mechanisms of anesthetic action: historical perspective and review of current concepts. *Anesthesiology* 46:49-62
118. Kaur C, Ling EA. 2017. The circumventricular organs. *Histology and histopathology* 32:879-92
119. Kehoe LA, Bernardinelli Y, Muller D. 2013. GluN3A: an NMDA receptor subunit with exquisite properties and functions. *Neural plasticity* 2013:145387
120. Krause G, Winkler L, Mueller SL, Haseloff RF, Piontek J, Blasig IE. 2008. Structure and function of claudins. *Biochimica et biophysica acta* 1778:631-45
121. Krause G, Winkler L, Piehl C, Blasig I, Piontek J, Muller SL. 2009. Structure and function of extracellular claudin domains. *Annals of the New York Academy of Sciences* 1165:34-43
122. Kumar AR, Grewal NS, Chung TL, Bradley JP. 2009. Lessons from operation Iraqi freedom: successful subacute reconstruction of complex lower extremity battle injuries. *Plastic and reconstructive surgery* 123:218-29
123. Kumar AR, Grewal NS, Chung TL, Bradley JP. 2009. Lessons from the modern battlefield: successful upper extremity injury reconstruction in the subacute period. *The Journal of trauma* 67:752-7
124. Langer J, Gerkau NJ, Derouiche A, Kleinhans C, Moshrefi-Ravasdjani B, et al. 2017. Rapid sodium signaling couples glutamate uptake to breakdown of ATP in perivascular astrocyte endfeet. *Glia* 65:293-308
125. Le Freche H, Brouillette J, Fernandez-Gomez FJ, Patin P, Caillierez R, et al. 2012. Tau phosphorylation and sevoflurane anesthesia: an association to postoperative cognitive impairment. *Anesthesiology* 116:779-87
126. Lennie P. 2003. The cost of cortical computation. *Current biology : CB* 13:493-7
127. Lenz C, Rebel A, van Ackern K, Kuschinsky W, Waschke KF. 1998. Local cerebral blood flow, local cerebral glucose utilization, and flow-metabolism coupling during sevoflurane versus isoflurane anesthesia in rats. *Anesthesiology* 89:1480-8
128. Lepouse C, Lautner CA, Liu L, Gomis P, Leon A. 2006. Emergence delirium in adults in the post-anaesthesia care unit. *British journal of anaesthesia* 96:747-53
129. Lewansowsky M. 1900. Zur Lehre von der Cerbrospinalflussgkeit. *Clinical Medicine* 40:480-94

130. Li QF, Wang XR, Yang YW, Su DS. 2006. Up-regulation of hypoxia inducible factor 1alpha by isoflurane in Hep3B cells. *Anesthesiology* 105:1211-9
131. Li QF, Zhu YS, Jiang H. 2008. Isoflurane preconditioning activates HIF-1alpha, iNOS and Erk1/2 and protects against oxygen-glucose deprivation neuronal injury. *Brain research* 1245:26-35
132. Li W, Ju K, Li Z, He K, Chen J, et al. 2016. Significant association of GRM7 and GRM8 genes with schizophrenia and major depressive disorder in the Han Chinese population. *European neuropsychopharmacology : the journal of the European College of Neuropsychopharmacology* 26:136-46
133. Li Z, Cao Y, Li L, Liang Y, Tian X, et al. 2014. Prophylactic angiotensin type 1 receptor antagonism confers neuroprotection in an aged rat model of postoperative cognitive dysfunction. *Biochemical and biophysical research communications* 449:74-80
134. Liddelow SA. 2011. Fluids and barriers of the CNS: a historical viewpoint. *Fluids and barriers of the CNS* 8:2
135. Lin D, Zuo Z. 2011. Isoflurane induces hippocampal cell injury and cognitive impairments in adult rats. *Neuropharmacology* 61:1354-9
136. Lin DL, Kirk KL, Murphy KP, McHale KA, Doukas WC. 2004. Orthopedic injuries during Operation Enduring Freedom. *Military medicine* 169:807-9
137. Lindahl P, Johansson BR, Leveen P, Betsholtz C. 1997. Pericyte loss and microaneurysm formation in PDGF-B-deficient mice. *Science (New York, N.Y.)* 277:242-5
138. Lippoldt A, Liebner S, Andbjer B, Kalbacher H, Wolburg H, et al. 2000. Organization of choroid plexus epithelial and endothelial cell tight junctions and regulation of claudin-1, -2 and -5 expression by protein kinase C. *Neuroreport* 11:1427-31
139. Liu C, Cotten JF, Schuyler JA, Fahlman CS, Au JD, et al. 2005. Protective effects of TASK-3 (KCNK9) and related 2P K channels during cellular stress. *Brain research* 1031:164-73
140. Liu J, Wang P, Zhang X, Zhang W, Gu G. 2014. Effects of different concentration and duration time of isoflurane on acute and long-term neurocognitive function of young adult C57BL/6 mouse. *International journal of clinical and experimental pathology* 7:5828-36
141. Liu W, Wang P, Shang C, Chen L, Cai H, et al. 2014. Endophilin-1 regulates blood-brain barrier permeability by controlling ZO-1 and occludin expression via the EGFR-ERK1/2 pathway. *Brain research* 1573:17-26
142. Lochhead JJ, Ronaldson PT, Davis TP. 2017. Hypoxic Stress and Inflammatory Pain Disrupt Blood-Brain Barrier Tight Junctions: Implications for Drug Delivery to the Central Nervous System. *The AAPS journal* 19:910-20
143. Lockhart SH, Cohen Y, Yasuda N, Freire B, Taheri S, et al. 1991. Cerebral uptake and elimination of desflurane, isoflurane, and halothane from rabbit brain: an in vivo NMR study. *Anesthesiology* 74:575-80
144. Lockwood G. 2010. Theoretical context-sensitive elimination times for inhalation anaesthetics. *British journal of anaesthesia* 104:648-55

145. Luo T, Wang Y, Qin J, Liu ZG, Liu M. 2017. Histamine H3 Receptor Antagonist Prevents Memory Deficits and Synaptic Plasticity Disruption Following Isoflurane Exposure. *CNS neuroscience & therapeutics* 23:301-9
146. Lutz SE, Zhao Y, Gulinello M, Lee SC, Raine CS, Brosnan CF. 2009. Deletion of astrocyte connexins 43 and 30 leads to a dysmyelinating phenotype and hippocampal CA1 vacuolation. *The Journal of neuroscience : the official journal of the Society for Neuroscience* 29:7743-52
147. Makaryus R, Lee H, Yu M, Zhang S, Smith SD, et al. 2011. The metabolomic profile during isoflurane anesthesia differs from propofol anesthesia in the live rodent brain. *Journal of cerebral blood flow and metabolism : official journal of the International Society of Cerebral Blood Flow and Metabolism* 31:1432-42
148. Maldonado JR. 2017. Acute Brain Failure: Pathophysiology, Diagnosis, Management, and Sequelae of Delirium. *Critical care clinics* 33:461-519
149. Malgras B, Prunet B, Lesaffre X, Boddaert G, Travers S, et al. 2017. Damage control: Concept and implementation. *Journal of visceral surgery* 154 Suppl 1:S19-s29
150. Manda B, Mir H, Gangwar R, Meena AS, Amin S, et al. 2018. Phosphorylation hotspot in the C-terminal domain of occludin regulates the dynamics of epithelial junctional complexes. *Journal of cell science* 131
151. Mankertz J, Tavalali S, Schmitz H, Mankertz A, Riecken EO, et al. 2000. Expression from the human occludin promoter is affected by tumor necrosis factor alpha and interferon gamma. *Journal of cell science* 113 (Pt 11):2085-90
152. Marty MC, Alliot F, Rutin J, Fritz R, Trisler D, Pessac B. 2002. The myelin basic protein gene is expressed in differentiated blood cell lineages and in hemopoietic progenitors. *Proceedings of the National Academy of Sciences of the United States of America* 99:8856-61
153. Mashour GA, Forman SA, Campagna JA. 2005. Mechanisms of general anesthesia: from molecules to mind. *Best practice & research. Clinical anaesthesiology* 19:349-64
154. Matsugi T, Chen Q, Anderson DR. 1997. Adenosine-induced relaxation of cultured bovine retinal pericytes. *Investigative ophthalmology & visual science* 38:2695-701
155. Matter K, Balda MS. 1998. Biogenesis of tight junctions: the C-terminal domain of occludin mediates basolateral targeting. *Journal of cell science* 111 (Pt 4):511-9
156. Maynard EA, Schultz RL, Pease DC. 1957. Electron microscopy of the vascular bed of rat cerebral cortex. *The American journal of anatomy* 100:409-33
157. Mazare N, Gilbert A, Boulay AC, Rouach N, Cohen-Salmon M. 2018. Connexin 30 is expressed in a subtype of mouse brain pericytes. *Brain structure & function* 223:1017-24
158. McNeil E, Capaldo CT, Macara IG. 2006. Zonula occludens-1 function in the assembly of tight junctions in Madin-Darby canine kidney epithelial cells. *Molecular biology of the cell* 17:1922-32
159. McTigue DM, Tripathi RB. 2008. The life, death, and replacement of oligodendrocytes in the adult CNS. *Journal of neurochemistry* 107:1-19

160. Mediavilla Varas J, Philippens M, Meijer SR, van den Berg AC, Sibma PC, et al. 2011. Physics of IED Blast Shock Tube Simulations for mTBI Research. *Frontiers in neurology* 2:58
161. Medina R, Rahner C, Mitic LL, Anderson JM, Van Itallie CM. 2000. Occludin localization at the tight junction requires the second extracellular loop. *The Journal of membrane biology* 178:235-47
162. Milenkovic I, Zimprich A, Gencik M, Platho-Elwischger K, Seidel S. 2018. A novel nonsense autosomal dominant mutation in the GLRA1 gene causing hyperekplexia. *Journal of neural transmission (Vienna, Austria : 1996)*
163. Mohammadi MT, Dehghani GA. 2014. Acute hypertension induces brain injury and blood-brain barrier disruption through reduction of claudins mRNA expression in rat. *Pathology, research and practice* 210:985-90
164. Moller JT, Cluitmans P, Rasmussen LS, Houx P, Rasmussen H, et al. 1998. Long-term postoperative cognitive dysfunction in the elderly ISPOCD1 study. ISPOCD investigators. International Study of Post-Operative Cognitive Dysfunction. *Lancet (London, England)* 351:857-61
165. Monk TG, Weldon BC, Garvan CW, Dede DE, van der Aa MT, et al. 2008. Predictors of cognitive dysfunction after major noncardiac surgery. *Anesthesiology* 108:18-30
166. Montague P, McCallion AS, Davies RW, Griffiths IR. 2006. Myelin-associated oligodendrocytic basic protein: a family of abundant CNS myelin proteins in search of a function. *Developmental neuroscience* 28:479-87
167. Morita K, Furuse M, Fujimoto K, Tsukita S. 1999. Claudin multigene family encoding four-transmembrane domain protein components of tight junction strands. *Proceedings of the National Academy of Sciences of the United States of America* 96:511-6
168. Morita K, Sasaki H, Furuse M, Tsukita S. 1999. Endothelial claudin: claudin-5/TMVCF constitutes tight junction strands in endothelial cells. *The Journal of cell biology* 147:185-94
169. Morrisroe ER, S. Influence of Isoflurane Duration on Permeability on Blood Brain Barrier in Mice. *Proc. Australian Cognitive Neuroscience Conference Brisbane, Australia, 2012*:
170. Muoio V, Persson PB, Sendeski MM. 2014. The neurovascular unit - concept review. *Acta physiologica (Oxford, England)* 210:790-8
171. Murphy KL, Baxter MG. 2013. Long-term effects of neonatal single or multiple isoflurane exposures on spatial memory in rats. *Frontiers in neurology* 4:87
172. Nag S. 2003. Morphology and molecular properties of cellular components of normal cerebral vessels. *Methods in molecular medicine* 89:3-36
173. Navarrete A, van Schaik CP, Isler K. 2011. Energetics and the evolution of human brain size. *Nature* 480:91-3
174. Nicholson C. 2001. Diffusion and Related Transport Mechanisms in Brain Tissue. *Reports on Progress in Physics* 64:815-84
175. Nickel R, Forge A. 2008. Gap junctions and connexins in the inner ear: their roles in homeostasis and deafness. *Current opinion in otolaryngology & head and neck surgery* 16:452-7

176. Nitta T, Hata M, Gotoh S, Seo Y, Sasaki H, et al. 2003. Size-selective loosening of the blood-brain barrier in claudin-5-deficient mice. *The Journal of cell biology* 161:653-60
177. Noguchi KK, Johnson SA, Dissen GA, Martin LD, Manzella FM, et al. 2017. Isoflurane exposure for three hours triggers apoptotic cell death in neonatal macaque brain. *British journal of anaesthesia* 119:524-31
178. Olah M, Biber K, Vinet J, Boddeke HW. 2011. Microglia phenotype diversity. *CNS & neurological disorders drug targets* 10:108-18
179. Oldendorf WH, Cornford ME, Brown WJ. 1977. The large apparent work capability of the blood-brain barrier: a study of the mitochondrial content of capillary endothelial cells in brain and other tissues of the rat. *Annals of neurology* 1:409-17
180. Olsen RW, Li GD. 2011. GABA(A) receptors as molecular targets of general anesthetics: identification of binding sites provides clues to allosteric modulation. *Canadian journal of anaesthesia = Journal canadien d'anesthesie* 58:206-15
181. Owens BD, Kragh JF, Jr., Wenke JC, Macaitis J, Wade CE, Holcomb JB. 2008. Combat wounds in operation Iraqi Freedom and operation Enduring Freedom. *The Journal of trauma* 64:295-9
182. Oztas B, Akgul S, Arslan FB. 2004. Influence of surgical pain stress on the blood-brain barrier permeability in rats. *Life sciences* 74:1973-9
183. Oztas B, Sandalci U. 1984. Reversibility of blood-brain barrier dysfunction in acute hypertension induced by angiotensin. *Experimental neurology* 84:666-70
184. Pal D, Walton ME, Lipinski WJ, Koch LG, Lydic R, et al. 2012. Determination of minimum alveolar concentration for isoflurane and sevoflurane in a rodent model of human metabolic syndrome. *Anesthesia and analgesia* 114:297-302
185. Pardridge WM. 2015. Blood-brain barrier endogenous transporters as therapeutic targets: a new model for small molecule CNS drug discovery. *Expert opinion on therapeutic targets* 19:1059-72
186. Patel MM, Patel BM. 2017. Crossing the Blood-Brain Barrier: Recent Advances in Drug Delivery to the Brain. *CNS drugs* 31:109-33
187. Persidsky Y, Ramirez SH, Haorah J, Kanmogne GD. 2006. Blood-brain barrier: structural components and function under physiologic and pathologic conditions. *Journal of neuroimmune pharmacology : the official journal of the Society on NeuroImmune Pharmacology* 1:223-36
188. Perszyk RE, DiRaddo JO, Strong KL, Low CM, Ogden KK, et al. 2016. GluN2D-Containing N-methyl-d-Aspartate Receptors Mediate Synaptic Transmission in Hippocampal Interneurons and Regulate Interneuron Activity. *Molecular pharmacology* 90:689-702
189. Petecchia L, Sabatini F, Usai C, Caci E, Varesio L, Rossi GA. 2012. Cytokines induce tight junction disassembly in airway cells via an EGFR-dependent MAPK/ERK1/2-pathway. *Laboratory investigation; a journal of technical methods and pathology* 92:1140-8
190. Piontek J, Winkler L, Wolburg H, Muller SL, Zuleger N, et al. 2008. Formation of tight junction: determinants of homophilic interaction between classic claudins. *FASEB journal : official publication of the Federation of American Societies for Experimental Biology* 22:146-58

191. Potokar M, Jorgacevski J, Zorec R. 2016. Astrocyte Aquaporin Dynamics in Health and Disease. *International journal of molecular sciences* 17
192. Prasad S, Sajja RK, Naik P, Cucullo L. 2014. Diabetes Mellitus and Blood-Brain Barrier Dysfunction: An Overview. *Journal of pharmacovigilance* 2:125
193. Press NA. 2011. *Guide for the Care and Use of Laboratory Animals* Washington DC: National Academy Press
194. Proia P, Di Liegro CM, Schiera G, Fricano A, Di Liegro I. 2016. Lactate as a Metabolite and a Regulator in the Central Nervous System. *International journal of molecular sciences* 17
195. Qosa H, Miller DS, Pasinelli P, Trotti D. 2015. Regulation of ABC efflux transporters at blood-brain barrier in health and neurological disorders. *Brain research* 1628:298-316
196. Radtke FM, Franck M, Hagemann L, Seeling M, Wernecke KD, Spies CD. 2010. Risk factors for inadequate emergence after anesthesia: emergence delirium and hypoactive emergence. *Minerva anestesiologica* 76:394-403
197. Ramasamy A, Hill AM, Clasper JC. 2009. Improvised explosive devices: pathophysiology, injury profiles and current medical management. *Journal of the Royal Army Medical Corps* 155:265-72
198. Rampil IJ, Moller DH, Bell AH. 2006. Isoflurane modulates genomic expression in rat amygdala. *Anesthesia and analgesia* 102:1431-8
199. Redfors B, Shao Y, Omerovic E. 2014. Influence of anesthetic agent, depth of anesthesia and body temperature on cardiovascular functional parameters in the rat. *Laboratory animals* 48:6-14
200. Reed JM, Squire LR. 1997. Impaired recognition memory in patients with lesions limited to the hippocampal formation. *Behavioral neuroscience* 111:667-75
201. Reese TS, Karnovsky MJ. 1967. Fine structural localization of a blood-brain barrier to exogenous peroxidase. *The Journal of cell biology* 34:207-17
202. Ribatti D, Nico B, Crivellato E, Artico M. 2006. Development of the blood-brain barrier: a historical point of view. *Anatomical record. Part B, New anatomist* 289:3-8
203. Rohan D, Buggy DJ, Crowley S, Ling FK, Gallagher H, et al. 2005. Increased incidence of postoperative cognitive dysfunction 24 hr after minor surgery in the elderly. *Canadian journal of anaesthesia = Journal canadien d'anesthesie* 52:137-42
204. Rudolph JL, Marcantonio ER. 2011. Review articles: postoperative delirium: acute change with long-term implications. *Anesthesia and analgesia* 112:1202-11
205. Rudolph U, Antkowiak B. 2004. Molecular and neuronal substrates for general anaesthetics. *Nature reviews. Neuroscience* 5:709-20
206. Ruffer C, Gerke V. 2004. The C-terminal cytoplasmic tail of claudins 1 and 5 but not its PDZ-binding motif is required for apical localization at epithelial and endothelial tight junctions. *European journal of cell biology* 83:135-44
207. Rundshagen I. 2014. Postoperative cognitive dysfunction. *Deutsches Arzteblatt international* 111:119-25
208. Rustenhoven J, Jansson D, Smyth LC, Dragunow M. 2017. Brain Pericytes As Mediators of Neuroinflammation. *Trends in pharmacological sciences* 38:291-304

209. Saitou M, Furuse M, Sasaki H, Schulzke JD, Fromm M, et al. 2000. Complex phenotype of mice lacking occludin, a component of tight junction strands. *Molecular biology of the cell* 11:4131-42
210. Sankar S, Yellajoshyula D, Zhang B, Teets B, Rockweiler N, Kroll KL. 2016. Gene regulatory networks in neural cell fate acquisition from genome-wide chromatin association of Geminin and Zic1. *Scientific reports* 6:37412
211. Santhappan R, Crowder AT, Gouty S, Cox BM, Cote TE. 2015. Mu opioid receptor activation enhances regulator of G protein signaling 4 association with the mu opioid receptor/G protein complex in a GTP-dependent manner. *Journal of neurochemistry* 135:76-87
212. Schenning KJ, Noguchi KK, Martin LD, Manzella FM, Cabrera OH, et al. 2017. Isoflurane exposure leads to apoptosis of neurons and oligodendrocytes in 20- and 40-day old rhesus macaques. *Neurotoxicology and teratology* 60:63-8
213. Schiffer HH, Heinemann SF. 2007. Association of the human kainate receptor GluR7 gene (GRIK3) with recurrent major depressive disorder. *American journal of medical genetics. Part B, Neuropsychiatric genetics : the official publication of the International Society of Psychiatric Genetics* 144b:20-6
214. Schlageter KE, Molnar P, Lapin GD, Groothuis DR. 1999. Microvessel organization and structure in experimental brain tumors: microvessel populations with distinctive structural and functional properties. *Microvascular research* 58:312-28
215. Sedlakova R, Shivers RR, Del Maestro RF. 1999. Ultrastructure of the blood-brain barrier in the rabbit. *Journal of submicroscopic cytology and pathology* 31:149-61
216. Seeman P. 1972. The membrane actions of anesthetics and tranquilizers. *Pharmacological reviews* 24:583-655
217. Shen X, Liu Y, Xu S, Zhao Q, Guo X, et al. 2013. Early life exposure to sevoflurane impairs adulthood spatial memory in the rat. *Neurotoxicology* 39:45-56
218. Shi C, Yi D, Li Z, Zhou Y, Cao Y, et al. 2017. Anti-RAGE antibody attenuates isoflurane-induced cognitive dysfunction in aged rats. *Behavioural brain research* 322:167-76
219. Solari N, Hangya B. 2018. Cholinergic modulation of spatial learning, memory and navigation. *The European journal of neuroscience* 48:2199-230
220. Stein PD, Goldhaber SZ, Henry JW. 1995. Alveolar-arterial oxygen gradient in the assessment of acute pulmonary embolism. *Chest* 107:139-43
221. Steinmetz J, Christensen KB, Lund T, Lohse N, Rasmussen LS. 2009. Long-term consequences of postoperative cognitive dysfunction. *Anesthesiology* 110:548-55
222. Stevenson BR, Siliciano JD, Mooseker MS, Goodenough DA. 1986. Identification of ZO-1: a high molecular weight polypeptide associated with the tight junction (zonula occludens) in a variety of epithelia. *The Journal of cell biology* 103:755-66
223. Stewart PA, Wiley MJ. 1981. Developing nervous tissue induces formation of blood-brain barrier characteristics in invading endothelial cells: a study using quail--chick transplantation chimeras. *Developmental biology* 84:183-92

224. Subramanian RK, Sidharthan A, Maneksh D, Ramalingam L, Manickam AS, et al. 2013. Normative data for arterial blood gas and electrolytes in anesthetized rats. *Indian journal of pharmacology* 45:103-4
225. Szathmari A, Jouvet A, Mottolese C, Champier J, Fevre Montange M. 2015. Anatomical, molecular and pathological consideration of the circumventricular organs. *Neuro-Chirurgie* 61:90-100
226. Takehashi M, Kanatsu-Shinohara M, Miki H, Lee J, Kazuki Y, et al. 2007. Production of knockout mice by gene targeting in multipotent germline stem cells. *Developmental biology* 312:344-52
227. Tejwani GA, Rattan AK, Gudehithlu KP, McDonald JS. 1991. Modulation of mu, kappa and delta opioid receptors in the rat brain by isoflurane and enflurane. *Neuropharmacology* 30:643-9
228. Terrando N, Eriksson LI, Ryu JK, Yang T, Monaco C, et al. 2011. Resolving postoperative neuroinflammation and cognitive decline. *Annals of neurology* 70:986-95
229. Tetrault S, Chever O, Sik A, Amzica F. 2008. Opening of the blood-brain barrier during isoflurane anaesthesia. *The European journal of neuroscience* 28:1330-41
230. Thomas WE. 1999. Brain macrophages: on the role of pericytes and perivascular cells. *Brain research. Brain research reviews* 31:42-57
231. Timpl R, Brown JC. 1996. Supramolecular assembly of basement membranes. *BioEssays : news and reviews in molecular, cellular and developmental biology* 18:123-32
232. Traweger A, Fang D, Liu YC, Stelzhammer W, Krizbai IA, et al. 2002. The tight junction-specific protein occludin is a functional target of the E3 ubiquitin-protein ligase itch. *The Journal of biological chemistry* 277:10201-8
233. Tremoleda JL, Kerton A, Gsell W. 2012. Anaesthesia and physiological monitoring during in vivo imaging of laboratory rodents: considerations on experimental outcomes and animal welfare. *EJNMMI research* 2:44
234. Tress O, Maglione M, May D, Pivneva T, Richter N, et al. 2012. Panglial gap junctional communication is essential for maintenance of myelin in the CNS. *The Journal of neuroscience : the official journal of the Society for Neuroscience* 32:7499-518
235. Tsai TL, Sands LP, Leung JM. 2010. An Update on Postoperative Cognitive Dysfunction. *Advances in anesthesia* 28:269-84
236. Tsantoulas C, McMahon SB. 2014. Opening paths to novel analgesics: the role of potassium channels in chronic pain. *Trends in neurosciences* 37:146-58
237. Tsukita S, Furuse M. 1999. Occludin and claudins in tight-junction strands: leading or supporting players? *Trends in cell biology* 9:268-73
238. Tsukita S, Furuse M, Itoh M. 2001. Multifunctional strands in tight junctions. *Nature reviews. Molecular cell biology* 2:285-93
239. Uchimoto K, Miyazaki T, Kamiya Y, Mihara T, Koyama Y, et al. 2014. Isoflurane impairs learning and hippocampal long-term potentiation via the saturation of synaptic plasticity. *Anesthesiology* 121:302-10
240. Umeda K, Ikenouchi J, Katahira-Tayama S, Furuse K, Sasaki H, et al. 2006. ZO-1 and ZO-2 independently determine where claudins are polymerized in tight-junction strand formation. *Cell* 126:741-54

241. Umeda K, Matsui T, Nakayama M, Furuse K, Sasaki H, et al. 2004. Establishment and characterization of cultured epithelial cells lacking expression of ZO-1. *The Journal of biological chemistry* 279:44785-94
242. Van Itallie CM, Anderson JM. 1997. Occludin confers adhesiveness when expressed in fibroblasts. *Journal of cell science* 110 (Pt 9):1113-21
243. Vilhardt F. 2005. Microglia: phagocyte and glia cell. *The international journal of biochemistry & cell biology* 37:17-21
244. Vorbrodt AW, Dobrogowska DH. 2003. Molecular anatomy of intercellular junctions in brain endothelial and epithelial barriers: electron microscopist's view. *Brain research. Brain research reviews* 42:221-42
245. Vutskits L, Xie Z. 2016. Lasting impact of general anaesthesia on the brain: mechanisms and relevance. *Nature reviews. Neuroscience* 17:705-17
246. Wakita M, Kotani N, Nonaka K, Shin MC, Akaike N. 2013. Effects of propofol on GABAergic and glutamatergic transmission in isolated hippocampal single nerve-synapse preparations. *European journal of pharmacology* 718:63-73
247. Wang H, Jin Y, Dai J. 2015. Biological processes and pathway changes in isoflurane-induced anesthesia revealed by bioinformatics analysis of gene expression profiles. *Journal of anesthesia* 29:912-9
248. Wang MC, Temkin NR, Deyo RA, Jurkovich GJ, Barber J, Dikmen S. 2007. Timing of surgery after multisystem injury with traumatic brain injury: effect on neuropsychological and functional outcome. *The Journal of trauma* 62:1250-8
249. Wang Z, Yang Y, Xiang X, Zhu Y, Men J, He M. 2010. [Estimation of the normal range of blood glucose in rats]. *Wei sheng yan jiu = Journal of hygiene research* 39:133-7, 42
250. Wen H, Watry DD, Marcondes MC, Fox HS. 2004. Selective decrease in paracellular conductance of tight junctions: role of the first extracellular domain of claudin-5. *Molecular and cellular biology* 24:8408-17
251. Westphalen RI, Hemmings HC, Jr. 2003. Effects of isoflurane and propofol on glutamate and GABA transporters in isolated cortical nerve terminals. *Anesthesiology* 98:364-72
252. White PF, Johnston RR, Eger EI, 2nd. 1974. Determination of anesthetic requirement in rats. *Anesthesiology* 40:52-7
253. Wilding LA, Hampel JA, Khoury BM, Kang S, Machado-Aranda D, et al. 2017. Benefits of 21% Oxygen Compared with 100% Oxygen for Delivery of Isoflurane to Mice (Mus musculus) and Rats (Rattus norvegicus). *Journal of the American Association for Laboratory Animal Science : JAALAS* 56:148-54
254. Wong AD, Ye M, Levy AF, Rothstein JD, Bergles DE, Searson PC. 2013. The blood-brain barrier: an engineering perspective. *Frontiers in neuroengineering* 6:7
255. Xu B, Yang J, Kang F, Li J. 2015. The inflammatory response of two different kinds of anesthetics on vascular cognitive impairment rats and the effect on long term cognitive function. *International journal of clinical and experimental medicine* 8:16694-8
256. Yamamoto T, Iwamoto T, Kimura S, Nakao S. 2018. Persistent isoflurane-induced hypotension causes hippocampal neuronal damage in a rat model of chronic cerebral hypoperfusion. *Journal of anesthesia* 32:182-8

257. Yamanishi S, Katsumura K, Kobayashi T, Puro DG. 2006. Extracellular lactate as a dynamic vasoactive signal in the rat retinal microvasculature. *American journal of physiology. Heart and circulatory physiology* 290:H925-34
258. Yamazaki Y, Umeda K, Wada M, Nada S, Okada M, et al. 2008. ZO-1- and ZO-2-dependent integration of myosin-2 to epithelial zonula adherens. *Molecular biology of the cell* 19:3801-11
259. Yang C-F, Yu-Chih Chen M, Chen T-I, Cheng C-F. 2014. Dose-dependent effects of isoflurane on cardiovascular function in rats. *Tzu Chi Medical Journal* 26:119-22
260. Yanike M, Wirth S, Suzuki WA. 2004. Representation of well-learned information in the monkey hippocampus. *Neuron* 42:477-87
261. Yoon S, Seger R. 2006. The extracellular signal-regulated kinase: multiple substrates regulate diverse cellular functions. *Growth factors (Chur, Switzerland)* 24:21-44
262. Yu QJ, Tao H, Wang X, Li MC. 2015. Targeting brain microvascular endothelial cells: a therapeutic approach to neuroprotection against stroke. *Neural regeneration research* 10:1882-91
263. Zhao J, Hao J, Fei X, Wang X, Hou Y, Deng C. 2014. Isoflurane inhibits occludin expression via up-regulation of hypoxia-inducible factor 1alpha. *Brain research* 1562:1-10
264. Zhu XH, Qiao H, Du F, Xiong Q, Liu X, et al. 2012. Quantitative imaging of energy expenditure in human brain. *NeuroImage* 60:2107-17
265. Zipser BD, Johanson CE, Gonzalez L, Berzin TM, Tavares R, et al. 2007. Microvascular injury and blood-brain barrier leakage in Alzheimer's disease. *Neurobiology of aging* 28:977-86
266. Zlokovic BV. 2008. The blood-brain barrier in health and chronic neurodegenerative disorders. *Neuron* 57:178-201
267. Zola SM, Squire LR. 2001. Relationship between magnitude of damage to the hippocampus and impaired recognition memory in monkeys. *Hippocampus* 11:92-8